

**Regulation factors of productivity, nitrogen fixation and  
phytoplankton species composition in the upwelling area and the  
Mekong estuary off southern central Vietnam, South China Sea**

Dissertation

Zur Erlangung des akademischen Grades  
Doktor der Naturwissenschaften  
(doctor rerum naturalium)

Vorgelegt der  
Mathematisch-Naturwissenschaftlichen Fakultät  
der Universität Rostock

von  
Deniz Bombar  
geb. am 15. Februar 1978 in Worms

Rostock 2010

**URN: *urn:nbn:de:gbv:28-diss2010-0158-5***

**Gutachter:**

PD Dr. Maren Voss

Biologische Meereskunde

Leibniz-Institut für Ostseeforschung, Warnemünde

Prof. Dr. Joseph Montoya

Department of Environmental Science & Technology, School of Biology

Georgia Institute of Technology, Atlanta, USA

Prof. Dr. Friedrich Widdel

Abteilung Mikrobiologie

Max-Planck-Institut für Marine Mikrobiologie, Bremen

**Datum der öffentlichen Verteidigung:** 27.09.2010

# Contents

<b>List of Figures</b> .....	III
<b>List of Tables</b> .....	IV
<b>Summary</b> .....	V
<b>Zusammenfassung</b> .....	VII
<b>1. General Introduction</b> .....	1
1.1 Oceanic new production.....	1
1.2 Diversity and ecology of pelagic diazotroph prokaryotes in the tropical and subtropical ocean.....	7
1.3 The South China Sea and the upwelling area off Vietnam .....	14
1.4 Aim of the study.....	17
<b>2. Sources of new nitrogen in the Vietnamese upwelling region of the South China Sea</b> .....	19
2.1 Abstract .....	19
2.2 Introduction.....	20
2.3 Materials and methods .....	22
2.4 Results.....	24
2.4.1 Environmental conditions .....	24
2.4.2 Primary productivity.....	26
2.4.3 Nitrate uptake .....	27
2.4.4 N <sub>2</sub> fixation.....	29
2.4.5 Vertical nitrate flux.....	29
2.5 Discussion .....	31
2.5.1 Different upwelling intensity in July 2003 and July 2004.....	31
2.5.2 Primary productivity and nitrate supply in the upwelling zone.....	32
2.5.3 Primary productivity and nitrate supply at offshore stations .....	37
2.5.4 N <sub>2</sub> fixation as a source of new nitrogen .....	39
<b>3. The Mekong River plume fuels nitrogen fixation and determines phytoplankton species distribution in the South China Sea during low and high discharge season</b> ....	42
3.1 Abstract .....	42
3.2 Introduction.....	43
3.3 Materials and methods .....	44
3.3.1 Study area.....	44
3.3.2 Sampling .....	45
3.3.3 Analyses .....	46
3.4 Results.....	48
3.4.1 Hydrographic conditions and nutrient distributions.....	48
3.4.2 N <sub>2</sub> fixation and primary production.....	52
3.4.3 Phytoplankton species distribution.....	55
3.5 Discussion .....	57
3.5.1 Comparison of abiotic conditions during low and high discharge .....	57
3.5.2 Influence of the Mekong River plume on N <sub>2</sub> fixation, primary production, and phytoplankton community composition .....	59
3.5.3 Ecological importance of N <sub>2</sub> fixation in the Mekong River plume.....	61

<b>4. Distribution of diazotrophic microorganisms, <i>nifH</i> gene expression and N<sub>2</sub> fixation in the Mekong River Plume during intermonsoon</b> .....	63
4.1 Abstract .....	63
4.2 Introduction .....	64
4.3 Materials and methods .....	65
4.3.1 Sampling .....	65
4.3.2 Nutrient analyses .....	67
4.3.3 N <sub>2</sub> fixation .....	67
4.3.4 Nucleic acid sampling and extraction .....	67
4.3.5 <i>nifH</i> PCR, cloning, sequencing, and sequence analysis .....	68
4.3.6 cDNA synthesis .....	68
4.3.7 Quantitative PCR and RT-QPCR .....	70
4.3.8 Transformation onto Lagrangian coordinates and a Lagrangian tracer experiment .....	70
4.3.9 Statistical analyses .....	71
4.4 Results .....	71
4.4.1 Lagrangian tracer experiments .....	71
4.4.2 Environmental conditions .....	73
4.4.3 N <sub>2</sub> fixation .....	77
4.4.4 Abundances of diazotrophs and <i>nifH</i> gene expression .....	77
4.4.5 <i>nifH</i> diversity and phylotype distributions .....	80
4.5 Discussion .....	81
4.5.1 Hydrography of the Mekong River plume during intermonsoon and classification of stations .....	81
4.5.2 Influence of the river plume on the distribution and activity of different diazotrophs .....	82
<b>5. Conclusions and Perspectives</b> .....	88
<b>Bibliography</b> .....	94
<b>Publications, Manuscripts, and Conferences</b> .....	IX
<b>Acknowledgements</b> .....	XI
<b>Erklärung</b> .....	XII
<b>Curriculum vitae</b> .....	XIII

## List of Figures

1.1 Conceptual diagram of some major features of the oceanic nitrogen cycle.....	2
1.2 Scheme of the intracellular regulation of N <sub>2</sub> fixation.....	9
1.3 Conceptual model for the fate of nitrogen fixed by different diazotrophs.....	13
1.4 Map of the South China Sea and important seasonal hydrographic features.....	15
2.1 Map of the investigation areas in the South China Sea, SW-monsoon 2003/2004.....	21
2.2 Mixed layer depths and sea surface temperatures.....	25
2.3 Profiles of nitrate concentrations.....	26
2.4 Vertical distributions of primary productivity, nitrate uptake, and N <sub>2</sub> fixation.....	27
2.5 Areal rates of primary productivity, nitrate uptake, and N <sub>2</sub> fixation.....	28
2.6 Profiles of vertical eddy diffusivities.....	30
2.7 Comparison between rate measurements and estimated nitrate fluxes.....	33
2.8 Relationship between nitrate uptake and N-demands at upwelling stations.....	34
2.9 Cruise comparison between areal N <sub>2</sub> fixation; relationship to primary productivity.....	40
3.1 Map of the Mekong River estuary, sampling stations in Apr. 2007/Sept. 2008.....	45
3.2 Horizontal salinity- and nutrient distributions in the investigation area.....	49
3.3 N:P ratios in different salinity ranges.....	52
3.4 Rates of N <sub>2</sub> fixation in the investigation area.....	53
3.5 Course of N <sub>2</sub> fixation at time series stations.....	54
3.6 Relationships between N <sub>2</sub> fixation, turbidity, and N:P ratios.....	55
3.7 Horizontal phytoplankton distributions.....	57
4.1 Map of the Mekong River estuary, sampling stations in Apr. 2007.....	66
4.2 Distribution of salinity / turbidity in Eulerian and Lagrangian station grid.....	72
4.3 Propagation of the Mekong Plume according to Lagrangian tracer experiment.....	72
4.4 Nutrient regressions and ratios.....	74
4.5 Horizontal distribution of <i>nifH</i> gene copies of different phylotypes.....	78
4.6 <i>NifH</i> gene copies / transcripts and N <sub>2</sub> fixation at mooring station 19.....	79
5.1 Conceptual diagram of diazotrophy in the Mekong River plume.....	90
5.2 Concentrations of Si(OH) <sub>4</sub> and PO <sub>4</sub> <sup>3-</sup> vs. salinity.....	92

## List of Tables

2.1 Estimates of upwelling nitrate fluxes.....	30
2.2 Estimates of diffusive nitrate fluxes.....	31
2.3 Primary productivity estimates for different upwelling areas and offshore waters.....	35
3.1 N <sub>2</sub> fixation rates in April 2007 and September 2008.....	48
3.2 Pearson correlation matrix comparing salinity, turbidity, and nutrient concentrations....	50
3.3 Ranges, means, and standard deviations of all variables.....	51
4.1 Applied <i>nifH</i> primer and probe sets.....	69
4.2 Pearson correlation matrix comparing salinity, turbidity, and nutrient concentrations.....	73
4.3 Summary of mean <i>nifH</i> gene copy / transcript abundances, nitrate concentrations, and N <sub>2</sub> fixation in the different salinity ranges.....	75-76

## Summary

The southwest (SW) monsoon between June and September induces upwelling off the southern central Vietnamese coast in the South China Sea (SCS). Remote sensing and modeling studies suggest that this upwelling area is the most productive region of the SCS, but so far, no *in situ* studies have been conducted in this pelagic ecosystem. Therefore, one major aim of this thesis was to evaluate the primary productivity of the upwelling zone and of adjacent offshore waters during SW monsoon in July 2003 and 2004, and to assess the importance of nitrate as well as pelagic dinitrogen (N<sub>2</sub>) fixation in fueling this productivity. Estimates of vertical nitrate fluxes by Ekman upwelling (upwelling zone) and turbulent diffusion (offshore zone) were determined complementary to rate measurements of primary productivity, nitrate uptake, and N<sub>2</sub> fixation. The results show that primary productivity in the Vietnamese upwelling zone can be as high as in other upwelling areas of the world, e.g. off northwest Africa or off the Somali coast in the Arabian Sea, but due to El Niño influence, weaker upwelling and consequently lower productivity was found in July 2003 ( $28 \pm 18$  mmol C m<sup>-2</sup> d<sup>-1</sup>) compared to July 2004 ( $103 \pm 25$  mmol C m<sup>-2</sup> d<sup>-1</sup>). The predominant importance of upwelling nitrate as a source of new nitrogen was displayed by upwelling nitrate fluxes of up to  $17 \pm 2$  mmol N m<sup>-2</sup> d<sup>-1</sup> in July 2004, which would cover the entire N-demand of primary productivity. Diffusive nitrate fluxes in offshore waters were determined in July 2003 and are in the order of  $2.3 \pm 0.6$  mmol N m<sup>-2</sup> d<sup>-1</sup>, based on a maximal diffusivity of 1 cm<sup>2</sup> s<sup>-1</sup> in the nitracline. N<sub>2</sub> fixation was a significant nitrogen source in offshore waters, but surprisingly with lower rates in July 2003 ( $22 - 119$  μmol N m<sup>-2</sup> d<sup>-1</sup>) than in July 2004 ( $37 - 375$  μmol N m<sup>-2</sup> d<sup>-1</sup>), equalling 1 - 5% and probably 2 - 25% of diffusive nitrate fluxes, respectively.

Most of the elevated N<sub>2</sub> fixation rates were measured at stations where the Mekong River plume was noticeable, suggesting that riverine micronutrients and/or trace metals supported the growth of marine diazotrophs. Therefore, the impact of Mekong River outflow on pelagic N<sub>2</sub> fixation and phytoplankton species distributions was investigated in more detail during minimal and maximal river discharge in April 2007 and September 2008, respectively. During both cruises, ratios of NO<sub>3</sub><sup>-</sup> + NO<sub>2</sub><sup>-</sup> to PO<sub>4</sub><sup>3-</sup> (N:P) in surface waters sharply declined with increasing salinity. Sampling stations having N:P ratios lower than the typical oceanic Redfield ratio (16:1) were characterized by some of the highest rates of N<sub>2</sub> fixation ever measured in the marine pelagial, with up to 22.77 nmol N L<sup>-1</sup> h<sup>-1</sup> in April 2007, and up to 5.05 nmol N L<sup>-1</sup> h<sup>-1</sup> in September 2008. The highest rates would cover up to 47% of the N- demand of primary productivity in the Mekong Plume. The low N:P ratios indicate that N<sub>2</sub> fixation was triggered by a PO<sub>4</sub><sup>3-</sup>-surplus relative to phytoplankton nutrient requirements. Coincident with this PO<sub>4</sub><sup>3-</sup> surplus, concentrations of Si(OH)<sub>4</sub> were high, suggesting that nutrient conditions

particularly favoured the growth of symbioses between different diatom species and the heterocystous cyanobacterium *Richelia intracellularis* (Diatom-Diazotroph Associations, DDAs). Based on microscopy, diatom species including *Rhizosolenia* spp., *Chaetoceros* spp., *Guinardia* spp., *Hemiaulius* spp., and *Bacteriastrum* spp, which potentially hosted diazotroph symbionts, were indeed highly abundant during both cruises. The presence and activity of DDAs was confirmed for April 2007 by analyzing the distribution and expression of the nitrogenase (*nifH*) gene by quantitative PCR. This molecular approach also revealed that *Trichodesmium* spp. was an at least equally important diazotroph in the Mekong River plume. *NifH* gene copies and transcripts of unicellular cyanobacterial diazotrophs (groups B and C) and a  $\gamma$ -proteobacterial phylotype were exclusively found at oceanic stations, confirming that the nutrient gradients within tropical river plumes are responsible for unequal distribution patterns of different marine diazotrophs. The diversity of the diazotroph community was assessed by a nested PCR approach targeting *nifH*, and subsequent DNA-sequencing of representative *nifH* clones from clone libraries. Several *nifH* sequences represented new lineages of heterotrophic proteobacteria and diazotrophs belonging to *nifH* cluster III (including anaerobic sulfate reducers). These previously uncharacterized prokaryotes were possibly responsible for the unexpectedly high N<sub>2</sub> fixation ( $1.13 \pm 1.04 \text{ nmol N L}^{-1} \text{ h}^{-1}$ ) in parts of the plume which had lowest salinity and highest nutrient concentrations, and possibly resided within anoxic microzones of suspended particles. Overall, it was shown that the Mekong River plume can be a “hot spot” of N<sub>2</sub> fixation, hosts a diverse diazotroph community, and seems to particularly favor the growth of *Trichodesmium* spp. and DDAs. Tropical river plumes seem to generally enhance oceanic N<sub>2</sub> fixation by supplying phosphorus and iron, and thus might trigger a substantial contribution to global oceanic N<sub>2</sub> fixation.

## Zusammenfassung

Im südchinesischen Meer wird durch den Südwest- (SW) Monsun zwischen Juni und September vor der südlichen vietnamesischen Küste Auftrieb verursacht. Numerische Modelle und durch Satellitensensoren gemessene Chlorophyllkonzentrationen lassen vermuten, dass dieses Gebiet das produktivste des gesamten südchinesischen Meeres ist, jedoch wurde das pelagische Ökosystem bisher nie direkt untersucht. Ein Hauptziel dieser Doktorarbeit war deshalb die Bestimmung der Produktivität der Auftriebszone sowie der weiter küstenfern gelegenen oligotrophen Gewässer im Juli 2003 und Juli 2004. Außerdem sollten Nitrat und pelagische Distickstoff- ( $\text{N}_2$ ) Fixierung als Quellen für neuen Stickstoff quantifiziert werden. Zusätzlich zu Ratenmessungen der Primärproduktion, der Nitrataufnahme und der  $\text{N}_2$  Fixierung wurden Nitratreinträge durch Ekman-auftrieb (für die Auftriebszone) und turbulente Diffusion (für die oligotrophe, küstenferne Zone) berechnet. Die Ergebnisse zeigen, dass die Auftriebszone vor Vietnam ähnlich produktiv sein kann wie andere Auftriebsgebiete der Welt, z.B. vor Nordwest Afrika oder vor der somalischen Küste im Arabischen Meer. Allerdings war der Auftrieb und damit die Produktivität im Juli 2003 ( $28 \pm 18 \text{ mmol C m}^{-2} \text{ d}^{-1}$ ) durch El Niño-Auswirkungen schwächer als im Juli 2004 ( $103 \pm 25 \text{ mmol C m}^{-2} \text{ d}^{-1}$ ). In der Auftriebszone war Nitrat eindeutig die wichtigste Quelle neuen Stickstoffs. Die Nitratreinträge durch Ekman-auftrieb von bis zu  $17 \pm 2 \text{ mmol N m}^{-2} \text{ d}^{-1}$  (Juli 2004) würden den gesamten Stickstoffbedarf der gemessenen Primärproduktion decken. Für die oligotrophen, küstenfernen Gewässer lagen die Nitratreinträge durch Diffusion um  $2.3 \pm 0.6 \text{ mmol N m}^{-2} \text{ d}^{-1}$ , basierend auf maximalen Diffusivitäten von  $1 \text{ cm}^2 \text{ s}^{-1}$  in der Nutrikline. In diesen Gewässern wurden auch die höchsten Raten der  $\text{N}_2$  Fixierung gemessen, allerdings lagen sie im Juli 2003 niedriger ( $22 - 119 \mu\text{mol N m}^{-2} \text{ d}^{-1}$ ) als im Juli 2004 ( $37 - 375 \mu\text{mol N m}^{-2} \text{ d}^{-1}$ ). Diese Raten sind vergleichbar zu 1 - 5% (Juli 2003) und 2 - 25% (Juli 2004) der diffusiven Nitratreinträge.  $\text{N}_2$  Fixierung konnte somit als weitere, signifikante Stickstoffquelle identifiziert werden.

Die höchsten  $\text{N}_2$  Fixierungsraten wurden auf Stationen in der Mekong- Flussfahne gemessen. Dieser Befund legt nahe, dass das Wachstum der planktischen, diazotrophen Mikroorganismen womöglich durch im Flusswasser enthaltene Nährstoffe oder Spurenmetalle gefördert wurde. Um dies zu überprüfen wurden während der Niedrigabflusszeit im April 2007 sowie während der Hauptabflusszeit im September 2008 weitere Feldstudien durchgeführt. Während beider Ausfahrten zeigte das molare Verhältnis von  $\text{NO}_3^- + \text{NO}_2^-$  zu  $\text{PO}_4^{3-}$  (N:P) in Wasserproben von der Oberfläche einen deutlichen Abfall mit steigender Salinität. Auf Stationen, auf denen das N:P Verhältnis niedriger als das Redfield- Verhältnis von 16:1 lag, wurden extreme hohe  $\text{N}_2$  Fixierungsraten gemessen. Im April 2007 wurden Raten von bis zu  $22.77 \text{ nmol N L}^{-1} \text{ h}^{-1}$  gemessen, und im September 2008 von bis zu  $5.05 \text{ nmol N L}^{-1} \text{ h}^{-1}$ . Diese

Raten zählen zu den höchsten je im Meer gemessenen Raten und würden bis zu 47% des Stickstoffbedarfs der in der Mekongfahne gemessenen Primärproduktion decken. Die niedrigen N:P verhältnisse lassen vermuten, dass die Diazotrophen durch fluviale  $\text{PO}_4^{3-}$ -Einträge profitierten. Gleichzeitig wurden in der Flussfahne hohe Konzentrationen an  $\text{Si}(\text{OH})_4$  gemessen. Die Kombination dieser Nährstoffe ist förderlich für das Wachstum von Symbiosen zwischen verschiedenen Diatomeenarten und *Richelia intracellularis*, einem diazotrophen Cyanobakterium (Diatom-Diazotroph Associations, DDAs). Tatsächlich zeigten die mikroskopischen Auswertungen hohe Abundanzen von Diatomeen wie *Rhizosolenia* spp., *Chaetoceros* spp., *Guinardia* spp., *Hemiaulius* spp., und *Bacteriastrum* spp, welche bekanntermaßen mit *Richelia intracellularis* assoziiert sein können. Die Verifizierung der Anwesenheit und Aktivität von DDAs gelang für April 2007 durch die Analyse der Verteilung und der Expression des funktionellen  $\text{N}_2$  Fixierungs- (Nitrogenase-) Gens *nifH* mittels quantitativer PCR. Dieser molekulare Ansatz enthüllte zusätzlich, dass *Trichodesmium* spp. ein weiterer wichtiger diazotropher Mikroorganismus in der Flussfahne des Mekongs war. *NifH* Genkopien und Transkripte von einzelligen Cyanobakterien (Gruppen B/C) sowie von  $\gamma$ - Proteobakterien wurden dagegen ausschließlich auf ozeanischen Stationen gefunden. Diese Befunde bestätigen, dass die Nährstoffgradienten in tropischen Flussfahnen eine Ungleichverteilung verschiedener mariner  $\text{N}_2$  Fixierer verursachen. Die Diversität des *nifH* Gens im Salinitätsgradienten wurde mit Hilfe eines nested PCR- Ansatzes untersucht. Repräsentative *nifH* Klone aus Klonbibliotheken wurden sequenziert und mit bestehenden *nifH* Datenbanken verglichen. Einige Sequenzen repräsentierten neue Linien heterotropher Proteobakterien sowie von Diazotrophen aus dem *nifH* Cluster III (dazu zählen anaerobe Sulfatreduzierer). Diese bisher uncharakterisierten Prokaryoten waren möglicherweise für die unerwartet hohe  $\text{N}_2$  Fixierung ( $1.13 \pm 1.04 \text{ nmol N L}^{-1} \text{ h}^{-1}$ ) verantwortlich, die in den Bereichen der Flussfahne mit niedrigsten Salinitäten und höchsten Nährstoffkonzentrationen gemessen wurde. Solche Mikroorganismen könnten in anoxischen Mikrozonen suspendierter Partikel vorhanden gewesen sein. Zusammenfassend lässt sich sagen, dass die Flussfahne des Mekong hohe  $\text{N}_2$  Fixierung im SCS fördert, dass sie eine diverse Gemeinschaft diazotropher Mikroorganismen beheimatet, und dass *Trichodesmium* spp. und DDAs die quantitativ bedeutendsten  $\text{N}_2$  Fixierer sind. Diese Arbeit liefert somit zusätzliche Beweise dafür, dass tropische Flussfahnen durch ihre Einträge von Phosphat und Eisen generell die  $\text{N}_2$  Fixierung im Meer fördern, und es kann vermutet werden, dass sie dadurch einen bedeutenden Anteil zur globalen marinen  $\text{N}_2$  Fixierung beitragen.

## 1. General Introduction

This PhD thesis is part of the bilateral Vietnamese-German project “Land-Ocean-Atmospheric Interactions in the Coastal Zone of Southern Vietnam” which ran between 2003 and 2009. The participating institutes were the Institute of Oceanography in Nha Trang, Vietnam, the Institute of Oceanology in Hai Phong, Vietnam, the Institute of Oceanography in Hamburg, the Institute of Biogeochemistry and Marine Chemistry in Hamburg, the Institute of Geosciences in Kiel, the Center for Tropical Marine Ecology in Bremen, and the Leibniz Institute for Baltic Sea Research in Warnemünde (IOW). Researchers from the IOW were involved in two consecutive sub-projects, entitled “Pelagic Processes and Biogeochemical Fluxes in the South China Sea”, (2003 - 2006), and “Pelagic processes and nitrogen cycle studies in coastal waters off southern central Vietnam: mesocosm experiments, field work and modeling” (2006 - 2009). Based on results from the first project phase, this thesis focused on a closer evaluation of primary production, nitrate assimilation and  $N_2$  fixation in the upwelling zone and the adjacent offshore zone, and discussed available rate measurements in the context with different nitrate supply pathways in the respective zones (chapter 2). Furthermore, the magnitude and the ecological significance of  $N_2$  fixation in the Mekong River plume was determined (chapter 3), and the diazotroph community was investigated by traditional microscopic as well as molecular methods (chapter 3 and 4). The following chapters of this introduction give a comprehensive description of oceanic new production and its biogeochemical significance, and summarize important aspects about the diversity and ecology of some known marine pelagic diazotrophs. Afterwards follows a description of the investigation area, which highlights why the South China Sea is an excellent site for studying new production and pelagic ecosystem dynamics. Lastly, the aims of the study are addressed.

### 1.1 Oceanic new production

Nearly half of the global net primary production, i.e. the binding of atmospheric  $CO_2$  into the biomass of photoautotrophic organisms, is maintained by phytoplankton dispersed in the world's oceans (Field et al. 1998). As these phytoplankters eventually sink out of the euphotic zone or are eaten and end up in fecal pellets, they transfer fixed carbon to the ocean interior. The fraction of the deep ocean dissolved carbon pool attributable to this flux amounts to approximately  $2500 * 10^{15}$  g C, which equals 3.5 times the atmospheric carbon pool (Gruber and Sarmiento 2002). Thus, the “biological carbon pump” is considered as one of the fundamental controls on the atmospheric levels of  $CO_2$  (Gruber and Sarmiento 2002; Falkowski et al. 2003).

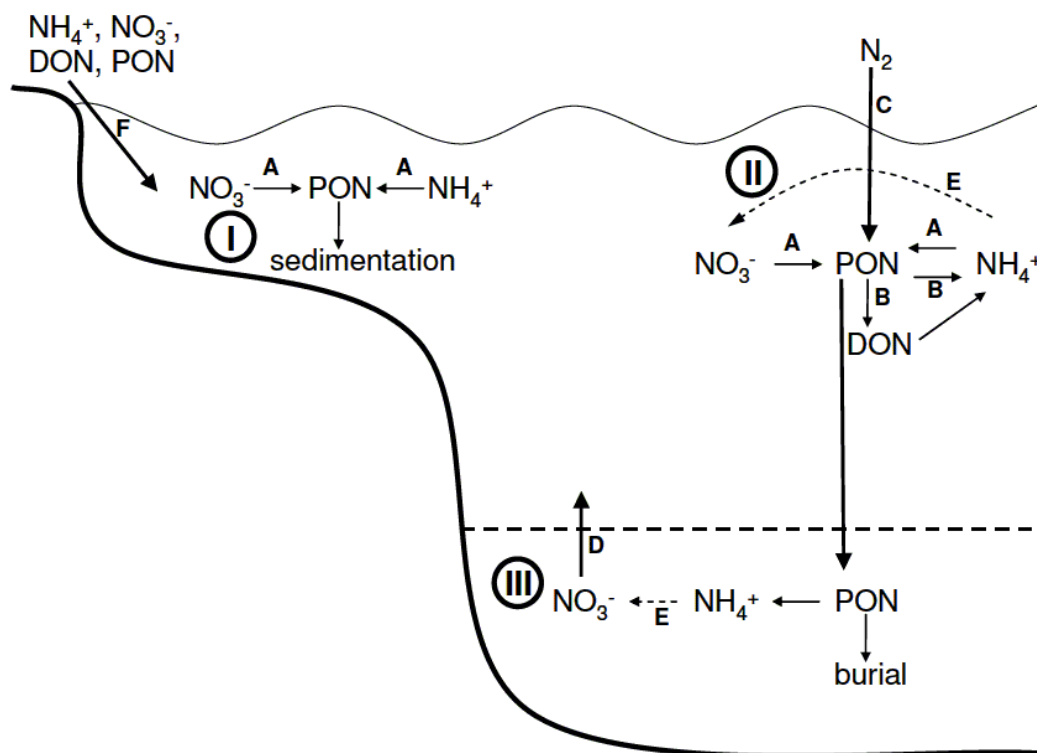


**Figure 1.1:** Conceptual diagram of major features of the nitrogen cycle in coastal shelf and upwelling ecosystems (I), surface waters of the open ocean (II), and deep water (III). PON, particulate organic nitrogen; DON, dissolved organic nitrogen. Dashed arrows indicate transformations involving multiple steps. The dashed line indicates the thermocline. Pathways: A, assimilation of dissolved inorganic nitrogen; B, ammonium regeneration; C,  $\text{N}_2$  fixation; D, nitrate diffusion/ upwelling from deep water; E, nitrification; F, continental inputs. Modified from Zehr and Ward (2002) and Sigman and Casciotti (2001).

In the largest parts of the oceans, phytoplankton productivity is primarily limited by the availability of nitrogen (Thomas 1966; Graziano et al. 1996, Davey et al. 2008), which is an essential component of cellular material including proteins and nucleic acids in all living cells. Therefore, nitrogen availability plays an important role in determining primary production in the oceans. About 94% of all nitrogen in the ocean is dissolved  $\text{N}_2$  (Gruber 2008), which is the most inert form of nitrogen and is therefore usually denoted as “biounavailable”. Apart from  $\text{N}_2$ , the oceanic pool of fixed nitrogen mainly consists of  $\text{NO}_3^-$  (about 88%), followed by dissolved organic nitrogen (DON), which makes up nearly all of the remaining 12% (Gruber 2008). The sum of the other nitrogen species including particulate organic nitrogen (PON),  $\text{NO}_2^-$ ,  $\text{NH}_4^+$ , and  $\text{N}_2\text{O}$  makes up less than 0.3% of the total fixed nitrogen pool (Gruber 2008). Below the thermocline, most organic nitrogen is remineralized to  $\text{NH}_4^+$  and subsequently nitrified to  $\text{NO}_3^-$  (Fig. 1.1). From there,  $\text{NO}_3^-$  can reach the upper ocean by upwelling or diffusion. In tropical and subtropical open seas which are not affected by upwelling, thermohaline stratification permanently separates the warm,  $\text{NO}_3^-$  - impoverished surface layer from colder,  $\text{NO}_3^-$  - rich deeper waters, and turbulent diffusion through the thermocline (diapycnal mixing) is the main process entraining  $\text{NO}_3^-$  into surface waters (Fig. 1.1).

In 1967, the conceptual model of “new” and “regenerated” production was introduced (Dugdale and Goering 1967). New production refers to primary production based on allochthonous N-sources, including  $\text{NO}_3^-$  influxes through upwelling and diffusion, N-inputs from rivers, and  $\text{N}_2$  fixation by marine prokaryotes (Fig. 1.1). In turn, regenerated production in the open ocean denotes carbon fixation sustained by autochthonous, recycled N-sources ( $\text{NH}_4^+$ , DON) provided by heterotrophic respiration and exudation within the euphotic zone. It was later proposed that over sufficiently long spatial and temporal scales, carbon export to the deep ocean is quantitatively equivalent to the fraction of total production that is supported by  $\text{NO}_3^-$  (Eppley and Peterson 1979). In other words, phytoplankton nitrogen metabolism was coupled to the cycling and export of carbon. Studying oceanic new production thereby promised to be a straightforward way to understand the efficiency of the biological carbon pump, and thus new production became a major focus of biogeochemical research (Ducklow et al. 2001). Eppley and Peterson (1979) also showed that total primary production seemed to be quantitatively related to new production, and this prompted hope that total primary production rates estimated from satellite-derived chlorophyll concentrations could be used to quantify export production on a global scale (Ducklow et al. 2001).  $\text{N}_2$  fixation, although explicitly mentioned by Dugdale and Goering (1967) as an additional source of new nitrogen, was initially neglected in the majority of field studies after 1969, and it took much longer until its impact was revealed (see below).

Overall, marine primary- and new production and especially the variability and interaction of these processes remain poorly constrained. Due to the limited scope of shipboard measurements, the use of ocean color satellite sensors has proven useful for studying the dynamics and spatial differences in oceanic primary production, and to model basin-scale and global estimates (Longhurst 1995; Behrenfeld and Falkowski 1997). Others have then used satellite-derived primary production to model global new (= export) production (Laws et al. 2000). However, it must be noted that such primary production estimates can vary twofold between different models, and are especially unreliable for areas having extreme concentrations of chlorophyll, suspended particles, and colored dissolved organic matter, such as the coastal ocean (Carr et al. 2006). Oceanic new- and export production have been studied in more detail using various approaches, including  $^{15}\text{NO}_3^-$  tracer incubations, particle flux estimates using sediment traps and measurements of radionuclide thorium-234, and geochemical balance estimates based on temporal changes in nutrient and oxygen stocks (see Ducklow et al. 2001 and Falkowski et al. 2003 for a review). Besides providing many important insights to upper ocean biogeochemistry, these intensive observations showed that the relationship between total production, new- and export

production is far more complex than initially assumed. For example, primary production measured in the subtropical North Pacific during the Hawaii Ocean Time-series (HOT) observations is poorly or even negatively correlated with sediment trap fluxes (Karl et al. 1996, 2001). The model by Laws et al. (2000) showed that the ratio of new (= export) production to primary production is mainly controlled by temperature, and it also explained the decoupling of primary production and export found at the HOT station. However, an assumption of that model is that new production is balanced by export production, as formulated in the initial paper by Eppley and Peterson (1979), but this may not be the case on shorter timescales. Additionally, more recent modeling studies showed that in highly dynamic areas such as coastal upwellings, there can be a substantial spatial decoupling of new- and export production, due to horizontal fluxes induced by Ekman offshore transport and meso- and submesoscale circulation structures (Plattner et al. 2005). More “fundamental” challenges to the new production concept arose from studies on the nitrogen metabolism of oceanic phytoplankton and bacteria. It was shown that nitrification can occur within the euphotic zone (Fig. 1.1), which contrasts earlier beliefs that this process is inhibited in the light, and which confounds the concept that  $\text{NO}_3^-$  is solely an allochthonous nitrogen source. (Dore and Karl 1996). Yool et al. (2007) assessed that nitrification within the euphotic zone could be quantitatively significant enough to mark earlier assessments of new production as severe overestimates. On the other hand, Bronk et al. (1994) showed that failure to correct for DON release by phytoplankton during  $^{15}\text{NO}_3^-$  incubations may result in substantial underestimation of new production rates.

An additional, alternative approach to study oceanic new production is to quantify the  $\text{NO}_3^-$  supply to surface waters by physical transport mechanisms. The underlying concept is that there must be a balance between vertical  $\text{NO}_3^-$  supply and biological consumption and export, irrespective of how this  $\text{NO}_3^-$  is cycled within the food web. Therefore, a precise quantification of  $\text{NO}_3^-$  - fluxes would also represent a rate of new production and would help to understand how much primary- and export production can be maintained in different areas of the ocean (Chavez and Toggweiler 1995). Reported estimates of diffusive  $\text{NO}_3^-$  fluxes in tropical and subtropical open seas vary by an order of magnitude ( $0.14 - 4.1 \text{ mmol N m}^{-2} \text{ d}^{-1}$ , see e.g. Lewis et al. 1986; Jenkins 1988; Zhang et al. 2001), partly reflecting latitudinal differences between sampling sites, but possibly also the fact that different methods of measuring diffusion coefficients integrate over varying time- and space scales (Oschlies 2002). In spite of these uncertainties, these methods have helped to confirm a general characteristic of the most oligotrophic areas, i.e. that regenerated production by far dominates over  $\text{NO}_3^-$  - based new production, and that rates of primary production are typically among the lowest

rates found in the ocean (Neuer et al. 2002). Nevertheless, due to the vast expansion of these areas (covering nearly 75% of the global ocean surface), they account for at least 80% of total oceanic primary production, and for a large share of new production as well (Longhurst et al. 1995; Laws et al. 2000). In contrast, the coastal ocean covers less than 20% of the global ocean, but a significant proportion of the global primary- and new production occurs there, due to high  $\text{NO}_3^-$  - based production resulting from wind driven coastal upwelling as well as runoff from land and river discharge (Walsh 1991, Chavez and Toggweiler 1995; Gruber 2008; Beman et al. 2005). According to Chavez and Toggweiler (1995), new production occurring in coastal upwelling areas alone might account for 11% of global new production. For the upwelling area off Vietnam, South China Sea, there are so far only satellite-derived primary production estimates available, and new production has never been studied *in situ* before. Therefore, one aim of this thesis was to quantify primary production and  $\text{NO}_3^-$  assimilation of that region based on *in situ* rate measurements, and to additionally determine vertical  $\text{NO}_3^-$  - fluxes by Ekman upwelling (upwelling affected zone) and turbulent diffusion (offshore waters), in order to compare these supply pathways and to evaluate the relative importance of  $\text{NO}_3^-$  in fueling primary production (chapter 2).

The recognition that  $\text{N}_2$  fixation is a key component of the marine nitrogen cycle successively emerged from several independent lines of evidence.  $\text{N}_2$  fixing organisms were initially believed to be scarce in the marine pelagial, but microbiologists continued to discover various diazotrophs in the field, including heterocystous and non-heterocystous cyanobacteria, diverse representatives of the proteobacteria, archaea, and other prokaryotes (Carpenter and Capone 2009) (see chapter 1.2 for details). The traditional assumption that pelagic  $\text{N}_2$  fixation is a minor source of nitrogen was also drawn into doubt as studies proposed a higher nitrogen demand of primary production than could be accounted for by vertical  $\text{NO}_3^-$  fluxes alone (Michaels et al. 1994; Montoya et al. 2002; Lee et al. 2002). Since convenient methods to measure rates of  $\text{N}_2$  fixation (i.e. the  $\text{C}_2\text{H}_2$  reduction method, Stewart et al. 1967, and the  $^{15}\text{N}_2$  tracer uptake method, Montoya et al. 1996), were available and applied in various field campaigns, the accumulating data showed that  $\text{N}_2$  fixation is readily detectable and significant throughout the tropical and subtropical seas (see e.g. review by Karl et al. 2002). Besides direct rate measurements,  $\text{N}_2$  fixation has also been quantified by indirect biogeochemical methods, since a decrease in  $\delta^{15}\text{N}$  values of particulate organic nitrogen (Montoya et al. 2002; Capone et al. 2005) as well as non-Redfield elevated ratios of  $\text{NO}_3^-$  to  $\text{PO}_4^{3-}$  produced from regenerated particulate material (“ $\text{N}^*$ ” -approach, Gruber and Sarmiento 1997; Hansell et al. 2004) are indicative of  $\text{N}_2$  fixation. A compilation of the most recent global estimates of pelagic  $\text{N}_2$  fixation is given as  $120 \pm 50 * 10^{12}$  g N year<sup>-1</sup>, which exceeds total riverine nitrogen fluxes to

the ocean ( $\sim 80 * 10^{12}$  g N year<sup>-1</sup>) as well as atmospheric depositions ( $50 \pm 20 * 10^{12}$  g N year<sup>-1</sup>) (Gruber 2008). Thus, it is acknowledged nowadays that pelagic N<sub>2</sub> fixation is the largest external source of fixed nitrogen to the ocean.

In tropical oligotrophic seas, N<sub>2</sub> fixation as a source of new nitrogen can be comparable or even higher than diffusive vertical NO<sub>3</sub><sup>-</sup> fluxes (Capone et al. 2005). This has implications for carbon cycling, since N<sub>2</sub> fixation can support a net flux of CO<sub>2</sub> from the atmosphere to the ocean, whereas upward NO<sub>3</sub><sup>-</sup> fluxes are accompanied by respired CO<sub>2</sub> in approximate Redfieldian proportions, therefore yielding no net CO<sub>2</sub> drawdown (Eppley and Peterson 1979; Michaels et al. 2001). A striking feature of all of the latest estimates of global N<sub>2</sub> fixation is that they fall well below the global estimate of  $\sim 400 * 10^{12}$  g N year<sup>-1</sup> of loss of oceanic nitrogen as N<sub>2</sub> to the atmosphere by denitrification and the anammox reaction (Codispoti et al. 2007). The fixed nitrogen content of the oceans is mainly determined by these opposing pathways, and in the long term, they are assumed to be tightly coupled by negative feedback mechanisms so that the marine nitrogen cycle remains balanced (Gruber 2008). However, others have proposed that N<sub>2</sub> fixation and denitrification can be decoupled enough to cause changes in the pool size of oceanic nitrogen, which in turn would alter marine productivity and consequently the partitioning of CO<sub>2</sub> between the ocean and the atmosphere (Altabet 1995; Falkowski 1997). For example, Altabet et al. (1995) investigated sediment cores from the Arabian Sea and observed intriguing links between decreases of oceanic denitrification (indicative of an increase in the oceanic nitrogen pool) and glacial maxima (presumably due to a large flux of atmospheric CO<sub>2</sub> to the deep ocean via enhanced export production based on higher nitrogen availability).

So far, however, most evidence suggests that the discrepancy between recent estimates of N<sub>2</sub> fixation and denitrification/anammox is simply due to the fact that N<sub>2</sub> fixation is still underestimated. For example, in the tropical North Atlantic, the areal integration of N<sub>2</sub> fixation by the best-studied cyanobacterium *Trichodesmium* accounts for only 40-59% of the geochemically inferred N<sub>2</sub> fixation (Capone et al. 2005; Mahaffey et al. 2005). While this alone is a very significant fraction, it remains largely unknown to which extent other pelagic diazotroph species contribute to overall N<sub>2</sub> fixation (see chapter 1.2). Further, some recent findings suggest that the mentioned estimates of global N<sub>2</sub> fixation must be incomplete, since they do not include N<sub>2</sub> fixation in previously unconsidered marine environments. Dekas et al. (2009) discovered that deep-sea archaea fix N<sub>2</sub> at low rates, but since these organisms occur throughout continental margin sediments and at cold seeps, they could be quantitatively important. A study in the temperate oligotrophic Pacific Ocean reported low but significant N<sub>2</sub> fixation rates by unicellular diazotrophs in waters with temperatures below 20-25°C, whereby

so far, N<sub>2</sub> fixation budgets only extrapolate measured rates to waters having seasonally averaged temperatures greater than or equal to 25°C (Needoba et al. 2007). It is also questionable whether the geochemical approaches to quantify N<sub>2</sub> fixation capture all diazotroph inputs that occur within the water column. For instance, Scharek et al. (1999b) showed that intact cells of diatoms hosting diazotroph symbionts (Diazotroph-Diatom-Associations, DDAs) can be detected in sediment traps at 4000m depth following bloom events. If such rapid settling rates were to be a general characteristic for the widespread DDAs, their whole contribution to N<sub>2</sub> fixation would possibly not be represented by the quantification approaches using N:P regeneration stoichiometry, since the DDA cells would be remineralized much deeper compared to the depth horizons for which e.g. N\* values are typically used to calculate rates (maximal between 70m and 700m; Gruber and Sarmiento 1997). The most important lesson from all of these recent discoveries is clearly that the dynamics of the oceanic nitrogen cycle cannot be revealed without assessing the full diversity of marine diazotrophs, and without a better understanding of the distribution and ecology of the different species. The next chapter introduces the diversity of some currently known and quantitatively important pelagic diazotrophs and highlights the molecular methodological advances that have helped in identifying new diazotroph species and in studying how their distribution in the ocean is controlled by environmental factors.

## 1.2 Diversity and ecology of pelagic diazotroph prokaryotes in the tropical and subtropical ocean

Early studies on N<sub>2</sub> fixation in the open ocean mainly focused on the photosynthetic, filamentous, non-heterocystous cyanobacterium *Trichodesmium*, which exclusively occurs in surface waters with temperatures >20°C (LaRoche and Breitbarth 2005). Colonies of this species are visible to the naked eye and can occur as dense surface blooms that extend for up to thousands of kilometres in tropical oceans (Capone et al. 1997). As mentioned above, *Trichodesmium* alone accounts for substantial inputs of new nitrogen (Capone et al. 1997, 2005).

Diatoms hosting diazotroph symbionts have also been identified as widespread and quantitatively important in N<sub>2</sub> fixation. The diatom hosts come from various genera. *Hemiaulus*, *Rhizosolenia*, *Guinardia* and *Bacteriastrum* associate with the heterocystous, photoautotroph cyanobacterium *Richelia intracellularis*, while diatoms of the genus *Chaetoceros* are typically found in symbiosis with *Calothrix rhizosoleniae*, another diazotroph cyanobacterium which is closely related to *Richelia* (Carpenter 2002; Foster and Zehr 2006). The trichomes of *Richelia intracellularis* reside as an endosymbiont between the plasmalemma and the frustule of the diatom in *Hemiaulus*, *Rhizosolenia* and *Guinardia* (Villareal 1992). In the DDAs *Bacteriastrum*-

*Richelia intracellularis* and *Chaetoceros-Calothrix rhizosoleniae*, the symbiont resides as an epiphyte on the spines of the diatom (Carpenter 2002; Foster and O'Mullan 2008). A less well-studied symbiosis exists between the chain-forming pennate diatom, *Climacodium frauenfeldianum*, and a unicellular cyanobacterium which is similar in morphology to *Crocospaera watsonii* (R. A. Foster, pers. Comm.).

The mutual benefits for host and diazotroph in such symbioses have long been assumptive. Some of the early observations in the oligotrophic North Pacific central gyre showed highest abundances of *Rhizosolenia-Richelia* during the late summer months when nutrient concentrations in the upper water column were near the detection limit, suggesting that *Richelia* fixed and shared nitrogen with the diatom hosts to cover their demand for nitrogen (Venrick 1974). High rates of  $N_2$  fixation (measured by  $C_2H_2$  reduction) were detected in such blooms (Mague et al. 1974), and based on a strong concordance between the abundances of DDAs and other major diatom species, it was speculated that DDAs even released dissolved inorganic nitrogen and thereby sustained the growth of the whole phytoplankton assemblage (Venrick 1974). Later, batch culture experiments showed that the percentage of symbiotic *Rhizosolenia* increased from 5% to 65% within 12 days in N-deplete medium, while asymbiotic *Rhizosolenia* cells were only able to grow in N-replete medium, further proving the dependence of the diatom hosts on the diazotrophy of *Richelia* (Villareal 1990). In the western Pacific Ocean, Gomez et al. (2005) observed *Calothrix* associated with *Chaetoceros* diatoms which lacked chloroplasts, possibly indicating that *Calothrix* also transferred fixed carbon to their hosts (Gomez et al. 2005; Foster and O'Mullan 2008). Recently, Foster et al. (unpubl.) used high-resolution nanometer scale secondary ion mass spectrometry (nanoSIMS) to analyze samples of *Rhizosolenia-Richelia*, *Hemiaulus-Richelia*, and *Chaetoceros-Calothrix* recovered from  $^{15}N_2$  incubation experiments. The results convincingly show that 1) nitrogen was fixed by the symbiont and transferred to the host, 2) the host growth was largely supported by the symbiont, and 3) that carbon was fixed by both symbionts and hosts (R. A. Foster, pers. comm.). Thus, the diazotrophy of such symbionts has obviously enabled a variety of diatom host species to colonize the surface waters of the open oligotrophic ocean, in contrast to asymbiotic diatoms which generally dominate phytoplankton communities only where silicate and other nutrients are non-limiting (Kudela 2008; Foster and O'Mullan 2008). The diazotroph symbionts, in turn, are thought to benefit from the positive buoyancy of the diatoms by which they remain positioned in the euphotic zone (Carpenter 2002), while direct evidence for transfer of metabolites from host to symbiont is lacking so far.

Although *Trichodesmium* and DDAs were recognized early as important members of the pelagic diazotroph community, it seemed unlikely that they alone could be responsible for the

overall  $N_2$  fixation in the oceanic environment where N-limitation should clearly select for species with this physiological ability. And indeed, previously unrecognized unicellular cyanobacteria, proteobacteria, clostridia, sulphate reducers and archaea were discovered in later studies (Zehr et al. 1998). Abundance estimates and *in situ* measurements of  $N_2$  fixation rates showed that unicellular cyanobacterial diazotrophs are likely to make a substantial contribution to new production globally (Montoya et al. 2004; Church et al. 2005a). Non-cyanobacterial, heterotrophic diazotrophs which presumably lack a light-dependent metabolism typically dominate diazotroph assemblages below 200m depth, and can be found down to 2600m in the bathypelagial (Mehta et al. 2005; Farnelid and Riemann 2008; Moisander et al. 2008). Heterotrophic diazotrophs have received least attention so far, but their as yet known diversity and distribution suggests that they are quantitatively important  $N_2$  fixers as well (Farnelid and Riemann 2008).

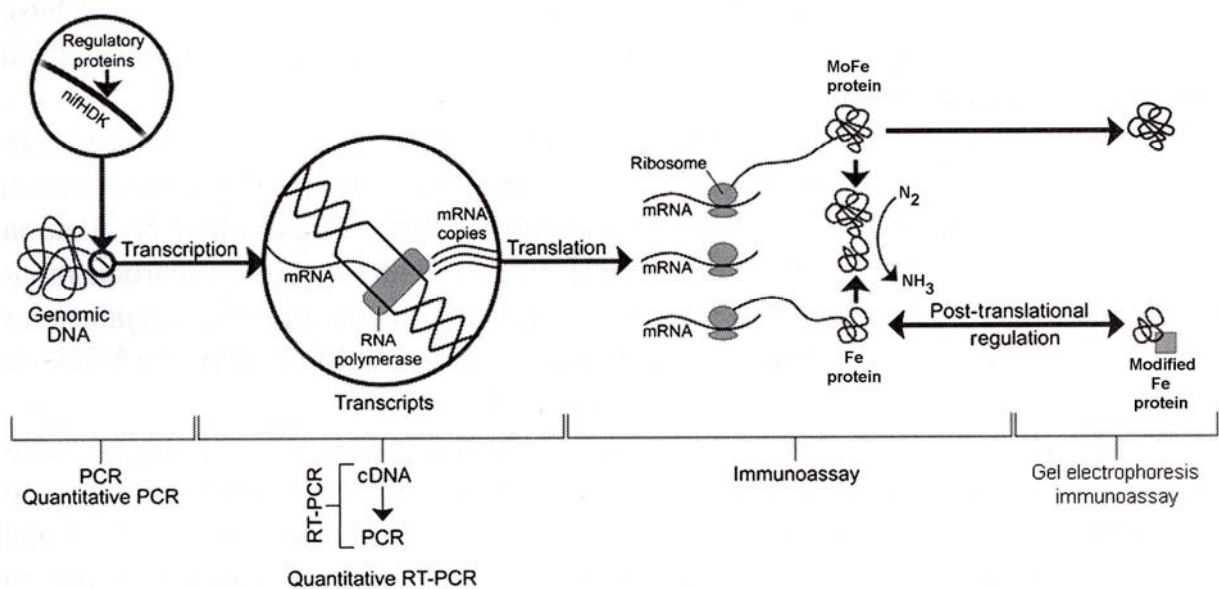


**Figure 1.2:** Scheme of the regulation of  $N_2$  fixation at transcriptional, translational and post-translational levels. Molecular genetic, immunological and proteomic methods can be used to study these different levels of regulation. Many ecological studies have used genetic methods targeting the *nifH* gene itself. PCR can be used to obtain information about phylogeny. Quantitative PCR (QPCR) quantifies *nifH* gene copies (which often approximately equals cell abundances). Reverse-transcription (RT) QPCR quantifies mRNA copies, which indicates diazotroph activity of a phylotype. Taken from Zehr and Paerl (2008).

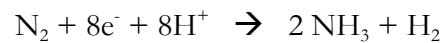
All of these important discoveries were the result of studies that aimed to analyze the full diversity of microorganisms with the potential for  $N_2$  fixation by characterizing the diversity of the *nifH* gene sequence in ocean waters. The structural *nifH* gene encodes for an iron-containing subunit of the nitrogenase enzyme, which is found in all diazotroph species (Fig. 1.2). Certain regions of the *nifH* gene sequence are highly conserved across different phylogenetic groups (i.e. they share a high degree of similarity), and can therefore serve as universal priming sites using “degenerate” primers in polymerase chain reaction (PCR) (Zehr and McReynolds 1989; Zehr and Turner 2001). These degenerate primers are a mixture of all

possible codon sequences that could encode the conserved amino acid sequence, so that the phylogenetic variety of known and unknown *nifH* genes can be captured during PCR (Zehr and Capone 1996). The amplified *nifH* sequences also contain less conserved regions, which can be used to distinguish between different taxonomic groups, and it was shown that *nifH* phylogeny is roughly consistent with the phylogeny based on 16S ribosomal DNA (Kirshtein et al. 1991; Zehr et al. 2003). The identification of previously unknown unicellular diazotroph species was possible through PCR amplification of the *nifH*-region from environmental DNA, and subsequent cloning and sequencing (Zehr et al. 1998). In later studies, the isolation and analysis of *nifH*-messenger-RNA from environmental samples showed that unicellular cyanobacteria and proteobacteria do also express (transcribe) the *nifH* gene (Zehr et al. 2001). Ultimately, the application of quantitative polymerase chain reaction assays (QPCR/RT-QPCR) was used to estimate abundances and patterns of gene expression of different *nifH*-containing organisms (Short and Zehr 2005) (see chapter 4 for method details). As indicated in Figure 1.2, gene transcription is followed by translation into the enzyme protein, and post-translational modifications of the protein also occur. This shows that the expression of a gene is not necessarily directly related to the rate of enzymatic activity. However, it is known that *nifH* expression is tightly regulated by environmental factors, resulting e.g. in a circadian rhythm of *nifH* expression and rates of N<sub>2</sub> fixation in *Trichodesmium* spp. (Chen et al. 1998). Thus, analyses of *nifH* expression are a useful approach to identify microorganisms that are active N<sub>2</sub> fixers, and to determine regulatory environmental factors of N<sub>2</sub> fixation.

While rate measurements of N<sub>2</sub> fixation can quantify diazotroph inputs at the time point of investigation (if they occur), molecular methods give additional information about the presence or absence of different diazotroph phylotypes, and can be used to understand how environmental factors regulate N<sub>2</sub> fixation on the gene level. For example, Langlois et al. (2005) showed that *nifH* sequences of unicellular cyanobacteria in the tropical northern Atlantic are closely related to *nifH* sequences from the Pacific Ocean, and in contrast to *Trichodesmium*, these sequences were also found deeper in the water column at lower temperatures and at detectable NO<sub>3</sub><sup>-</sup> concentrations. Analyses of *nifH* gene expression by RT-QPCR revealed the differing diurnal periodicity in N<sub>2</sub> fixation of cyanobacteria and proteobacteria in the environment, and showed that active N<sub>2</sub> fixation by proteobacteria occurs below the nutricline (Church et al. 2005b). In experimental incubations containing natural populations of diazotrophs collected in the Pacific Ocean, it was shown that phosphorus additions did not change abundances and *nifH* expression of different diazotrophs within 36h, indicating that diazotrophy must be constrained by other factors in this system (Zehr et al. 2007). Thus, by using these molecular approaches, it is possible to follow distinct

physiological responses of diazotrophs to changes in environmental conditions, and this information helps to better understand and predict how N<sub>2</sub> fixation is controlled on an ecosystem level.

By taking a closer look at the structural and biochemical characteristics of the nitrogenase enzyme system, it becomes obvious which environmental factors must directly regulate the activity of oceanic diazotrophs. The complete functional nitrogenase enzyme consists of two main proteins, termed dinitrogenase (component I, a MoFe protein encoded by *nifD* and *nifK* genes) and dinitrogenase-reductase (component II, an Fe-protein, encoded by *nifH*) (Fig. 1.2). As shown in Fig. 1.2, ammonia (NH<sub>3</sub>) is the primary product of N<sub>2</sub> fixation, obtained in the reaction



whereby the eight electrons come from reduced ferredoxin, which in turn is either produced in chloroplasts by photosystem I in phototrophs, or alternatively by oxidative processes in heterotrophic microorganisms. N<sub>2</sub> fixation is thus energetically costly, so it strongly depends on energy sources (light in phototrophs, or metabolic substrates in heterotrophs) (Carpenter and Capone 2008). The high energy demand of N<sub>2</sub> fixation is generally believed to cause diazotrophs to switch to the uptake of combined nitrogen species (NO<sub>3</sub><sup>-</sup>, NH<sub>4</sub><sup>+</sup>, DON) once they become available. This has mostly been tested in studies with the model organism *Trichodesmium*, and nitrogenase inhibition seems to only occur under micromolar N concentrations (Mulholland et al. 2001; Holl and Montoya 2005). The N<sub>2</sub> fixation reaction is a reductive process, causing nitrogenase activity to be very sensitive to oxygen inhibition. As a result, different species have evolved structural and physiological adaptations in order to maintain diazotroph activity, including the development of heterocysts (which are mainly found in freshwater and brackish species, except for the mentioned *Richelia*), diel rhythms to temporally separate photosynthesis from N<sub>2</sub> fixation (e.g. in unicellular *Crocosphaera*), or even the complete abdication of O<sub>2</sub>-producing photosystem II in *Cyanothece*-like unicellular cyanobacteria (Fay 1992; Zehr et al. 2008). Due to the high iron content of the catalytic centre of nitrogenase, diazotrophs have an approximately 10-fold greater iron requirement than other phytoplankton (Berman-Frank et al. 2001; Kustka et al. 2003). Consequently, several studies have found elevated N<sub>2</sub> fixation in areas receiving substantial wet and dry deposition of iron (Mahaffey et al. 2003; Johnson et al. 2003; Mills et al. 2004). Phosphorus is not directly involved in the N<sub>2</sub> fixation reaction, but is an essential nutrient for growth. Phosphorus only reaches the ocean by continental weathering and river discharge, and is thus an important

limiting factor for diazotrophs in the open ocean (Sanudo-Wilhelmy et al. 2001; Mills et al. 2004). Denitrification and anammox in the oxygen minimum zones of the oceans generate water masses with low nitrogen- but high phosphorus concentrations, which can then fuel N<sub>2</sub> fixation on large spatial scales once they reach the overlying euphotic zone. A recent modeling study suggests that these mechanisms might control N<sub>2</sub> fixation on a global scale (Deutsch et al. 2007). The DDAs are exceptional among diazotrophs, since the diatom hosts have an absolute requirement for silicon. This is likely part of the explanation for why some of the highest abundances of DDAs and their *nifH* genes have been found in areas where tropical rivers supply nutrients (Si, Fe, P) to the adjacent oligotrophic sea, e.g. in the Amazon- or the Congo River plume (Carpenter et al. 1999; Foster et al. 2007; Subramaniam et al. 2008; Foster et al. 2008).

Thus, a complex interplay between physical, chemical, and biotic factors governs the unequal distribution of different oceanic diazotrophs. For the tropical North Atlantic Ocean, there is evidence for a basin-scale difference in the importance of large diazotrophs such as *Trichodesmium* and DDAs, which dominate in the western part, and unicellular diazotrophs, which dominate east of 40° W (Montoya et al. 2007). This large scale “niche partitioning” between diazotroph groups likely reflects different selective pressures acting on diazotrophs in the form of river discharge, which heavily affects the western Atlantic (Subramaniam et al. 2008), and upwelling and dust depositions of iron and phosphorus, which primarily influence large parts of the eastern Atlantic (Mills et al. 2004; Montoya et al. 2007). Given that the fate of recently fixed nitrogen largely depends on the diazotroph species (Mulholland 2007), the assessment of these variable distributions is important for understanding the impact of diazotrophy on oceanic biogeochemistry. For example, *Trichodesmium* has few known grazers, is positively buoyant, and is rarely found in sediment traps, and consequently fixed nitrogen and carbon are primarily recycled within the surface ocean after exudation or cell lysis (O’Neil and Roman 1992; Mulholland 2007; Hewson et al. 2004). Unicellular cyanobacteria are assumed to be more rapidly consumed by protists, but thereby also rather fuel the microbial food web within the euphotic zone (Caron et al. 1991). As mentioned above, the DDAs have high sinking rates; therefore they transfer fixed nitrogen to the deep sea and also efficiently contribute to the sequestration of atmospheric carbon (Scharek et al. 1999a,b; Subramaniam et al. 2008). Considering this, the elevated DDA abundances and rates of N<sub>2</sub> fixation in tropical river plumes are especially important examples for niche-partitioning (Fig. 1.3). In the Amazon River plume, large blooms of *Hemiaulus-Richelia* symbioses coincided with some of the highest rates of N<sub>2</sub> fixation ever measured in the marine pelagial; the rates exceeded vertical diffusive NO<sub>3</sub><sup>-</sup> fluxes, and up to  $0,45 * 10^{12}$  g N were fixed in one DDA-bloom that covered

approximately  $10^6$  km<sup>2</sup> and lasted for 10 days (Carpenter et al. 1999). Compared to stations within the adjacent oligotrophic Atlantic, a more than twofold higher biological carbon drawdown and a nearly fourfold higher mass flux to sediment traps resulted from these blooms (Subramaniam et al. 2008).

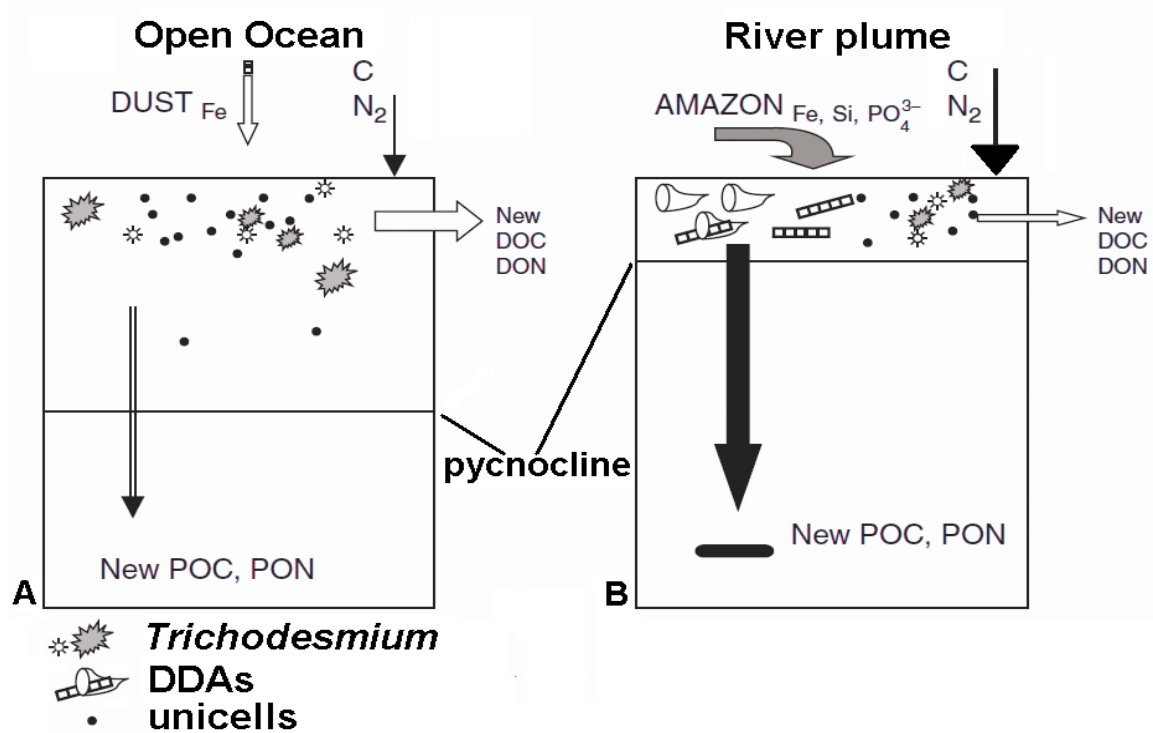


**Figure 1.3:** Conceptual model for different fates of filamentous cyanobacterial diazotrophs and unicells in the open ocean (A) compared to DDA blooms in River plumes (B). DOC/DON: dissolved organic carbon/nitrogen; POC/PON: particulate organic carbon/nitrogen. Modified from Carpenter and Capone (2008).

Tropical rivers generally carry high phosphorus-, iron- and silica loads (Nitterouer et al. 1995; Conley 1997). It was therefore assumed that high N<sub>2</sub> fixation, in particular by DDAs, could be a general phenomenon, but few other studies focussing on diazotrophy have been conducted in river plume systems. Five of the ten largest rivers of the world by discharge lie in tropical latitudes (Perry et al. 1996), suggesting that if their plumes are “hot spots” of N<sub>2</sub> fixation, their influence on overall oceanic N<sub>2</sub> fixation could be substantial. The Mekong River is the 10<sup>th</sup> largest river in the world by discharge (Perry et al. 1996), and our results from investigations in the SCS off southern central Vietnam showed a link between the Mekong River plume and elevated rates of N<sub>2</sub> fixation (Voss et al. 2006). Therefore, as part of this thesis, the influence of the Mekong River on phytoplankton species distribution and N<sub>2</sub> fixation was studied in more detail. Methods included *in situ* rate measurements of N<sub>2</sub> fixation, analyses of phytoplankton distributions, analyses of the distribution and expression of *nifH*, and an assessment of *nifH*-diversity (see chapters 3 and 4).

### 1.3 The South China Sea and the upwelling area off Vietnam

The SCS is a marginal sea of the tropical North Pacific Ocean and is one of the largest marginal seas on earth. With an area of approximately  $3.5 * 10^6 \text{ km}^2$  it extends between the equator and  $23^\circ\text{N}$ , and between  $99^\circ\text{E}$  and  $121^\circ\text{E}$  (Fig. 1.4A). A deep central basin (maximal depth 5000m) accounts for almost half of the surface area, while shallow shelf areas are found in the gulf of Thailand and the gulf of Tonkin. The southwest (SW) monsoon between June and September and the northeast (NE) monsoon between November and March strongly affect the surface circulation and the biogeochemistry in the SCS. Higher average wind speeds (9m/s) during NE monsoon result in an overall cyclonic circulation pattern within the basin, and inherently currents flow southward along the Vietnamese coast and suppress upwelling (Hu et al. 2000; Isobe and Namba 2001; Fang et al. 2002) (Fig. 1.4B, D). In contrast, during SW monsoon (average of 6m/s) the wind forcing is spatially inhomogeneous and forms an anticyclonic circulation cell in the southern SCS, but a cyclonic cell in the northern SCS in the atmosphere and ocean (Fig. 1.4C). These two gyres meet at approximately  $12^\circ\text{N}$  off the Vietnamese coast and form a stretching deformation resulting in upwelling and an offshore current (Dippner et al. 2007). Further, the vertical movement of water masses off the Vietnamese coast is driven by Ekman upwelling and the related “dynamical” upwelling, i.e. the clockwise-rotating poleward undercurrent (Dippner et al. 2007). The SW monsoon also brings intense rainfall to Indochina, producing large pulses of riverine flow into the SCS via the Mekong River, which discharges 85% of its annual total outflow (about  $500 \text{ km}^3$ ) during this season (Hoa et al. 2007). During the NE monsoon, the Mekong River plume flows near shore in south-westerly direction, whereas in summer, it gets advected towards the northeast due to the SW monsoon and the anticyclonic gyre in the southern SCS (Hu et al. 2000) (Fig. 1.4D, E). As a result, during SW monsoon the SCS off southern central Vietnam concurrently receives nutrient inputs via coastal upwelling and river runoff.

Single upwelling events off Vietnam last between 2 and 9 days and bring nutrient rich water from approximately 125m depth towards the surface (Hu et al. 2001; Dippner et al. 2007). It was noted that N:P ratios of the upwelled nutrients are lower than the Redfield ratio of 16:1 and thus potentially favor diazotroph growth further offshore (Voss et al. 2006). During post El Niño years, the SW monsoon is weaker and consequently only subsurface layers are fertilized by upwelled nutrients (Chao et al. 1996; Dippner et al. 2007). According to the biogeochemical model by Liu et al. (2002), the upwelling area off Vietnam is the most productive region of the SCS, accounting for approximately 12% of the basin-wide annual primary production.

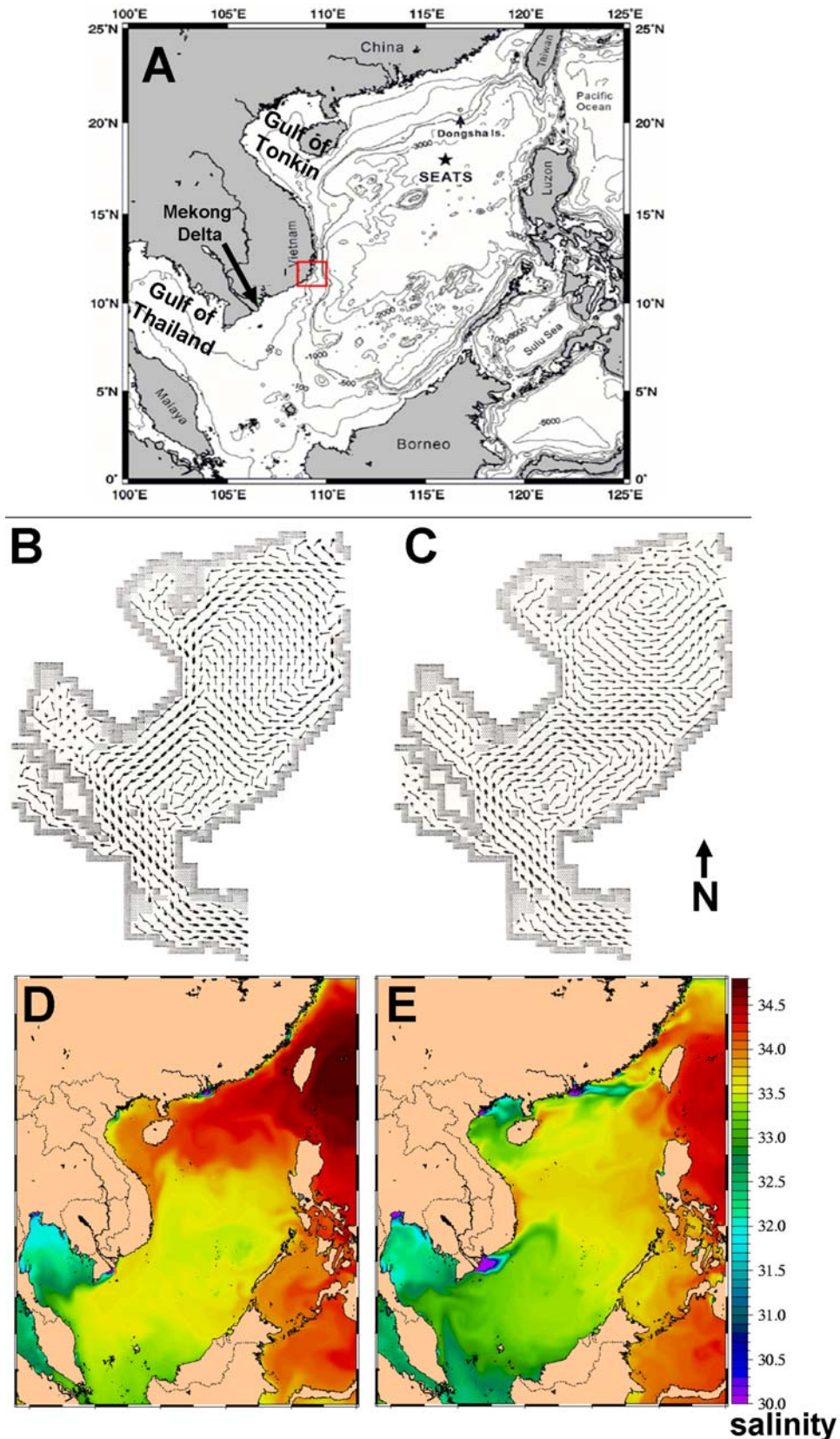


**Figure 1.4:** A) Map of the South China Sea with isobaths (in meters). The red square marks the position of the investigation area within the Vietnamese upwelling area. The asterisk indicates the position of the South East Asian Time Series station (SEATS). Redrawn from Chou et al. 2006. B) Model output of mean winter – and C) mean summer baroclinic circulation (after Pohlmann 1987). D) and E) show a snapshot of modeled horizontal distributions of surface salinity in March and July, respectively (<http://www7320.nrlssc.navy.mil/>). In E), note that a river-influenced water mass flows towards the northeast where concurrently upwelling of deep water occurs off the Vietnamese coast (indicated here by the slightly elevated salinities).

The impact of Mekong runoff on the biogeochemistry in the SCS has rarely been described in the literature. Reliable data on concentrations of dissolved nutrients in the Mekong River are sparse, with little information on seasonality. Measurements at the monitoring station My Tho in the lower Mekong basin show that the river water contains concentrations of over  $40 \mu\text{mol L}^{-1}$  of  $\text{NO}_3^- + \text{NO}_2^-$ , about  $1 \mu\text{mol L}^{-1}$  of  $\text{PO}_4^{3-}$ , and over  $100 \mu\text{mol L}^{-1}$  of  $\text{SiO}_2$  ([www.gemstat.org](http://www.gemstat.org)). These concentrations would give a N:P ratio of 40:1 and a Si:P ratio of 100:1, suggesting that the river should relieve N limitation and mainly support diatom growth once it discharges into the SCS (Egge and Asknes 1992). The elevated chlorophyll concentrations which occur off the Vietnamese coast during SW monsoon have mainly been investigated by remote sensing (Tang et al. 2004a, b). The observed chlorophyll distributions suggest that phytoplankton blooms develop both near the Mekong river mouth and within the upwelling area, and then merge as they get advected offshore into the central SCS with the predominant large-scale circulation (Tang et al. 2004b). However, *in situ* observations during SW monsoon 2003/2004 showed that a distinct river-influenced water mass (Mekong and Gulf of Thailand Water, MKGTW) can be identified in the upwelling area, approximately 260 km northeast of the actual river mouth (Voss et al. 2006; Dippner et al. 2007). This water mass was largely depleted in nutrients, but was characterized by elevated rates of  $\text{N}_2$  fixation, suggesting that it contained a distinct phytoplankton community including diazotrophs that initially benefited from riverine phosphorus or iron (Voss et al. 2006).

In the framework of the South East Asian Time Series Study (SEATS), comprehensive field work has been carried out since 1999 at a station in the northern SCS (Fig.1.4A), and some results from these studies might be viewed as general biogeochemical characteristics of the SCS. Several investigations included nutrient enrichment experiments, which yielded evidence for N limitation of phytoplankton growth (Wu et al. 2003; Chen et al. 2004; Chen 2005). These conditions can be considered to favor diazotrophs, and indeed,  $\text{NO}_3^-$  anomalies in the upper nutricline and mass balance calculations of the net community production point to a significant input of N to the ecosystem via  $\text{N}_2$  fixation (Wong et al. 2002; Chou et al. 2006). The diazotroph inputs derived from  $\text{NO}_3^-$  anomalies were greatest during winter, presumably due to atmospheric deposition of iron-rich dust which primarily occurs between fall and early spring and is thought to relieve a proposed iron limitation of diazotrophs (Wong et al. 2002). Interestingly, winter is also the season when  $\text{NO}_3^-$ -based new production is highest in the open SCS, due to enhanced vertical mixing by the strong NE monsoon (Chen 2005). Evidence for iron limitation of diazotroph growth in the SCS was derived from the fact that phosphorus concentrations in the surface layer remained unexpectedly high ( $>5\text{nM}$ ) during summer stratification in July 2000 (Wu et al. 2003). Possibly, in the southern SCS, large

inputs of bioavailable iron by the Mekong River alleviate this iron limitation during summer, which could thus explain the elevated rates of  $N_2$  fixation in the river plume (Voss et al. 2006).

The organisms that are responsible for  $N_2$  fixation in the SCS have not been studied in great detail at the SEATS station. *Trichodesmium* and *Richelia intracellularis* associated with *Rhizosolenia*, *Hemiaulus*, and *Chaetoceros* were found, but abundances were low (Wu et al. 2003; Chen et al. 2004). By using *nifH* amplification, a more recent study confirmed that unicellular diazotrophic cyanobacteria are also present (Chou et al. 2006). So far, the most comprehensive molecular characterization of diazotrophs was carried out in the southern SCS off the Vietnamese coast (Moisander et al. 2008). Based on *nifH* gene diversity and quantification, all the major oceanic diazotrophs are present in the SCS, with *Trichodesmium* as the most abundant phylotype besides unicellular cyanobacteria, *Richelia*, as well as  $\alpha$ - and  $\gamma$  proteobacteria (Moisander et al. 2008).

Overall, the SCS off Vietnam appears as an excellent site for studying pelagic ecosystem dynamics, with a focus on  $NO_3^-$  - based new production and  $N_2$  fixation. Wind-induced coastal upwelling and runoff from the Mekong River supply nutrients to the oligotrophic SCS and thereby influence primary productivity and phytoplankton species succession. A direct assessment of the relative importance of  $NO_3^-$  and  $N_2$  fixation in the upwelling system and the adjacent oligotrophic offshore region is currently lacking. The Mekong River plume provides the opportunity to study the proposed mechanistic link between  $N_2$  fixation and discharge by tropical rivers. These issues need to be addressed in order to learn more about the pelagic ecosystem of the SCS, but resolving them may also help to better understand the factors that generally constrain diazotrophy in the world's oceans.

#### 1.4 Aim of the study

The aim of the present study is the investigation of nitrogen cycling in the SCS, with a focus on the Vietnamese upwelling, Mekong River inputs, and pelagic  $N_2$  fixation. Chapter 2 focuses on the primary productivity of the Vietnamese upwelling, and on a detailed description of the magnitude of  $NO_3^-$  assimilation, using profiles of rate measurements as well as quantifications of vertical  $NO_3^-$  fluxes. Regarding these flux estimates, Ekman upwelling is distinguished from turbulent diffusion at stations in adjacent offshore waters. This part is based on data from cruises conducted during SW monsoon in July 2003 and 2004.

The goals of chapter 3 are to describe and compare the biogeochemical settings of the Mekong River plume during lowest and highest annual discharge in April 2007 and September 2008, respectively, and to assess how these settings are related to  $N_2$  fixation and to the

distribution of phytoplankton, including asymbiotic diatoms, *Trichodesmium* spp., and different diatom species that potentially host diazotroph symbionts.

In chapter 4, a molecular approach is used to unambiguously identify the  $N_2$  fixing microorganism, and to further clarify how the Mekong River influenced  $N_2$  fixation and the horizontal distribution and activities of diazotrophs in the SCS in April 2007. QPCR and RT-QPCR assays specific for 9 diazotroph phylotypes were used to estimate *nifH* gene abundances and expression in the investigation area. Additionally, the *nifH* gene diversity was assessed along the salinity gradient. In order to better understand and interpret the link between the Mekong River plume and the community of diazotrophs, the surface flow of the river plume along the coast was simulated using a hydrodynamic model.

This PhD thesis has been part of an interdisciplinary project in which the results of different scientists intertwine. Full comprehension of the results of this thesis can only be achieved with respect to the results from other project partners. Therefore, chapters 2-4 are presented within the context of designated external results in a manuscript-like structure (author contributions are explained under “Publications, Manuscripts and Conferences” at the end of the thesis). In chapter 5, the results of this thesis are related to global marine carbon and nitrogen cycling and some implications for future research are drawn.

## 2. Sources of new nitrogen in the Vietnamese upwelling region of the South China Sea

### 2.1 Abstract

In the South China Sea, the southwest-monsoon between June and September induces upwelling off the southern central Vietnamese coast. During field campaigns in July 2003 and 2004 we evaluated the importance of nitrate and dinitrogen ( $\text{N}_2$ ) fixation as sources of new nitrogen for phytoplankton primary productivity, both in the actual upwelling zone and the oligotrophic area further offshore. Complementary to rate measurements of primary productivity, nitrate uptake and  $\text{N}_2$  fixation, we determined vertical nitrate fluxes by Ekman upwelling (upwelling zone) and turbulent diffusion (offshore waters). Due to El Niño influence, upwelling was weaker in July 2003, with average primary productivity of  $28 \pm 18$   $\text{mmol C m}^{-2} \text{d}^{-1}$ , compared to  $103 \pm 25$   $\text{mmol C m}^{-2} \text{d}^{-1}$  in July 2004. Calculated upwelling nitrate fluxes of  $17 \pm 2$   $\text{mmol N m}^{-2} \text{d}^{-1}$  in July 2004 are consistent with N-demands of primary productivity, if Redfield stoichiometry is assumed. In July 2003, upwelling fluxes of  $14 \pm 2$   $\text{mmol N m}^{-2} \text{d}^{-1}$  exceed N-demands, indicating that new production was not fully realized. Diffusive nitrate fluxes in offshore waters were determined in July 2003 and are in the order of  $2.3 \pm 0.6$   $\text{mmol N m}^{-2} \text{d}^{-1}$ , based on maximal diffusivities of  $1 \text{ cm}^2 \text{ s}^{-1}$  in the nitracline.  $\text{N}_2$  fixation was a significant N-source in offshore waters, but with lower rates in July 2003 ( $22 - 119 \text{ } \mu\text{mol N m}^{-2} \text{d}^{-1}$ ) than in July 2004 ( $37 - 375 \text{ } \mu\text{mol N m}^{-2} \text{d}^{-1}$ ), equalling 1 - 5% and probably 2 - 25% of diffusive nitrate fluxes, respectively.

## 2.2 Introduction

Nutrient enrichment in surface waters of the South China Sea (SCS) is largely determined by the influence of the seasonally reversing East Asian monsoon on upper ocean circulation and wind-induced mixing. Between November and March, nutrients are provided to the mixed layer of the open SCS by convective overturn and enhanced vertical mixing by the strong northeast (NE-) monsoon (Tseng et al. 2005). Additionally, wind-induced upwelling of nutrient rich water is found northwest of the Strait of Luzon and north of the Sunda Shelf during this period (Shaw and Chao 1994; Chao et al. 1996). Consequently, the NE-monsoon is regarded as the most productive season for the SCS as a whole, with primary productivity in offshore waters reaching  $25 \text{ mmol C m}^{-2} \text{ d}^{-1}$  (Liu et al. 2002; Tseng et al. 2005).

Along parts of the coast of Vietnam, however, a contrary seasonality in primary productivity can be observed. Here, the SW-monsoon induces coastal upwelling between approximately  $10$  and  $15^{\circ}\text{N}$  between June and September (Wyrki 1961; Xie et al. 2003). Remote sensing- and modelling studies denote the Vietnamese upwelling area as the most productive region of the SCS, with surface chlorophyll concentrations of up to  $2 \text{ mg m}^{-3}$  and modelled primary productivity of up to  $80 \text{ mmol C m}^{-2} \text{ d}^{-1}$  in August (Liu et al. 2002; Tang et al. 2004a, b). However, these estimates were never validated by ground truth data.

Besides the seasonal upwelling, the outflow from the Mekong River is another potentially important nutrient source for Vietnamese coastal waters. Almost concurrently with the onset of upwelling-favourable winds, water levels in the lower basin of the Mekong River start to rise with the beginning of the rainy season, and runoff into the SCS increases from around  $1.500 \text{ m}^3 \text{ s}^{-1}$  in March/April to up to  $45.000 \text{ m}^3 \text{ s}^{-1}$  in September/October (Lu and Siew 2005), and references therein). The monsoon deflects the river plume north-eastward towards the area where upwelling occurs (Hu et al. 2000; Isobe and Namba 2001). From satellite chlorophyll data, Tang et al. (2004b) assumed that the high-chlorophyll patches around  $12^{\circ}\text{N}$  observed during summer off the Vietnamese coast result from both Mekong-runoff and upwelling of nutrient-rich waters.

In order to evaluate the relative importance of nitrogen inputs from upwelling, river discharge and  $\text{N}_2$  fixation for the high productivity off southern central Vietnam, a joint research project between the Leibniz Institute of Baltic Sea Research, Warnemuende, and the Institute of Oceanography, Nha Trang, was carried out between 2003 and 2008. A station grid (Fig. 2.1) was repeatedly sampled during different seasons, including during SW-monsoon 2003/2004 when upwelling occurred. During both of these cruises, the Mekong river plume was identifiable in the investigation area by its salinity signature, but it was depleted of both

nutrients and chlorophyll, suggesting that river-runoff cannot be considered as a significant source of nutrients for the upwelling area north of the Mekong delta (Voss et al. 2006; Dippner et al. 2007). The offshore extension of an upwelling zone is defined by the Rossby radius of deformation (Gill and Donn 1982). From physical observations during SW-monsoon 2003, a radius of deformation of approximately 42km was derived (Dippner et al. 2007). Within this upwelling zone, Ekman upwelling supplies nitrate to the euphotic layer. During SW-monsoon 2003/2004, the predominant importance of upwelling nitrate for primary producers and higher trophic levels was clearly displayed by natural abundances of stable nitrogen isotopes in phytoplankton and different zooplankton size classes (Loick et al. 2007). For offshore stations however, a 2-source mixing model with  $\delta^{15}\text{N}$  values of subthermocline nitrate and atmospheric  $\text{N}_2$  as end members showed that  $\text{N}_2$  fixation on average provided 9-13% of new nitrogen entering the food web during SW-monsoon 2003 and 2004, respectively (Loick et al. 2007).

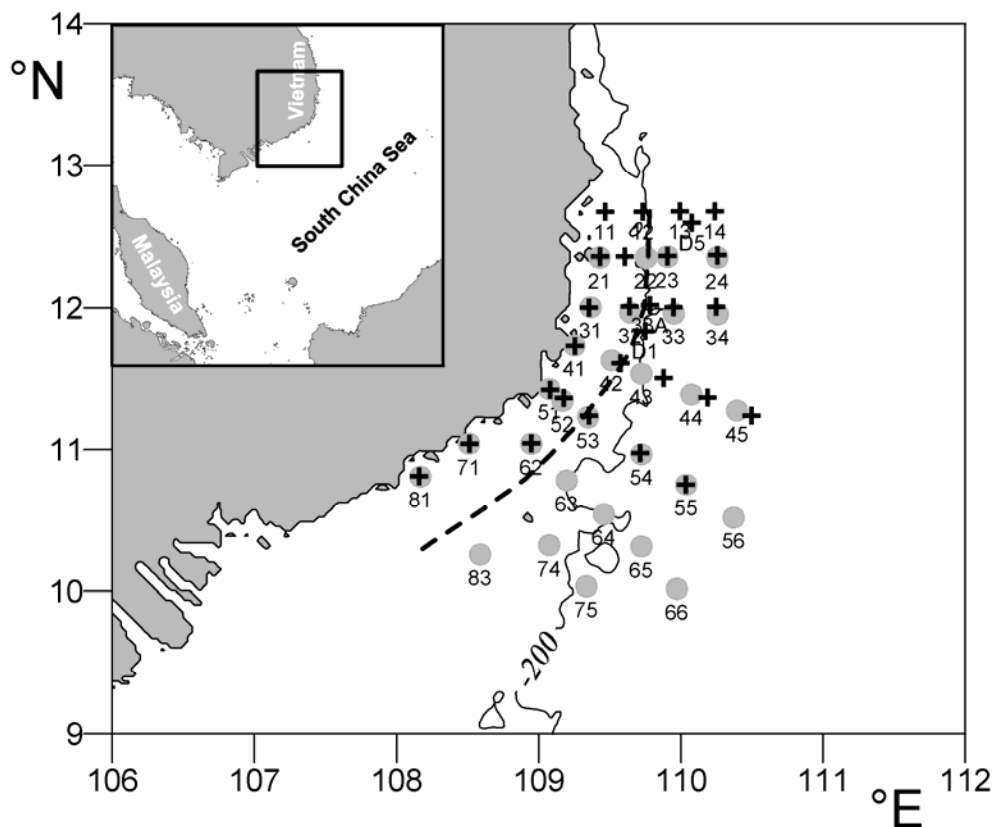


**Figure 2.1:** Map of the investigation area in the South China Sea and locations of sampling stations which were analyzed in this study. Black crosses: VG3 in July 2003, grey dots: VG7 in July 2004. Here and in other figures, the dashed line represents the seaward extension of the upwelling zone ( $\sim 42\text{km}$  offshore), as theoretically defined by the deformation radius.

The aims of the present paper are a more detailed description of the magnitude of nitrate assimilation within the euphotic zone of the Vietnamese upwelling, both by rate measurements and a quantification of vertical nitrate fluxes. Regarding these flux estimates, we distinguish

Ekman upwelling from turbulent diffusion at stations in adjacent offshore waters. These estimates might help to further assess the relative importance of different new nitrogen sources and how sensitive the system may be against future changes including climate change and anthropogenic pressures.

## 2.3 Materials and methods

Data are from stations visited on two cruises during SW-monsoon (cruise VG3, 9-28 July 2003, and VG7, 8-26 July 2004, Fig. 2.1). A Seabird CTD rosette system was used to sample the water column for nutrient analyses and experimental incubations. At each station, samples were taken for nutrient analyses from the surface (0-5m) and standard depths (10, 20, 30, 40, 50, 60, 70, 80, 90, 100 and 150m). All nutrients ( $\text{NO}_3^-$ ,  $\text{PO}_4^{3-}$  and Si) were analyzed colorimetrically after Grasshoff (1983). Under the local circumstances, the detection limit for this method was  $0.1\mu\text{mol L}^{-1}$  for all nutrients.

Rates of primary productivity and  $\text{N}_2$  fixation were measured after Montoya et al. (1996). Duplicate samples from different depths were poured into 2.3 L polycarbonate bottles and sealed with screw-caps containing Teflon coated butyl-rubber septa. To initiate the assays, 460 $\mu\text{l}$  of a 0.1 molar  $^{13}\text{C}$  labelled bicarbonate solution (99%  $\text{H}^{13}\text{CO}_3^{2-}$ ) and 2.5ml of  $^{15}\text{N}_2$  enriched gas (98% enrichment, Campro Scientific) were added to the sample bottles with a syringe. Samples were incubated for six hours under simulated *in situ* conditions on deck using neutral density screens and running surface sea water for cooling. By the use of the neutral density screens, the light levels for incubations were chosen to meet the approximate light conditions at sampling depths. We incubated water from the surface under 100% of surface irradiance, from 5m under 75%, from 10 m under 50%, from 20m under 23%, from 30-40m under 14%, and the deepest samples (40-80m) under 6%. Some of the deepest samples may have received slightly more radiation than in the field.

For nitrate uptake assays, the same experimental setup was used, but by adding a  $\text{Na}^{15}\text{NO}_3$  -solution as 10 % of ambient nitrate concentrations to duplicate samples from different depths within the nitracline (Dugdale and Goering 1967). In samples from depths where nitrate concentrations were near the limit of detection, minimal  $\text{Na}^{15}\text{NO}_3$ -additions ( $20\text{nmol L}^{-1}$ ) to incubations resulted in substrate enrichment between 30 and 50%. These potential nitrate uptake rates are specially marked in the results. Nitrate uptake incubations lasted for 2-3 hours.

All incubations were ended by gentle filtration through precombusted Whatman GF/F filters (0.7  $\mu\text{m}$  pore size). The filters were immediately dried for 48 hrs at  $60^\circ\text{C}$  in a drying oven and then stored at room temperature. In the lab the filters were fumed for 2 hrs with HCl and

dried again. Isotopic measurements of the filters were done with a Delta S (Thermo) isotope ratio mass spectrometer connected to an elemental analyser CE1108 via an open split interface. Calibration for tracer measurements was done with enriched IAEA standards, 310 for nitrogen (50‰ and 200‰) and 309 for carbon (100‰ and 550‰). Calibration for C and N was done with acetanilide at the start of each sample run that comprised app. 20 filter measurements. After each fifth sample an internal standard, a protein solution (Peptone, Merck Chemicals), was measured. The precision is  $<\pm 0.2\%$  for both elements.

Areal rates of primary productivity,  $N_2$  fixation and nitrate uptake were depth-integrated using the trapezoidal method, and daily rates were calculated by extrapolation to 12 hours of daylight. The nitrogen (N-) demand of primary productivity was calculated by assuming a Redfield C:N uptake ratio of 6.6.

The vertical distribution of photosynthetically active radiation (PAR) in the water column was measured with a LICOR spherical light sensor at 3 upwelling- and 4 offshore stations during VG7 in July 2004. The euphotic zone depth (EZD) was calculated as the depth at which PAR had been reduced to 1% of the surface value. In contrast to the LICOR-profiles Secchi depth readings were carried out during both cruises at 41 stations in total. The Secchi readings were done by different investigators, and not always concurrently with LICOR profiles, and can therefore not be validated and used to calculate EZDs. However, the Secchi depths may be used to infer that light conditions were roughly similar during both cruises (VG3 upwelling zone:  $22 \pm 6$  m,  $n=7$ ; offshore zone:  $32 \pm 11$  m,  $n=6$ , and VG7 upwelling zone:  $19 \pm 5$  m,  $n=10$ ; offshore zone:  $24 \pm 5$  m,  $n=17$ ).

Mixed layer depths (MLD) were estimated from the maximum in the buoyancy frequency of the water column. Velocities of the wind-induced Ekman upwelling were estimated as described in Dippner et al. (2007) as

$$W_E = \frac{1}{f\rho_0} \frac{\partial \tau^y}{\partial x} = \frac{\tau^y}{Rf\rho_0} \quad (1)$$

where  $f$  is the Coriolis parameter,  $\rho_0$  a reference density,  $\tau^y$  the north-south component of the wind stress, and  $R$  the first mode of the radius of deformation. For the calculation of the wind stress, we used bulk transfer coefficients for momentum according to Kondo (1975).

We assume that upwelling and offshore oligotrophy would be clearly separated by the estimated Rossby radius of deformation (Dippner et al. 2007). Therefore, as a first approach, we grouped all sampling stations as within- and outside of the upwelling zone.

The upwelling flux of nitrate into the euphotic zone ( $\text{mmol N m}^{-2} \text{d}^{-1}$ ) was calculated as

$$NO_3^- Flux_{upw} = W_E \times [NO_3^-]_{MSW} \quad (2)$$

where  $W_E$  is the velocity of the wind-induced upwelling ( $m\ s^{-1}$ ), and  $[NO_3^-]_{MSW}$  is the nitrate concentration ( $mmol\ N\ m^{-3}$ ) in the Maximum Salinity Water (MSW), which is the source water for upwelling (Dippner et al. 2007).

Vertical nitrate fluxes by turbulent diffusion were calculated for stations offshore of the upwelling zone as

$$NO_3^- Flux_{Diff} = D_v \frac{\partial}{\partial z} [NO_3^-] \quad (3)$$

where  $\frac{\partial}{\partial z} [NO_3^-]$  is the nitrate gradient at the nitracline ( $mmol\ m^{-4}$ ) and  $D_v$  the eddy diffusivity ( $cm^2\ s^{-1}$ ). At all offshore stations during VG3, vertical velocity profiles were measured down to 130 m using an acoustic current meter (NOBSKA, MAVS 2, 1.42 Hz). The vertical eddy diffusivity  $D_v$  is computed from CTD casts and current meter measurements, using the “Level 2” model of Mellor and Yamada (1974), and can be expressed as:

$$D_v = lqS_H \quad (4)$$

where  $l$  is a mixing length,  $q$  is twice the turbulent kinetic energy.  $S_H$  is a flux Richardson number dependent on stability functions for heat. The vertical eddy diffusivity is calculated from the *in situ* observations in the following way: From the velocity profile, the vertical shear and the turbulent kinetic energy is computed ( $q = U^2 + V^2$ ). From the CTD measurements the temperature gradient is computed. With the thermal expansion multiplied by gravity ( $\beta g = -1.73 \cdot 10^{-3}\ m\ s^{-2}\ K^{-1}$ ), and using the computed vertical shear, the Richardson numbers and the stability functions can be computed. By integrating the turbulent kinetic energy, the mixing length is obtained. Details are given in Mellor and Yamada (1974).

## 2.4 Results

### 2.4.1 Environmental conditions

MLD and SST showed well-defined offshore gradients and interannual differences (Fig. 2.2). During both cruises, upwelling stations had shallower MLDs and lower SST compared to offshore stations. Especially among VG7 offshore stations, MLD further increased from stations near the upwelling zone towards stations further offshore and further south (Fig. 2.2a, b). Additionally, during VG7 the offshore gradient in SST extended across stations outside of the upwelling zone (values between  $\leq 28^\circ C$  and  $\geq 29^\circ C$ ), whereas SST was comparatively uniform ( $29 - 30^\circ C$ ) in the offshore zone during VG3 (Fig. 2.2c, d). Overall, compared to VG3, the MLDs were shallower throughout the investigation area during VG7, and the gradient in SST was steeper.

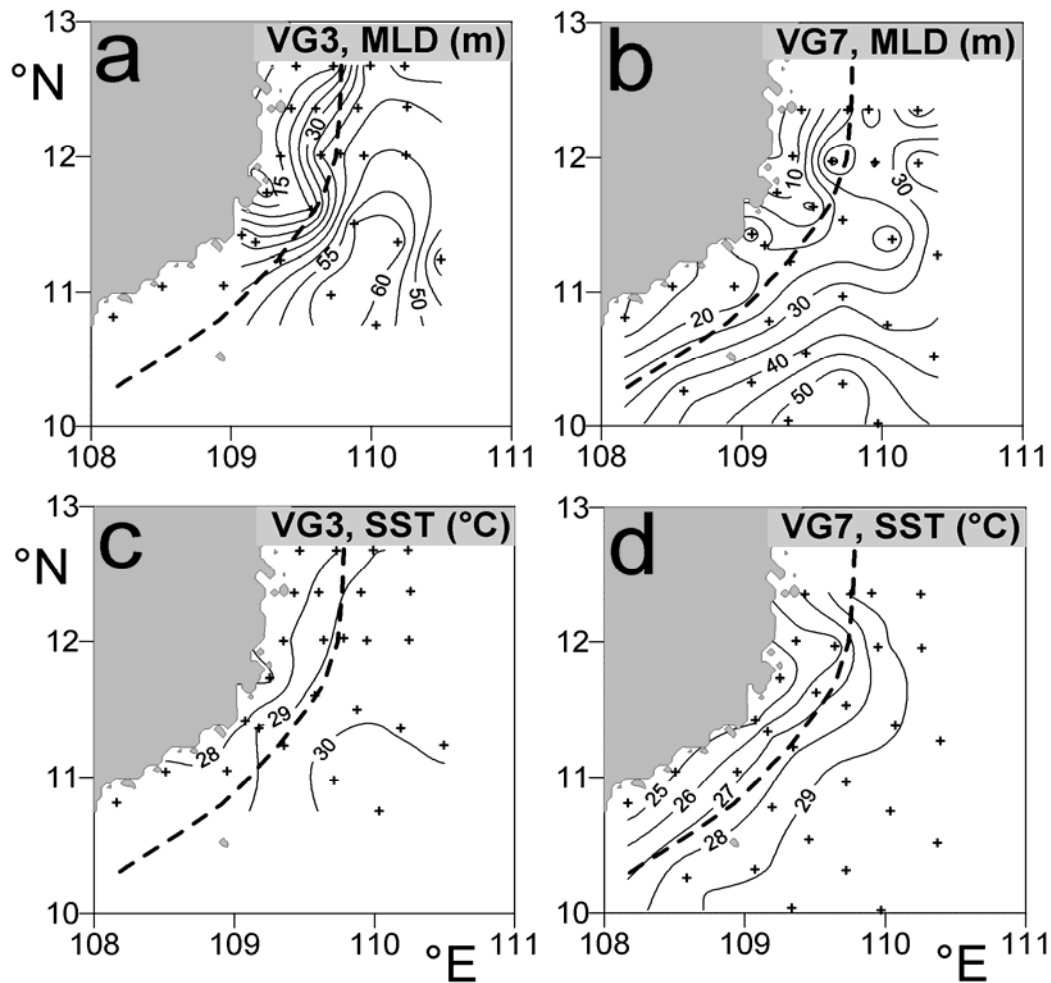


**Figure 2.2:** Mixed layer depths (MLD, m) during VG3 (a) and VG7 (b) and Sea Surface Temperature (SST, °C) during VG3 (c) and VG7 (d). Contour intervals are 5m for MLD and 1°C for SST. Black crosses mark sampling stations.

Concentrations of nitrate were below detection in surface waters at all stations and during both cruises (Fig. 2.3). At upwelling stations, nutrient enrichment was usually noted at the base or just below the MLD, and hence at shallower depths compared to offshore stations. The nitrate concentration at VG7 upwelling stations was typically equal or higher at similar depths compared to VG3. For offshore stations, profiles of nitrate concentrations appear to fall into two groups. One group (black offshore-profiles in Fig. 2.3) mainly consists of profiles from stations near the edge of the upwelling zone, with relatively shallow MLDs (VG3 stations 23, 33, 53 and VG7 stations 23, 33, 43, 53, 63 and 83). At stations lying further offshore, nitrate concentrations were  $\leq 0.5 \mu\text{mol L}^{-1}$  down to at least 70m depth (grey offshore-profiles in Figure 2.3, representing VG3 stations 44, 45, 54, and VG7 stations 65, 66, 75). These latter stations were characterized by deeper MLD ( $>60\text{m}$  for VG3,  $\geq 50\text{m}$  for VG7), except for VG3-station 45, which had a MLD of 36m.

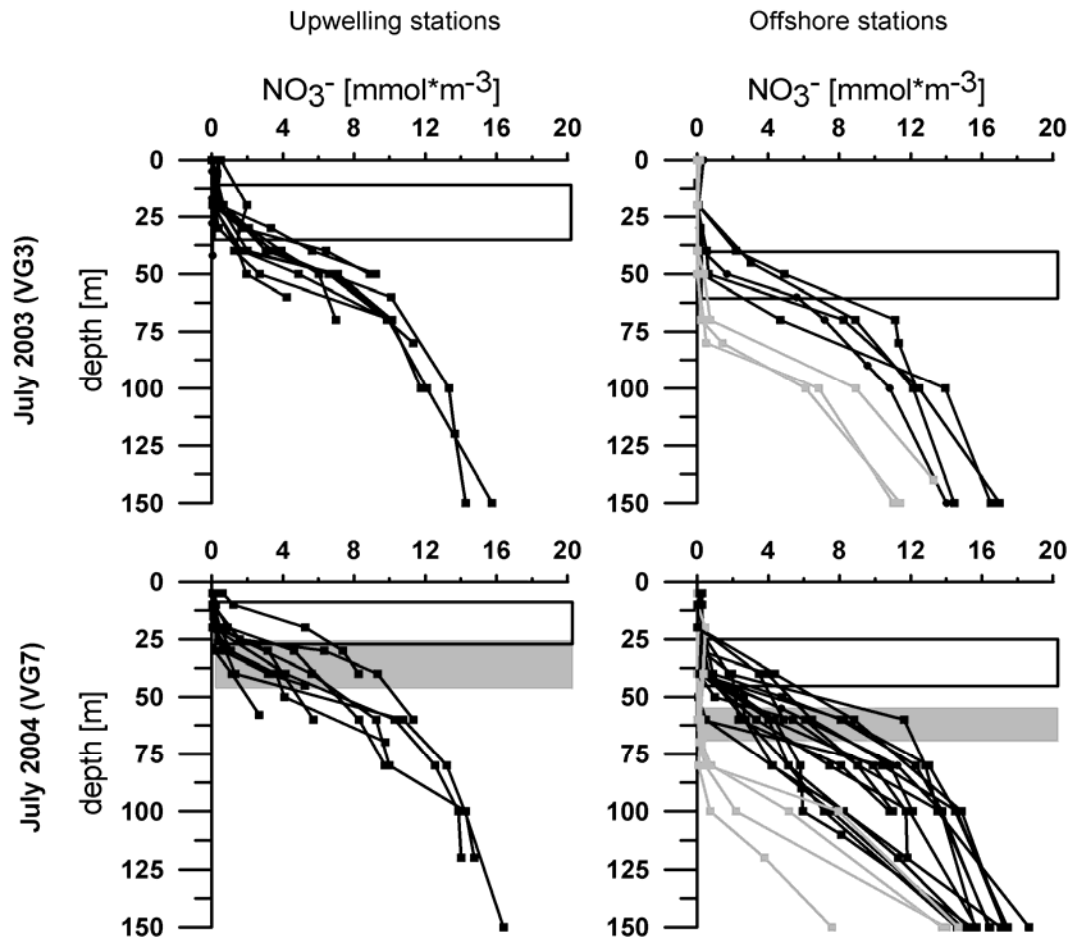


**Figure 2.3:** Profiles of nitrate concentrations for all stations within the upwelling- (left column) and the offshore zone (right column) during cruises VG3 and VG7. The white boxes represent mean  $\pm$  standard deviation of mixed layer depths, and the grey boxes in VG7 plots represent mean  $\pm$  standard deviation of euphotic zone depths. Grey nitrate profiles are from offshore stations that lay furthest offshore (see text in section 2.4.1).

EZD were determined from LICOR readings only during VG7, and were  $35 \pm 11$  m (range 23-45m,  $n=3$ ) in the upwelling zone and  $62 \pm 5$  m (range 60-70m,  $n=4$ ) in the offshore zone. These average EZD exceeded average MLD in both the upwelling- and the offshore zone during that cruise (Fig. 2.3).

### 2.4.2 Primary productivity

Rates of primary productivity were measured at several upwelling- and offshore stations during both cruises (Fig. 2.4, Fig. 2.5a). The rates were generally higher at upwelling stations compared to offshore stations (Fig. 2.4); this difference was more pronounced during VG7, when primary productivity of up to  $395.2 \text{ nmol C L}^{-1} \text{ h}^{-1}$  was measured (upwelling-station 62\_2, 10m), whereas rates did not exceed  $137.3 \text{ nmol C L}^{-1} \text{ h}^{-1}$  during VG3 (upwelling-station 42, 40m). Highest rates at upwelling stations generally occurred in subsurface maxima, and during VG7, the maxima were found at shallower depths (above 30m) compared to VG3 (between 30m and 40m depth). Deepest measurements at 70m during VG3 (station 33A, 42) yielded no detectable primary productivity. At VG7 stations 52 and 62\_1, the rates were still

high at the deepest measured depth (151.8 nmol C L<sup>-1</sup> h<sup>-1</sup> at station 52, 30m; 197.8 nmol C L<sup>-1</sup> h<sup>-1</sup> at station 62\_1, 40m). Overall, the upwelling zone was clearly more productive during VG7 (103 ± 25 mmol C m<sup>-2</sup> d<sup>-1</sup>, n = 4) than during VG3 (28 ± 18 mmol C m<sup>-2</sup> d<sup>-1</sup>, n=4) (Fig. 2.5a).

At offshore stations, primary productivity also differed between the years, with an average areal rate of 10 ± 5 mmol C m<sup>-2</sup> d<sup>-1</sup> (n=4) during VG3, which is roughly 34% of the mean value determined for VG7 (29 ± 15 mmol C m<sup>-2</sup> d<sup>-1</sup>, n=7) (Fig. 2.5a). Subsurface maxima were detected at most VG3 offshore stations (Fig. 2.4, stations 24, 33, 53), whereas during VG7, highest rates were found at the surface at 4 out of 7 offshore stations where primary productivity was measured (stations 33, 65\_1, 65\_2 and 83). At station 83, primary productivity ranged from 144.7 nmol C L<sup>-1</sup> h<sup>-1</sup> to 194.7 nmol C L<sup>-1</sup> h<sup>-1</sup> between the surface and 20m depth, clearly exceeding the rates measured at the other VG7 offshore stations. Finally, primary productivity was undetectable in samples from greatest depths during both cruises (at 80m at VG3 stations 53 and 45, and at 70m at VG7 station 65\_2).

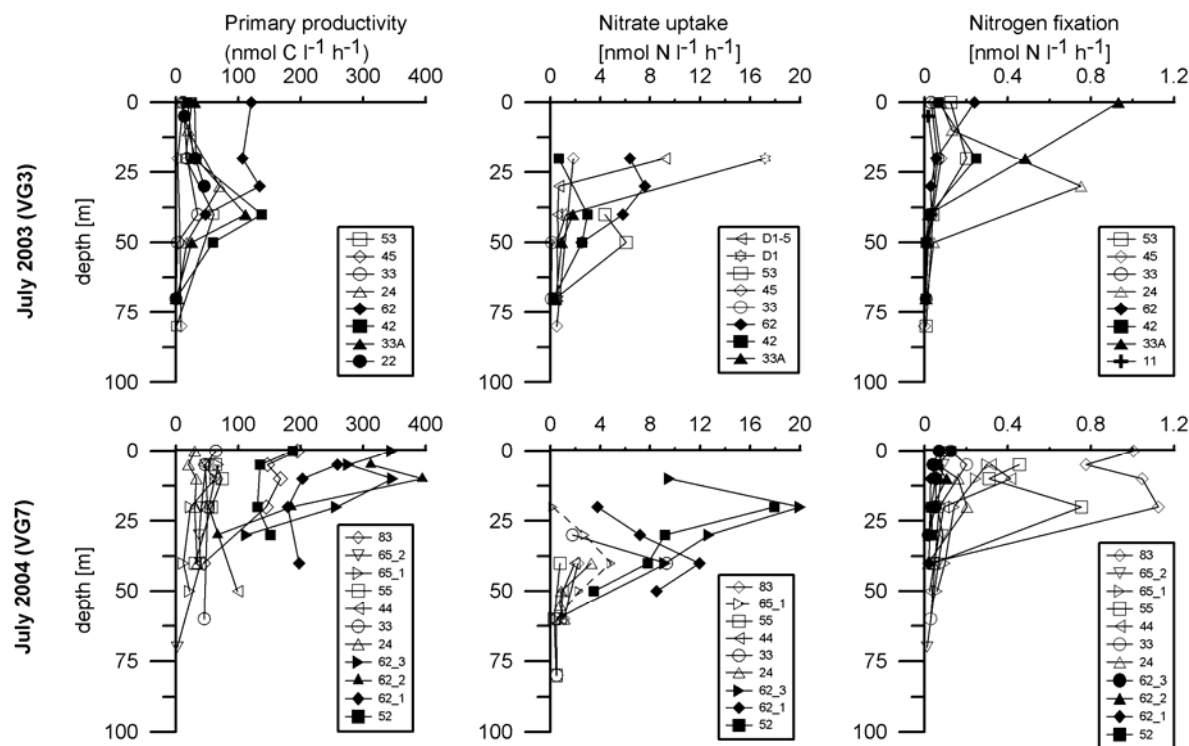


**Figure 2.4:** Vertical distributions of primary productivity, nitrate uptake and N<sub>2</sub> fixation within the upwelling- (filled symbols) and the offshore zone (open symbols) during VG3 and VG7. The dashed profile of nitrate uptake rates at station 65\_1 (VG7) represents potential rates (up to 50% substrate enrichment with <sup>15</sup>NO<sub>3</sub><sup>-</sup> in experimental incubations).

### 2.4.3 Nitrate uptake

Rates of nitrate uptake were distributed similarly to those of primary productivity, with the highest rates occurring above 30m depth in the upwelling zone during VG7 (up to 20.0 nmol N L<sup>-1</sup> h<sup>-1</sup> at 20m, station 62\_3; Fig. 2.4). Nitrate uptake was still high at the deepest measured depth at VG7 station 62\_1 (8.5 nmol N L<sup>-1</sup> h<sup>-1</sup>, at 50m). The maximal rate of nitrate uptake at a

VG3 upwelling station was  $7.6 \text{ nmol N L}^{-1} \text{ h}^{-1}$  (station 62, 30m). At 70 and 80m depth, nitrate uptake was undetectable or very low ( $0.4\text{-}0.5 \text{ nmol N L}^{-1} \text{ h}^{-1}$ ) during both cruises.

Nitrate uptake at offshore stations did generally not exceed  $4.9 \text{ nmol N L}^{-1} \text{ h}^{-1}$  during VG7 (30m depth, station 65\_1), with the exception of one higher value at 40m depth at station 33 ( $9.3 \text{ nmol N L}^{-1} \text{ h}^{-1}$ ). During VG3, comparatively high nitrate uptake occurred at 20m at offshore stations D1 and D5; however, these rates will not be discussed further, since they likely represent nutrient entrainment into the mixed layer by wind induced mixing, given that stations D1 and D5 were sampled after a storm on the last day of cruise VG3.

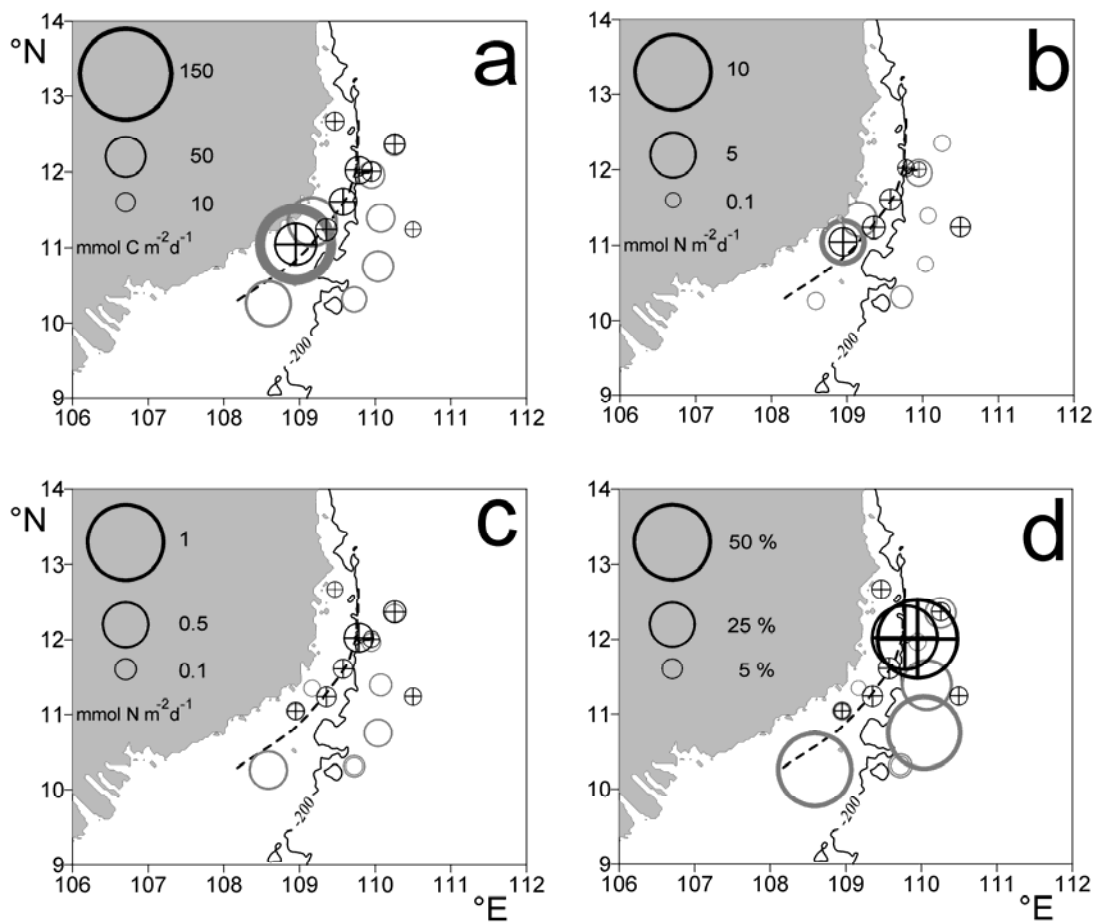


**Figure 2.5:** Areal rates of (a) primary productivity, (b) nitrate uptake and (c)  $\text{N}_2$  fixation measured during cruises VG3 (July 03, black circles with centered cross) and VG7 (July 04, grey circles). d) The percent contribution of  $\text{N}_2$  fixation to total new production ( $\text{N}_2$  fixation + nitrate uptake), estimated for all stations where both parameters were measured. Circles which appear thicker or double are stacked circles from stations which were repeatedly sampled.

The areal rates of nitrate uptake highlight the interannual differences, with an average value of  $4.2 \pm 0.9 \text{ mmol N m}^{-2} \text{ d}^{-1}$  ( $n=3$ ) for VG7 upwelling stations, compared to  $1.2 \pm 0.9 \text{ mmol N m}^{-2} \text{ d}^{-1}$  ( $n=3$ ) for VG3 (Fig. 2.5b). Average nitrate uptake at offshore stations ( $0.7 \pm 0.6 \text{ mmol N m}^{-2} \text{ d}^{-1}$ ,  $n=3$ ) was not distinguishable from the upwelling zone value during VG3, but during VG7, the average rate for the offshore zone ( $0.7 \pm 0.7 \text{ mmol N m}^{-2} \text{ d}^{-1}$ ,  $n=6$ ) was clearly lower than the average nitrate uptake in the upwelling zone.

#### 2.4.4 N<sub>2</sub> fixation

Rates of N<sub>2</sub> fixation exhibited strongest zonal differences during VG7 (Fig. 2.4, Fig. 2.5c). The overall lowest rates of N<sub>2</sub> fixation ( $23 \pm 6 \mu\text{mol N m}^{-2} \text{ d}^{-1}$ , n=4) were found in the upwelling zone during VG7, when primary productivity and nitrate uptake were highest (Fig. 2.5c). However, during the same cruise, the offshore zone was characterized by the highest rates of N<sub>2</sub> fixation ever measured ( $138 \pm 120 \mu\text{mol N m}^{-2} \text{ d}^{-1}$ , n=7). In contrast, highly variable rates of N<sub>2</sub> fixation were measured during VG3, with no clear difference between the upwelling- ( $88 \pm 97 \mu\text{mol N m}^{-2} \text{ d}^{-1}$ , n=4) and the offshore zone ( $59 \pm 45 \mu\text{mol N m}^{-2} \text{ d}^{-1}$ , n=4).

The highest N<sub>2</sub> fixation rate during VG3 occurred at the surface at upwelling station 33A ( $0.9 \text{ nmol N L}^{-1} \text{ h}^{-1}$ ). At offshore station 24, N<sub>2</sub> fixation reached a similarly high value, but in a subsurface maximum at 30m depth ( $0.8 \text{ nmol N L}^{-1} \text{ h}^{-1}$ ). During VG7, the highest rates of N<sub>2</sub> fixation were found between 0m and 20m depth at offshore station 83 (reaching  $1.1 \text{ nmol N L}^{-1} \text{ h}^{-1}$  at 20m), where also primary productivity was high. During both cruises, rates determined for depths between 40 and 50m were  $\leq 0.1 \text{ nmol N L}^{-1} \text{ h}^{-1}$ , and undetectable for depths of  $\geq 70\text{m}$ .

#### 2.4.5 Vertical nitrate flux

##### Ekman upwelling

Ekman velocities of  $1.64 \cdot 10^{-5} \text{ m s}^{-1}$  and  $2.06 \cdot 10^{-5} \text{ m s}^{-1}$  were calculated for VG3 and VG7, respectively. The calculation of upwelling fluxes was not possible for some stations (11, 21, 71, 81 during VG3 and stations 21, 51, 62\_1, 62\_3 during VG7), because they were too shallow or well mixed, and consequently the typical structure of the water column, with the MSW water mass around 50m depth, was not found. For all remaining upwelling stations, average nitrate fluxes were  $14 \pm 2 \text{ mmol N m}^{-2} \text{ d}^{-1}$  (n = 9) and  $17 \pm 2 \text{ mmol N m}^{-2} \text{ d}^{-1}$  (n = 7) during VG3 and VG7, respectively (Table 2.1).

##### Diffusive nitrate flux at offshore stations

During VG3, vertical eddy diffusivities were computed for twelve offshore stations, in order to get an impression of typical vertical patterns and the order of magnitude of diffusion coefficients in offshore waters. All surface values covered a range between  $0.1$  and  $4.1 \text{ cm}^2 \text{ s}^{-1}$ , with the exception of one maximum value of  $54 \text{ cm}^2 \text{ s}^{-1}$  at station 13. Fig. 2.6 shows four representative profiles. Below 60m water depth, mixing was found at stations 43 and 24 ( $3 \text{ cm}^2 \text{ s}^{-1}$  in 105 and 125 m). The profiles in Figure 2.6 also show local maxima between 15 and 40 m water depth. These maxima are connected to a temperature inversion in the water column,

which occurred at all offshore stations during VG3, except for station 43. The reason for this temperature inversion is not clear and will be the subject of future investigations.

Between 30m and 60m depth (which is the interval where nitraclines were generally found in the offshore zone) maximal diffusivities around  $1.0 \text{ cm}^2 \text{ s}^{-1}$  appeared which give an average diffusive nitrate flux of  $2.3 \pm 0.6 \text{ mmol N m}^{-2} \text{ d}^{-1}$  (Table 2.2). If similar eddy diffusivities are assumed for VG7, average diffusive nitrate fluxes would be  $1.8 \pm 0.5 \text{ mmol N m}^{-2} \text{ d}^{-1}$ .

**Table 2.1:** Estimates of nitrate fluxes from Maximum Salinity Water (MSW) by Ekman upwelling. The MSW-characteristics are taken from Dippner et al. (2007).

Cruise	Ekman velocity ( $\text{m s}^{-1}$ )	Depth (m)	Salinity (PSS)	Temp. ( $^{\circ}\text{C}$ )	$\text{NO}_3^- + \text{NO}_2^-$ ( $\text{mmol m}^{-3}$ )	$\text{NO}_3^-$ upwelling flux ( $\text{mmol N m}^{-2} \text{ d}^{-1}$ )
MSW- characteristics <sup>a</sup>		50-175	$\geq 34.5$	15-20	7-17	
VG3 (9 stations)	$1.64 \cdot 10^{-5}$	50-100	$34.5 \pm 0$	$19.0 \pm 1.1$	$9.7 \pm 1.4$	$14 \pm 2$
VG7 (7 stations)	$2.06 \cdot 10^{-5}$	40-70	$34.6 \pm 0$	$19.6 \pm 0.2$	$9.4 \pm 0.9$	$17 \pm 2$

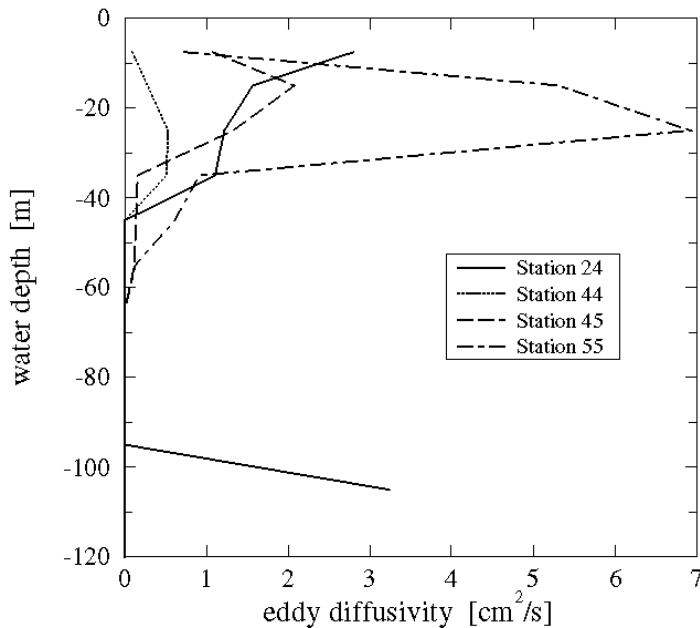


**Figure 2.6:** Four selected profiles of vertical eddy diffusivities computed from *in situ* observations during July 03 (VG3) using the “Level 2” model according to Mellor and Yamada (1974).

**Table 2.2:** Estimates of diffusive nitrate fluxes for offshore stations during VG3 and VG7. The eddy diffusivity ( $D_v$ ) of  $1.0 \text{ cm}^2 \text{ s}^{-1}$  used here represents the maximum value measured between 30m and 60m depth at offshore stations during VG3. Eddy diffusivities were not explicitly determined during VG7, so diffusive fluxes are assumptive for this cruise.

cruise	Number of offshore stations	$\text{NO}_3^-$ Gradient [ $\text{mmol N m}^{-4}$ ]	Diffusive $\text{NO}_3^-$ - flux ( $\text{mmol N m}^{-2} \text{ d}^{-1}$ )
VG3 (July03)	8	$0.27 \pm 0.07$	$2.3 \pm 0.6$
VG7 (July04)	22	$0.21 \pm 0.06$	$1.8 \pm 0.5$

## 2.5 Discussion

### 2.5.1 Different upwelling intensity in July 2003 and July 2004

The intensity of the Vietnamese upwelling is influenced by the northward extension of the intertropical convergence zone and by El Niño /Southern Oscillation (ENSO) events (Chao et al. 1996; Dippner et al. 2007). During SW-monsoon seasons which follow ENSO-events, average wind speeds are lower compared to the climatological mean, and upwelling intensity is reduced. For the coastal region off southern-central Vietnam, Xie et al. (2003) report Ekman velocities between 2 and  $2.5 * 10^{-5} \text{ m s}^{-1}$ , averaged over SW-monsoon periods June to August 2000-2002. Interestingly, all these years represent conditions of the climatological mean, i.e. clear upwelling structures can be observed on SST-satellite-images (Dippner et al. 2007). The Ekman velocity of  $2.06 * 10^{-5} \text{ m s}^{-1}$  determined for July 2004 (VG7) is in good agreement with the values by Xie et al. (2003). In contrast, VG3 took place in a post El Niño year 2003, and consequently a reduced Ekman velocity of  $1.64 * 10^{-5} \text{ m s}^{-1}$  was observed. The difference in upwelling intensity between VG3 and VG7 was clearly reflected by surface isotherms (Fig. 2.2c, d). The steeper SST gradient during VG7 suggests that stronger upwelling occurred.

Given that the SST gradient extended across stations outside of the upwelling zone during VG7, it appears likely that some of the offshore stations that lay close to the upwelling zone were still affected by upwelling. This is supported by the horizontal distribution of the MLDs (Fig 2.2b), which were  $\geq 40\text{m}$  at only few offshore stations on southern transects during VG7. The situation during VG3 seems more compatible with our station classification (upwelling/offshore), since only temperatures around  $30 \text{ }^\circ\text{C}$  and MLD between 40 and 60m were found at offshore stations, while lower SST and MLD shallower than 30m were largely confined to stations within the upwelling zone.

### 2.5.2 Primary productivity and nitrate supply in the upwelling zone

Previous field studies in the SCS included nutrient enrichment experiments, which consistently showed that primary productivity was enhanced by nitrate additions, but never by additions of phosphate or iron (Wu et al. 2003; Chen et al. 2004; Chen 2005). These observations suggest that nitrogen availability represents the most important control on primary productivity in the SCS. We therefore assume that in our investigation area, there was a direct link between enhanced primary productivity and the nitrate supply by upwelling.

The spatial extent on which nitrate-based new production is realized in an upwelling area mainly depends on the velocity of upward transport and the nitrate concentrations in the upwelling source water (MacIsaac et al. 1985; Dugdale et al. 1990). Ekman upwelling off the Vietnamese coast occurred with a vertical motion of not more than  $1.8\text{ m d}^{-1}$  (corresponding to  $2.06 \times 10^{-5}\text{ m s}^{-1}$  during VG7), and nitrate concentrations in MSW were relatively low (Table 2.1). This intensity of upwelling is much lower than e.g. off Peru, where Ekman velocities as high as  $36\text{ m d}^{-1}$  result in uniform nitrate concentrations of  $25\mu\text{mol L}^{-1}$  between 0m and 80m depth (Brink et al. 1981). Under conditions of such rapid upwelling, a phytoplankton community undergoes physiological transformations to adapt to conditions of high light and high nutrient concentrations as the upwelling plume flows away from the area of initial upwelling. Consequently, off the Peruvian coast, the highest rates of nitrate uptake as well as chlorophyll maxima are typically found in surface waters at stations representing several days of “down plume” transport (Brink et al. 1981; MacIsaac et al. 1985). A similar pattern can be found in the upwelling area off northwest Africa around  $21.5^{\circ}\text{N}$  (Ekman velocities of  $9\text{ m d}^{-1}$ , Huntsman and Barber 1977). In the Vietnamese upwelling area, rates of nitrate uptake and primary productivity were in most cases highest at stations within the upwelling zone, and showed subsurface peaks at most upwelling stations during both cruises (Fig. 2.4, Fig. 2.5). We did not observe elevated concentrations of nitrate in surface waters, neither in the upwelling zone nor at any offshore station (Fig. 2.3). Furthermore, highest chlorophyll concentrations were measured at upwelling stations and peaked between 20 and 40m during VG3, and between 10 and 40m during VG7 (data not shown). Thus, off the Vietnamese coast, the maximal upwelling-induced productivity seemed to be realized within the actual upwelling zone. Elevated primary productivity may also be found in an offshore jet protruding from the Vietnamese coast between approximately  $12^{\circ}$  and  $13^{\circ}\text{N}$  during SW-monsoon (Tang et al. 2004a,b; Tan and Shi 2009); however, on satellite pictures, this jet feature seems less productive than the coastal zone which was covered by our sampling, and which was directly affected by Ekman upwelling.

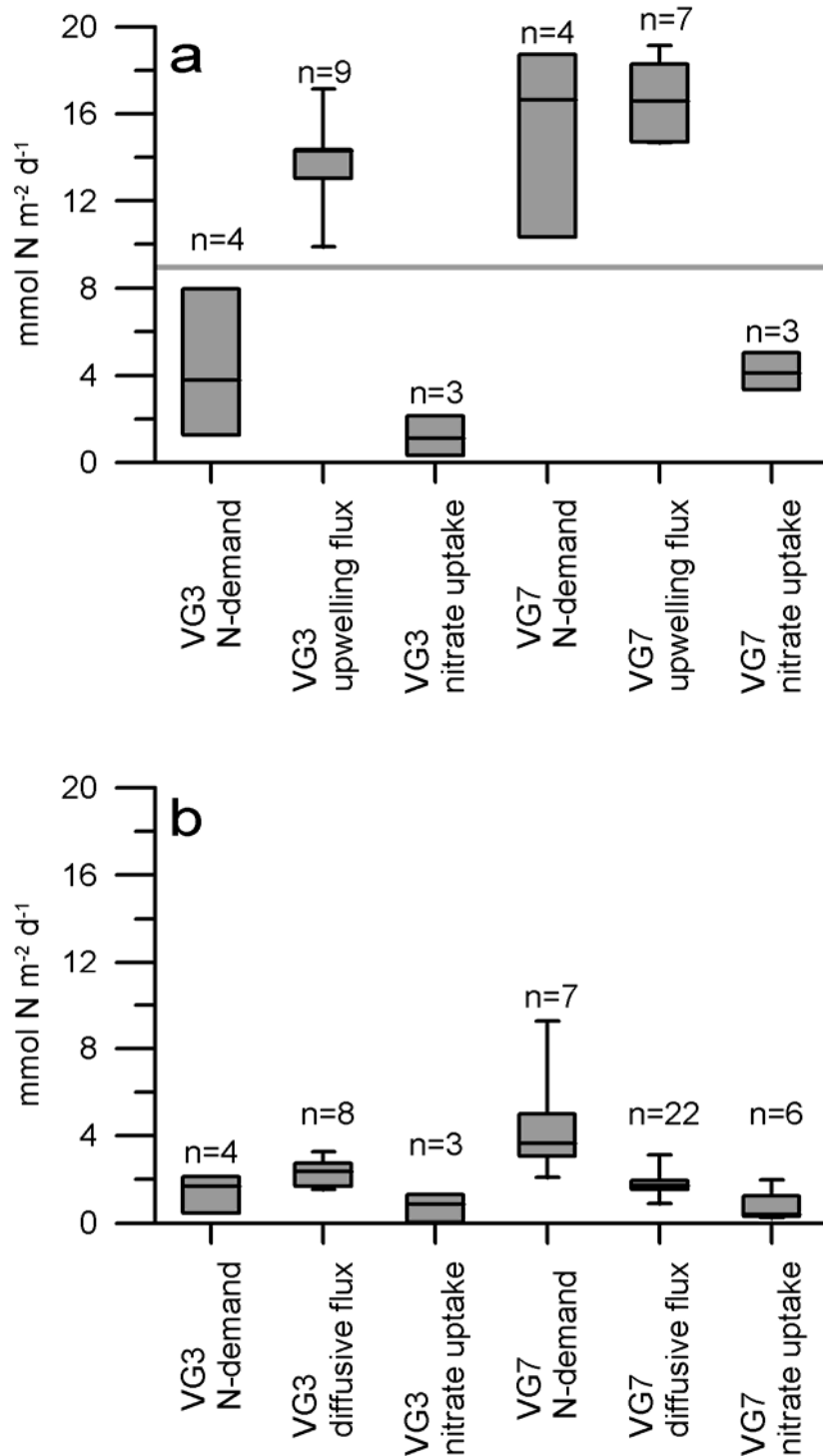


**Figure 2.7:** Comparison between N-demands of primary productivity (converted via Redfield ratio, C:N=6.6), rates of nitrate uptake, and estimated nitrate fluxes for (a) upwelling and (b) offshore stations during both cruises. Each box is defined by the lower and upper quartile, and the line crossing the box is the median. The whiskers extend to the minima and maxima of the data. In plot (a), the horizontal grey line represents modelled upwelling fluxes of nitrate for the Vietnamese upwelling area (Liu et al. 2002). To calculate diffusive fluxes, an eddy diffusivity  $D_v$  of  $1 \text{ cm}^2 \text{ s}^{-1}$  was chosen.  $n$  = number of sampling stations.

During both cruises, the calculated upwelling nitrate fluxes exceeded the rates of nitrate uptake (Fig. 2.7a). This would imply that nitrate accumulated in surface waters, which is not compatible with our observations described above and which rather suggest that the upwelling supply of nitrate was balanced by nitrate uptake. The discrepancy either indicates an

underestimation of nitrate uptake rates, an overestimation of upwelling fluxes, or both. The areal rates of nitrate uptake were also lower than N-demands of primary productivity (Fig. 2.7a). There was a significant positive correlation between these parameters (Fig. 2.8), suggesting that primary productivity in the upwelling zone was mainly based on upwelled nitrate, but all nitrate uptake data fall well below a 1:1 line. The slope of the regression line in Fig. 2.8 represents an overall C:N uptake ratio of 21, which appears high but lies within the range of  $\Delta\text{DIC}/\Delta\text{NO}_3$  depletion ratios of 10.1-28.6 which were reported for the Venezuelan and Peruvian upwelling ecosystems (Walsh 1996). C:N uptake ratios exceeding the Redfield ratio of 6.6 are commonly found in coastal- and open ocean ecosystems (Sambrotto et al. 1993 and references therein), and possibly represent preferential recycling of limiting nutrients (Thomas et al. 1999). Unfortunately, we lack comparable data to confirm elevated C:N uptake ratios for our study site, which would partly reconcile the discrepancy between N-demands of primary productivity and nitrate uptake rates. However, the elevated C:N uptake ratios would not explain the discrepancy between nitrate uptake and upwelling fluxes.

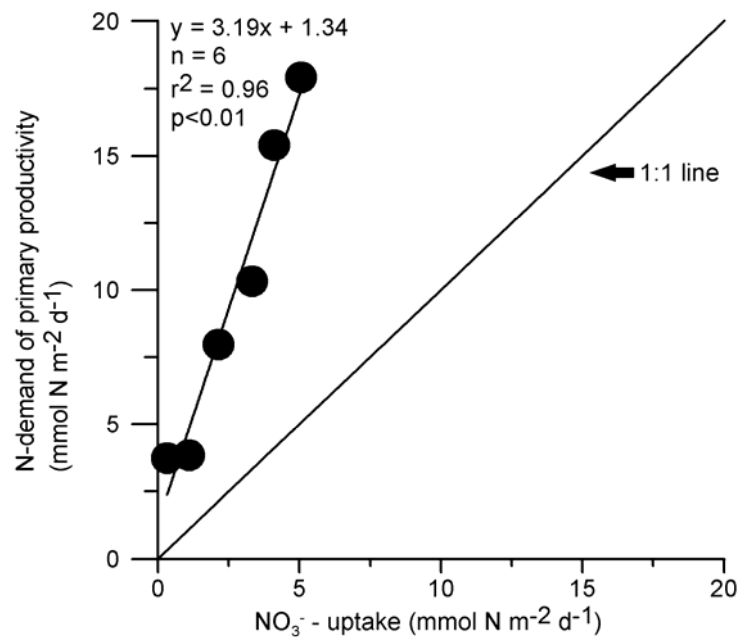


**Figure 2.8:** Relationship between nitrate uptake and N-demand of primary productivity at upwelling stations (pooled data from VG3 and VG7). Given that the N-demand of primary productivity was calculated assuming C:N uptake ratio of 6.6, the 1:1 line indicates the Redfield slope.

**Table 2.3:** Summary of pelagic primary productivity estimates for coastal upwelling areas and oligotrophic waters. Where available, primary productivity is given as mean  $\pm$  standard deviation, with the full range of values in parentheses.

Ocean region	Dates	Primary productivity (mmol C m <sup>-2</sup> d <sup>-1</sup> )	Number of stations/ observations	Reference
<i>coastal upwelling areas</i>				
Vietnamese upwelling zone	SW monsoon, July 2003 (VG3)	28 $\pm$ 18 (8-53)	4	this study
Vietnamese upwelling zone	SW-monsoon, July 2004 (VG7)	103 $\pm$ 25 (68 - 124)	4	this study
Vietnamese upwelling zone	Modeled average for July	70	na	Liu et al. 2002
northwestern Arabian Sea, off Somalia	SW-monsoon, July/August 1992	104 (66 - 233)	7	Veldhuis et al. 1997
Arabian Sea, off Omani coast	SW monsoon August – September 1995	123 $\pm$ 9	20	Barber et al. 2001
off northwest Africa, 21°40'N	March-May 1974	83 - 250	na	Huntsman and Barber 1977
<i>Offshore waters</i>				
Southern SCS offshore waters	SW monsoon, July 2003 (VG3)	10 $\pm$ 5 (3 - 14)	4	this study
Southern SCS offshore waters	SW monsoon, July 2004 (VG7)	29 $\pm$ 15 (14 - 61)	7	this study
Northern SCS offshore waters (app. 18°N)	SW monsoon, July 2000	16	1	Chen 2005
Northern SCS, Station SEATS (18°N, 116°E)	June 2001 - December 2003	9	11	Tseng et al. 2005
Tropical Atlantic at 21°N, 31°W	May-June 1992	29 $\pm$ 6	4	Claustre and Marty 1995
Oligotrophic Pacific at 12°N/S	1992	29 $\pm$ 2	6	Barber et al. 1996
Station ALOHA, Pacific, 0-50m	1991-92	28 $\pm$ 7	18	Karl et al. 1995

A number of reasons led us to assume that nitrate uptake was indeed underestimated. Nitrate uptake was measured at only 3 upwelling stations on each cruise, and variability was high, so we possibly did not sample areas where higher nitrate uptake occurred. Additionally, the depth resolution of nitracline sampling appears suboptimal at a few stations during VG7, where e.g. the profile from station 62\_1 appears truncated at 50m depth (Fig. 2.4). Areal daily rates of nitrate uptake were calculated by extrapolating hourly rates (from short morning incubations) to 12h of daylight, whereas upwelling fluxes represent a nitrate supply within 24h. Thus, areal rates do not represent any potential night time uptake by phytoplankton that used energy reserves from photosynthesis. Nearly constant nitrate uptake over a day-night cycle may occur especially at the bottom of the euphotic zone (Cochlan et al. 1991). Nitrate uptake during night was measured in various ocean regions including the upwelling systems off northwest Africa and Peru, where average night time rates were 20% and 25% of day rates, respectively (Eppley et al. 1970; Collos and Slawyk 1976; MacIsaac 1978; Cochlan et al. 1991). Lastly, our rate measurements likely do not include bacterial nitrate assimilation, since the water from nitrate uptake incubations was filtered over GF/F filters with a pore size of 0.7  $\mu\text{m}$ . Bacterial nitrate assimilation (*nasA*, *narB*) genes are widely distributed in marine environments (Allen et al. 2001; Paerl et al. 2008), and should mainly represent cells from 0.2-0.8 $\mu\text{m}$  size fraction (Allen et al. 2001). The contribution of bacteria to total nitrate assimilation was reported to be as high as 32% in some areas (Kirchman and Wheeler 1998).

On the other hand, expecting a balance between fluxes and rates would also require the calculated upwelling fluxes to be realistic estimates of the amount of nitrate that became available to primary producers within the euphotic zone. The estimates of nitrate supply by Ekman upwelling are higher than modeled July-averaged upwelling fluxes of about 9  $\text{mmol N m}^{-2} \text{d}^{-1}$  (Fig. 2.7a) (Liu et al. 2002). For VG7 data, our fluxes agree well with the N-demand of primary productivity, suggesting that they are still of realistic magnitude, but this was not the case for VG3 (Fig. 2.7a). During each cruise, nitrate concentrations in the MSW as well as the upwelling nitrate fluxes did not vary much, but there was considerable variation in the depth of the MSW horizon (Table 2.1). Since the MSW water will have mixed with water of lower nitrate concentration as it traveled upwards, it is likely that the daily nitrate uptake within the EZD (which was  $\leq 45\text{m}$  according to the few VG7 LICOR readings) was lower than the calculated nitrate fluxes out of the MSW. The notion that the nitrate uptake mainly occurred shallower than at MSW depth is supported by the available rate profiles of nitrate uptake (Fig. 2.4), as well as by the mentioned chlorophyll maxima which were not deeper than 40m during both cruises. The MSW overall lay deeper during VG3 (Table 2.1), whereas EZDs should have been similar to VG7, and this could explain the larger discrepancy between flux estimates and

nitrate uptake rates as well as between flux estimates and N-demands of primary productivity during VG3. We therefore assume that the initial nitrate flux estimates represent a potential maximum of new production, which was realized to a greater extent during stronger upwelling in 2004.

Primary productivity at VG7 upwelling stations is similar to values from the Arabian Sea (Table 2.3), where the SW-monsoon induces upwelling between 7° and 11°N along the coast of Somalia and off the Omani coast (Veldhuis et al. 1997; Barber et al. 2001; Marra and Barber 2005). Average primary productivity of 104 mmol C m<sup>-2</sup> d<sup>-1</sup> (off Somalia, Veldhuis et al. 1997) and 123 ± 9 mmol C m<sup>-2</sup> d<sup>-1</sup> (off Oman, Barber et al. 2001) lie in the upper range of values reported here. Much higher productivity is yet found in eastern boundary upwelling systems like for example off northeast Africa (Table 2.3) (Huntsman and Barber 1977). Productivity during VG3 was considerably lower, reflecting the reduced upwelling intensity due to ENSO influence (Table 2.3). Liu et al. (2002) estimated that volume-integrated primary production during the seasonal upwelling off Vietnam could account for 12% of the basin wide total annual primary production in the SCS. Their modelled July-averaged primary productivity of approximately 70 mmol C m<sup>-2</sup> d<sup>-1</sup> exceeds all VG3 rates but lies in the lower range of VG7 values (Table 2.3). Our data thus confirm that primary production in the Vietnamese upwelling is of great relevance for carbon cycling in the SCS, but is also subject to pronounced interannual variability. It is therefore essential to further investigate the modulation of upwelling intensity due to interannual climate variability, and the influence of this variability on the productivity of the SCS as a whole, in order to truly understand the biogeochemistry of this marginal sea.

### 2.5.3 Primary productivity and nitrate supply at offshore stations

Pronounced seasonal variability of primary productivity can also be found in offshore regions of SCS. At the South East Asian Time-series Study site (SEATS station, 18°N, 116°E), primary productivity typically peaks during winter months (up to 25 mmol C m<sup>-2</sup> d<sup>-1</sup>), when mixed layer depths down to 90m exceed nitracline depths between 50 and 70m, due to convective overturning and enhanced vertical mixing by the strong NE-monsoon (Tseng et al. 2005). During the rest of the year, the MLD stay relatively shallow (20-40m), but nitracline depths remain about equal (Wu et al. 2003; Tseng et al. 2005). As a consequence, low average primary productivity of 9 mmol C m<sup>-2</sup> d<sup>-1</sup> is found (Tseng et al. 2005). The nitraclines in the open SCS are shallower than e.g. at station ALOHA in the permanently stratified, tropical Pacific (120 ± 20m, Chen et al. 2003, 2004; Karl et al. 2003; Tseng et al. 2005). This suggests that diffusive

nitrate fluxes should have a particularly strong influence on primary productivity, especially under conditions of increased stratification and N-limitation during summer.

Coefficients of turbulent diffusion computed for offshore stations during VG3 represent only a snapshot of diffusive processes, but they may be used here to get an impression of the possible magnitude of diffusive vertical nitrate fluxes. The surface values between 0.1 and 4.1  $\text{cm}^2 \text{s}^{-1}$  reflect weak wind speeds of 2–4  $\text{m s}^{-1}$  in July 2003. The local surface maximum of 54  $\text{cm}^2 \text{s}^{-1}$  at station 13 was caused by a short wind event with speeds of more than 18  $\text{m s}^{-1}$  (Dippner et al. 2007). Diffusion coefficients of around 3  $\text{cm}^2 \text{s}^{-1}$  at 105 and 125 m water depth at stations 43 and 24 can be attributed to the strong shear of an upwelling-induced counter current at the shelf edge (Dippner et al. 2007). Apart from the local near-surface maxima (Fig. 2.6), diffusivities of  $\leq 1.0 \text{ cm}^2 \text{ s}^{-1}$  between 30 and 60m depth lie in the same order of magnitude as values for other open ocean systems (Lewis et al. 1986; Ledwell et al. 1993; Michaels et al. 1996; Zhang et al. 2001). Zhang et al. (2001) found average diffusion coefficients of  $1.0 \pm 0.3 \text{ cm}^2 \text{ s}^{-1}$  in an oligotrophic anticyclonic eddy in the northeast Atlantic at 46°N, using SF6 tracer-injection experiments. Lower values were reported from sites south of 30°N in the tropical Atlantic, varying between 0.1 and 0.4  $\text{cm}^2 \text{ s}^{-1}$  (e.g. Lewis et al. 1986; Ledwell et al. 1993). Wind-induced mixing in the SCS should overall be stronger than in the tropical Atlantic due to the monsoonal forcing, suggesting that diffusion coefficients in the order of 1.0  $\text{cm}^2 \text{ s}^{-1}$  determined for VG3 might be characteristic values.

The average diffusive nitrate flux of  $2.3 \pm 0.6 \text{ mmol N m}^{-2} \text{ d}^{-1}$  (Table 2.2) is e.g. similar to a value determined for the Sargasso Sea ( $2.3 \pm 0.7 \text{ mmol N m}^{-2} \text{ d}^{-1}$ , Jenkins and Doney 2003), but high compared to a maximum value of 0.74  $\text{mmol N m}^{-2} \text{ d}^{-1}$  reported for the tropical Atlantic in a paper by Capone et al. (2005). In that study, nitrate gradients were  $0.23 \pm 0.015 \text{ mmol m}^{-4}$  ( $n=24$ ), which are similar to ours (Table 2.2), but the maximal eddy diffusivity of 0.36  $\text{cm}^2 \text{ s}^{-1}$ , taken from Lewis et al. (1986), appears too low for our area because of the wind forcing. Although the measured rates of nitrate uptake (Fig. 2.7b) are comparable to values reported for offshore waters in the northern SCS ( $\geq 0.4 \text{ mmol N m}^{-2} \text{ d}^{-1}$ , Chen 2005), we assume that they could be underestimations for the mentioned reasons (see section 2.5.2). In all, we found a roughly consistent range of diffusive nitrate fluxes, N-demands of primary productivity, and nitrate uptake rates (Fig. 2.7b), suggesting that the diffusive fluxes are realistic values which likely represent an upper boundary of diffusive nitrate supply at VG3 offshore stations. The available rate measurements did not reflect the slight variations in MLD and nitracline depths in the offshore zone. Rates of primary productivity were variable, but the overall VG3 average of  $10 \pm 5 \text{ mmol C m}^{-2} \text{ d}^{-1}$  is in good agreement with rates between 9 and

16 mmol C m<sup>-2</sup> d<sup>-1</sup> which were determined for offshore waters in the northern SCS (Tseng et al. 2005; Chen 2005) (Table 2.3).

If we assume a coefficient of turbulent diffusion similar to cruise VG3, the average diffusive nitrate flux for VG7 offshore stations would be  $1.8 \pm 0.5$  mmol N m<sup>-2</sup> d<sup>-1</sup> (Table 2.2). This estimate is similar to areal rates of nitrate uptake at station 33 (2.0 mmol N m<sup>-2</sup> d<sup>-1</sup>) and 65\_1 (1.2 mmol N m<sup>-2</sup> d<sup>-1</sup>). However, unlike for VG3, the range of N-demand of primary productivity exceeds the range of diffusive fluxes (Fig. 2.7b). Except for station 83, the range of primary productivity is still in agreement with values from other tropical open ocean areas (Table 2.3), but similarly low primary productivity as at VG3-station 45 or the SEATS station were never observed during VG7. Since upwelling was stronger, productivity at stations close to the upwelling zone was likely not only fuelled by diffusive fluxes from below, but also by laterally advected nitrogen species from the upwelling zone, possibly in the form of regenerated nitrogen that accumulated in aged upwelling waters. This could also explain the prevalence of surface maxima in primary productivity at VG7 offshore stations, whereas during VG3, mainly subsurface maxima were found (Fig. 2.4).

#### 2.5.4 N<sub>2</sub> fixation as a source of new nitrogen

The areal rates of N<sub>2</sub> fixation overall cover a range between 10 and 375 μmol N m<sup>-2</sup> d<sup>-1</sup> (Fig 2.9a). These numbers fall into the lower range of values from the western part of the tropical North Atlantic, where average N<sub>2</sub> fixation measurements vary between  $85 \pm 23$  and  $898 \pm 234$  μmol N m<sup>-2</sup> d<sup>-1</sup>, with an average  $239 \pm 38$  μmol N m<sup>-2</sup> d<sup>-1</sup> (Capone et al. 2005). Based on this dataset, it was suggested that N<sub>2</sub> fixation in the tropical Atlantic is between 50% and 180% of the nitrate supply by turbulent diffusion through the thermocline (Capone et al. 2005).

A comparison of rates of N<sub>2</sub> fixation and nitrate uptake implies that N<sub>2</sub> fixation contributed up to around 50% to total new production at some stations (VG3 station 33, 33A, VG7 stations 83, 55; Fig. 2.5d). The lowest contributions were found within the upwelling zone during VG7 (0.8% maximum at station 52). However, as outlined in section 2.5.2, nitrate uptake was likely underestimated at some stations, so these numbers should be interpreted with caution. Compared to our estimates of vertical nitrate fluxes, N<sub>2</sub> fixation appears as an insignificant N-source within the upwelling zone, with around 0.2% of VG7 upwelling fluxes, and maximal 1.3% of the vertical flux at VG3 upwelling station 33A. At stations in the adjacent offshore zone, N<sub>2</sub> fixation was between 1% and 5% of the vertical diffusive nitrate flux during VG3, and between 2% and 25% of the diffusive nitrate flux during VG7.

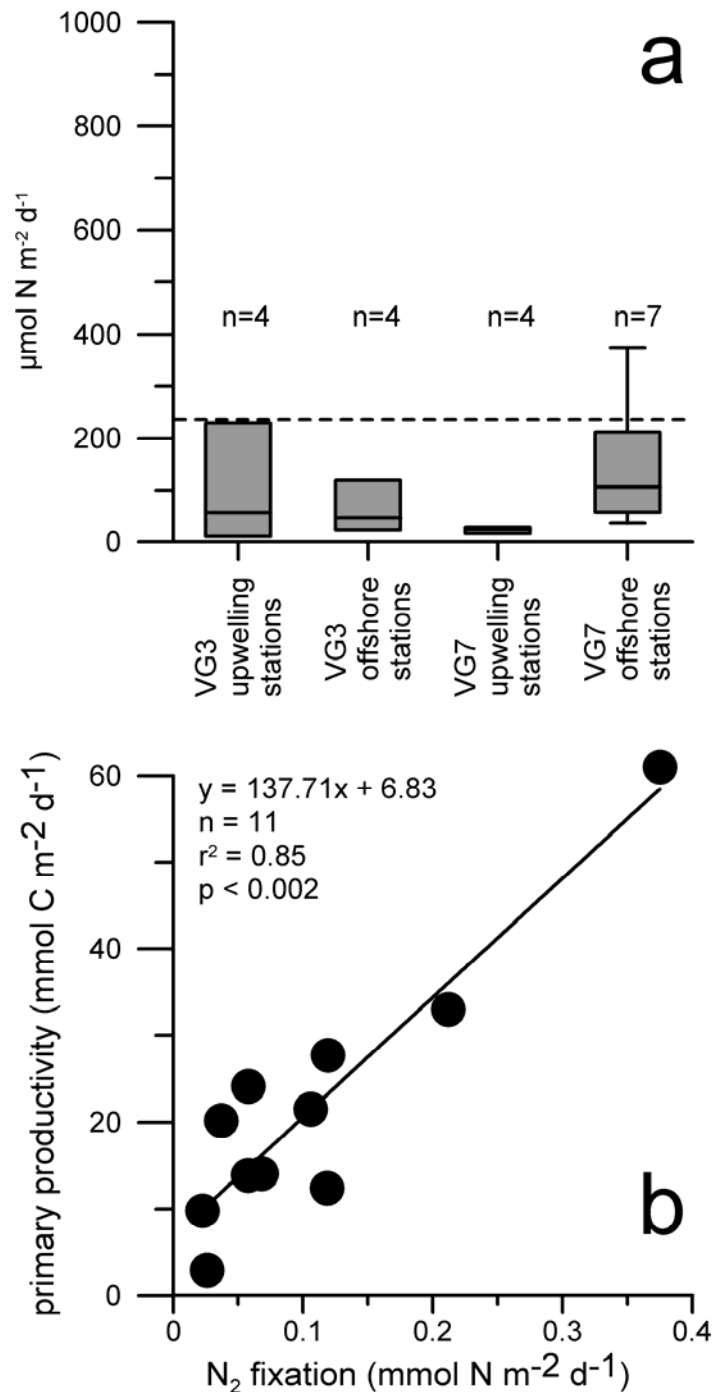


**Figure 2.9:** (a) Areal rates of  $N_2$  fixation at upwelling- and offshore stations during both cruises. The dashed horizontal line represents the average  $N_2$  fixation rate in the tropical north Atlantic (Capone et al. 2005). Note that the units are  $\mu\text{mol N m}^{-2} \text{d}^{-1}$ . Box-whisker plots are defined as mentioned in Fig. 2.7. n = number of stations. (b) Relationship between  $N_2$  fixation and primary productivity at offshore stations (pooled data from both cruises).

$N_2$  fixation supported between 0.1% and 8.2% of the N-demand of primary productivity during VG3 and VG7 (Voss et al. 2006). Stable isotope data reported by Loick et al. (2007) suggest that overall 9% (VG3) and 13% (VG7) of the nitrogen in the zooplankton food source was derived from  $N_2$  fixation. In a recent paper, Gaye et al. (2009) analyze the stable nitrogen isotopic composition of sediment trap material from 1200m at a station close to our station 34. The authors report that  $N_2$  fixation may have contributed up to 12% to the

total nitrogen flux during the years 1998/1999 and 2004/2005. Our estimates of the relative importance of  $N_2$  fixation are roughly consistent with the integrative isotope approaches. The rate measurements might be conservative estimates, since they do not represent any  $N_2$  fixation that possibly happened at night. In all, the results from independent approaches strongly support the role of  $N_2$  fixation as a significant source of new nitrogen in the area.

An interesting result is that highest rates of  $N_2$  fixation were not generally observed at “most oligotrophic” stations furthest offshore, but at stations which were likely still affected by upwelling. This is indicated by a significant positive correlation between areal rates of  $N_2$  fixation and primary productivity (Fig. 2.9b). This correlation also exist for VG7-data alone ( $p < 0.01$ ,  $n=7$ ), but not for VG3 data ( $p > 0.5$ ,  $n=4$ ). In a recent study, Bonnet et al. (2009) investigated  $N_2$  fixation in the western equatorial Pacific and found the highest rates in coastal waters off Papua New Guinea, possibly reflecting a positive response of diazotrophs to elevated concentrations of dissolved iron and phosphorus. Based on a clear link between low salinities and high rates of  $N_2$  fixation, it was argued that off the Vietnamese coast, the Mekong river plume sets favourable conditions for diazotrophs (and for diatom-diazotroph associations in particular) by introducing trace metals such as iron, as well as nutrient loads with low N:P- and high Si:N ratios (Voss et al. 2006). In the same paper, Voss et al. (2006) noted that upwelled nutrients had N:P ratios  $< 16$ , suggesting that a surplus of phosphorus from depth may also have positively affected  $N_2$  fixers. Further studies are necessary to test these assumptions and to identify important members of the diazotroph community in the area.

### 3. The Mekong River plume fuels nitrogen fixation and determines phytoplankton species distribution in the South China Sea during low and high discharge season

#### 3.1 Abstract

The influence of the Mekong River (South China Sea) on N<sub>2</sub> fixation and phytoplankton distribution was investigated during the lowest and highest discharge season in April 2007 and September 2008. The river plays an essential role in providing nutrients (nitrate, phosphate, silica) for the adjacent sea and creates different salinity and nutrient gradients over different seasons. River water (salinity 0), mesohaline waters (salinity 14-32), a transition zone with salinities between 32 and 33.5, and marine waters (salinity above 33.5) were sampled at different spatial resolutions in both cruises. High N<sub>2</sub> fixation rates were measured during both seasons, with rates of up to 5.05 nmol N L<sup>-1</sup> h<sup>-1</sup> in surface waters under nitrogen-replete conditions, increasing to 22.77 nmol N L<sup>-1</sup> h<sup>-1</sup> in nitrogen-limited waters. Asymbiotic diatoms were only found close to the river mouth, and diatoms which potentially hosted diazotroph symbionts were most abundant in waters where N<sub>2</sub> fixation rates were highest, nitrate concentrations were at the detection limit, and phosphate and silicate were still available. Filamentous cyanobacteria like *Trichodesmium* were only present in marine waters with salinities above 33.5. Overall, N<sub>2</sub> fixation accounted for 1% to 47% of the nitrogen demand of primary production.

### 3.2 Introduction

Dinitrogen (N<sub>2</sub>) fixation plays an important role in fueling the oligotrophic ocean with nitrogen (N) (Karl et al. 2002). Recent studies propose that N<sub>2</sub> fixation may also be significant in coastal and other nutrient rich environments (Deutsch et al. 2007; Bonnet et al. 2009). In this context, river plumes have been suggested to host other groups of N<sub>2</sub> fixing organisms than the typical open-ocean diazotrophs *Trichodesmium* and unicellular cyanobacteria (Capone et al. 1997; Church et al. 2005a); for example, in the Amazon River plume, diatom-diazotroph associations (DDAs) can displace *Trichodesmium* as the dominant diazotroph of the region, and rates of N<sub>2</sub> fixation in DDA blooms exceed vertical nitrate fluxes (Carpenter et al. 1999; Subramaniam et al. 2008). Diatoms hosting diazotroph symbionts come from various genera. *Hemiaulus*, *Rhizosolenia*, *Guinardia*, and *Bacteriastrum*, associate with the heterocystous cyanobacterium *Richelia intracellularis*, while diatoms of the genus *Chaetoceros* are typically found in symbiosis with *Calothrix rhizosoleniae*, another diazotroph cyanobacterium which is closely related to *Richelia* (Carpenter 2002; Foster and Zehr 2006). The trichomes of *Richelia intracellularis* reside as an endosymbiont between the plasmalemma and the frustule of the diatom in *Hemiaulus*, *Rhizosolenia*, and *Guinardia* (Villareal 1992). In the DDAs *Bacteriastrum-Richelia intracellularis* and *Chaetoceros-Calothrix rhizosoleniae*, the symbiont resides as an epiphyte on the spines of the diatom (Carpenter 2002; Foster and O'Mullan 2008). Studies by Foster and others (2007) later confirmed that DDAs (*Hemiaulus-Richelia*) dominate in the Amazon River plume waters with measurable concentrations of nitrate (NO<sub>3</sub>) (<0.01 - 0.13 μmol L<sup>-1</sup>), phosphate (PO<sub>4</sub>) (<0.02 - 0.13 μmol L<sup>-1</sup>), and silicate (Si(OH)<sub>4</sub>) (0.3 - 11.3 μmol L<sup>-1</sup>), while *Trichodesmium* and different groups of free-living unicellular cyanobacteria were more abundant in oceanic waters outside the river plume, where nutrients were below the detection limit (Foster et al. 2007; Subramaniam et al. 2008). Also in the Congo River plume in the Eastern Equatorial Atlantic, conditions seem to be favorable for DDAs, even though, *Trichodesmium* dominated the diazotroph community (Foster et al. 2008). The DDAs are thought to have a growth advantage in river plumes where nitrogen is limiting but phosphorus and silicate are still available, while nitrogen is supplied through N<sub>2</sub> fixation by the diazotroph symbiont (Janson et al. 1999; Carpenter 2002). Furthermore, tropical rivers provide trace metals such as iron (Nittrouer et al. 1995; Bergquist and Boyle 2006), which is an essential component of the dinitrogenase enzyme complex of all diazotrophs. All of these findings suggest that enhanced N<sub>2</sub> fixation in tropical river plumes might be a global phenomenon and would thus contribute substantially to oceanic N<sub>2</sub> fixation.

Like other tropical rivers, the Mekong River discharges relatively high concentrations of nutrients, with over 40  $\mu\text{mol L}^{-1}$  of nitrate plus nitrite ( $\text{NO}_3+\text{NO}_2$ ) and about 1  $\mu\text{mol L}^{-1}$  of  $\text{PO}_4$ , and over 100  $\mu\text{mol Si(OH)}_4$  (www.gemstat.org). These nutrients foster new production in the South China Sea (SCS) into which the Mekong River discharges. Previous results from the SCS show that the Mekong River plume is linked to elevated rates of N<sub>2</sub> fixation as far as 200 km northeast of the river mouth (Voss et al. 2006), which suggests a scenario similar to the one in the Amazon River plume. The study by Voss et al. (2006) investigated the Vietnamese upwelling area and the adjacent offshore oligotrophic region, where diazotroph species were possibly influenced by both riverine- and initially upwelled nutrients. In contrast to the study by Voss et al. (2006), we carried out a detailed sampling closer to the river mouth, where the changes in salinity- and nutrient concentrations are expected to have the greatest influence on species composition and rates of N<sub>2</sub> fixation. The diazotroph community in the SCS includes DDAs, *Trichodesmium*, and unicellular diazotrophs (<10  $\mu\text{m}$ ), comprising of coccoid cyanobacteria and proteobacteria (Moisander et al. 2008), and it can be expected that the Mekong River plume triggers unequal distribution patterns of these different groups. In the present study, we measured rates of N<sub>2</sub> fixation and determined phytoplankton species composition in SCS surface waters off the Mekong river mouth. The study compares two field investigations, one conducted in April 2007, coinciding with intermonsoon and the river's lowest annual outflow, and a second investigation, conducted in September 2008 during southwest (SW) monsoon and the river's highest annual outflow (Hoa et al. 2007). The goals of this study are to describe and compare the biogeochemical settings of the river plume during both seasons, and to assess how these settings are related to N<sub>2</sub> fixation and to the distribution of phytoplankton, including asymbiotic diatoms, *Trichodesmium* spp., and different diatom species that potentially host diazotroph symbionts.

### 3.3 Materials and methods

#### 3.3.1 Study area

The Mekong Delta lies between 9.0°N and 10.5°N in the Southeast Asian monsoon region. The SW monsoon between June and September coincides with the rainy season and the rivers largest annual outflow (40,000  $\text{m}^3 \text{s}^{-1}$ , Hoa et al. 2007). During this time of the year the winds have an approximate speed of 6  $\text{m s}^{-1}$  (Hellerman and Rosenstein 1983) and deflect the river plume northeast along the coast before it turns east into the open SCS. The northeast (NE) monsoon appears between November and March, coinciding with the dry season, and the prevailing winds have an average velocity of 9  $\text{m s}^{-1}$  (Hellerman and Rosenstein 1983). The

intermonsoon during April and May and during October and early November marks the transition between monsoon seasons (Fang et al. 2002). In April, at the end of the dry season, the river outflow reaches its annual low with an outflow of about  $2100 \text{ m}^3 \text{ s}^{-1}$  (Hoa et al. 2007) resulting in a relatively small river plume (covering approximately  $37,000 \text{ km}^2$  of the SCS), which is deflected southward. The total freshwater discharge of the Mekong River is about  $500 \text{ km}^3 \text{ yr}^{-1}$ , with 15% being discharged during the dry season, and 85% during the rainy season (Hoa et al. 2007). Compared to the Amazon and Congo River with  $6900 \text{ km}^3 \text{ yr}^{-1}$  and  $1300 \text{ km}^3 \text{ yr}^{-1}$ , respectively (Korzun 1978; World Hydrology Cycle Observing System, [www.whycos.org](http://www.whycos.org)) the discharge by the Mekong River is low, but it is the largest river draining into the SCS.

Annual loads of total nitrogen (TN) and total phosphorus (TP) are modeled for the river mouth reaching  $2.7 \times 10^4 \text{ t TN yr}^{-1}$  and  $9.0 \times 10^2 \text{ t TP yr}^{-1}$  (Yoshimura and Takeuchi 2007). The model also predicts a discharge of  $0.1 \text{ kg TN s}^{-1}$  during the dry season (December through May) and  $10 \text{ kg TN s}^{-1}$  during rainy season (May through November) (Yoshimura and Takeuchi 2007).

### 3.3.2 Sampling

Samples were collected aboard a Vietnamese monitoring vessel, BTh-0666 KN, between 15 April and 20 April 2007 (Fig. 3.1A) and between 18 September and 22 September 2008 (Fig. 3.1B). About 40% of the total water volume is discharged from the southernmost river arm (Sta. 3 in April 2007 and Sta. 24 in September 2008), whereas the other river arms represented by the Sta. 20 and Sta. 2 (April 2007) and Sta. 1 and Sta. 12 (September 2008) discharge  $\sim 30\%$  and  $13\%$ , respectively (Nguyen et al. 2008).

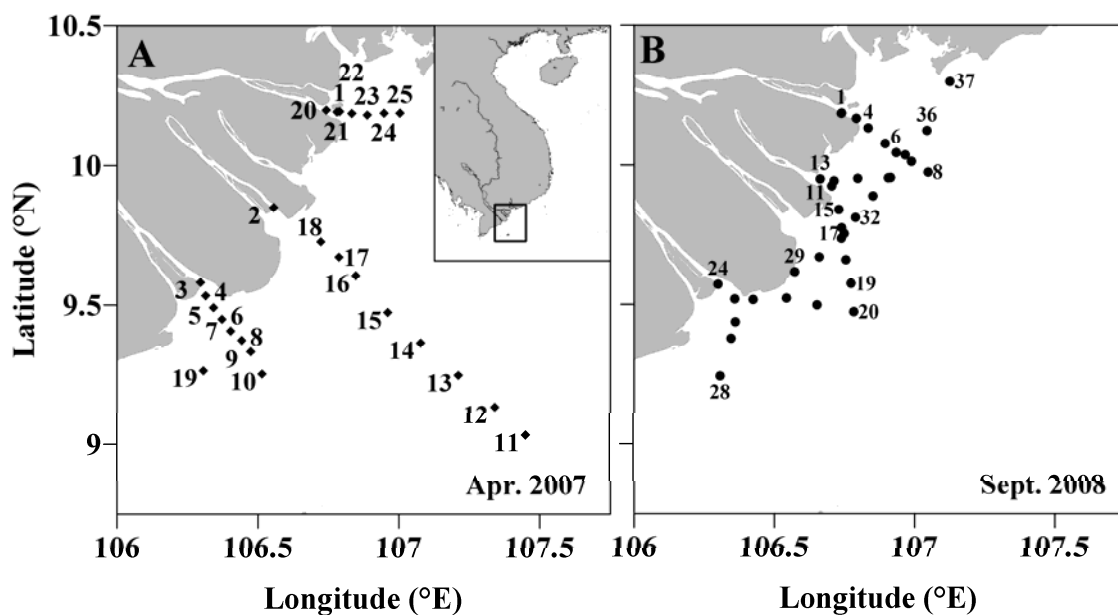


**Figure 3.1:** Map of the Mekong River Estuary with all CTD-stations of (A) April 2007 and (B) September 2008. The map was drawn with the Surfer ® 8.09 of Golden Software Inc.

Northeasterly winds of 10 to 12 m s<sup>-1</sup> occurred during a two-week period before the cruise in April 2007 and mixed the entire water column. Throughout the first four days of the cruise in April 2007 (Sta. 1-20) winds did not restrict sampling but on the northernmost transect (Sta. 21-25) winds of 6 m s<sup>-1</sup> allowed sampling only for nutrient concentrations and phytoplankton composition. Three transects were sampled, each started in a river arm and was directed out to the open sea. We planned to sample the same stations in September 2008, but because of constant winds between 5 and 10 m s<sup>-1</sup> sampling farther offshore was impossible and was kept close to the coast.

At all stations, the entire water column was measured for conductivity, temperature and depth (CTD) with Seabird sensors (SEB19 plus) and turbidity was measured with a Seapoint Turbidity Meter (recording Nephelometric Turbidity Units [NTU], waters below 10 NTU have moderate plant and animal life; waters below 1 NTU represent oligotrophic conditions; CWT 2004). A total of 25 (April 2007) and 35 (September 2008) surface samples (0 to 1 m) were taken with a 10 L Niskin bottle. A 24-hour time-series station (Sta. 19, Fig. 2.1A) was sampled between 05:30 h on 18 April 2007 and 07:00 h on 19 April 2007. The time-series station was sampled hourly with the CTD and provided a total of seven sampling points (SP) for nutrients, chlorophyll, phytoplankton, N<sub>2</sub> fixation, and primary production (sampling every 3 hours during the day, every six hours during the night). The same station (Sta. 28, Fig. 2.1B) was sampled again between 11:40 h on 20 September 2008 and 11:40 h on 21 September 2008, providing hourly measurements with a CTD between 11:40 h and 17:40 h (20 September 2008) as well as 05:40 h and 11:40 h (21 September 2008), and a total of four SP for chlorophyll, N<sub>2</sub> fixation, primary production, and phytoplankton (sampling every 6 hours) as well as six SP for nutrients (sampling every three hours). The geographical position of this time-series station was chosen in order to enable sampling of the hydrographic situation of the Mekong River plume throughout a complete tidal cycle.

### 3.3.3 Analyses

Water samples for the determination of NO<sub>3</sub>, NO<sub>2</sub>, PO<sub>4</sub>, and Si(OH)<sub>4</sub> were taken, filtered through Whatman GF/F glass fibre filters (0.7 μm pore size), and stored frozen onboard before they were analyzed at the Institute of Oceanography, Nha Trang. Standard colorimetric methods (Grasshoff 1983) were used. These methods usually reach a precision of 0.05 μmol L<sup>-1</sup> for NO<sub>3</sub>, 0.01 μmol L<sup>-1</sup> for NO<sub>2</sub>, 0.01 μmol L<sup>-1</sup> for PO<sub>4</sub>, and 0.1 μmol L<sup>-1</sup> for Si(OH)<sub>4</sub>. However, due to the local circumstances (nutrient traces in the only available distilled water), we could not achieve a precision better than 0.05 μmol L<sup>-1</sup> for NO<sub>3</sub>, NO<sub>2</sub>, and PO<sub>4</sub>. Nutrient

ratios (N:P, Si:N) were therefore not calculated for samples having unreliable concentrations  $\leq 0.1 \mu\text{mol L}^{-1}$ .

Chlorophyll *a* (Chl *a*) was measured at 12 stations in April 2007 and at 15 stations in September 2008. A water volume between 100 - 2000 mL was used to cover a Whatman GF/F glass fiber filter appropriately with organic material. Chlorophyll samples were stored frozen at  $-80^{\circ}\text{C}$  until analyzed. Chlorophyll was extracted in ethanol and measured with a Turner 10-AU-005 fluorometer (Wasmund et al. 2006).

Samples for phytoplankton identification (1.5 L) were taken at 21 stations (April 2007) and 13 stations (September 2008) and preserved with 0.5 mL Formaldehyde (33%) and 10 mL of Lugol solution, according to the Intergovernmental Oceanographic Commission protocol (Hallegraff et al. 1995). Phytoplankton identification and counting by light microscopy included only the size fraction  $>10 \mu\text{m}$  and was carried out using standard protocols after Utermöhl (1958). A fluorescence microscope for the detection of intracellular symbionts was not available.

Rates of N<sub>2</sub> fixation and primary production were measured using the tracer assay described by Montoya et al. (1996). Surface water was taken with Niskin bottles at 9 stations in April 2007 and at 13 stations in September 2008. The water was filled into three 2.3 L Nalgene bottles at each station. The Nalgene bottles were equipped with septum caps made of Teflon-lined butyl rubber. Subsequently, both <sup>15</sup>N<sub>2</sub> gas (2 mL; Sercon, 99 atom%) and  $0.1 \mu\text{mol L}^{-1}$  NaH<sup>15</sup>CO<sub>3</sub> solution (0.5 mL; Sigma Aldrich, 98 atom%), were added with syringes. The bottles were incubated on deck and cooled with surface seawater. During the day, the incubations lasted for 6 hours and the incubators were covered with neutral density screening (50%), which correspond to the light intensities of surface waters of mesotrophic waters or 10 m depth in oligotrophic waters. At night, the incubations lasted about 12 hours to assure a <sup>15</sup>N<sub>2</sub> uptake above the detection limit. Due to the limited cruise time during both investigations, N<sub>2</sub> fixation and primary production incubations were always initiated immediately after sampling so that most day-incubations lasted either from 06:00 h – 12:00 h or from 12:00 h – 18:00 h. Incubations during the night covered the entire dark period (Table 3.1).

The incubations were terminated by gentle vacuum filtration. In April 2007, N<sub>2</sub> fixation was measured in two size fractions ( $<$  and  $>10 \mu\text{m}$ ), and the total N<sub>2</sub> fixation rates were calculated by adding the respective rates. Samples were initially filtered through acid-washed gauze ( $10 \mu\text{m}$  pore-size). The filamentous cyanobacteria and diatoms ( $>10 \mu\text{m}$ ) were then rinsed onto precombusted Whatman GF/F glass fiber filters (4 h at  $500^{\circ}\text{C}$ ,  $0.7 \mu\text{m}$  pore size). The particles  $<10 \mu\text{m}$  in the filtrate were collected over additional glass fiber filter. In September 2008 the size fractions were not separated, and only total N<sub>2</sub> fixation rates were

measured. All filters were stored frozen at -20°C. In the laboratory, the filters were acidified over fuming hydrochloric acid (37%) for six hours, subsequently dried (40°C; 12 h), packed into tin cups, and pelletized. Isotopic measurements of the filters were done with a Delta S (Thermo) isotopic ratio mass spectrometer connected to an elemental analyzer CE1108 via open split interface. Rates of N<sub>2</sub> fixation and primary production were calculated as described by Montoya et al. (1996).

**Table 3.1:** Total N<sub>2</sub> fixation rates and percentage of each size fraction on total N<sub>2</sub> fixation for April 2007. For September 2008, only total rates are available. N<sub>2</sub> fixation incubations occurred during: day hours (sunrise - sunset) and lasted 6 hours; underlined values indicate incubations lasting 06:00 h – 12:00 h, bold values indicate incubations lasting 12:00 h – 18:00 h; night incubations (sunset – sunrise) lasted 12 hours and are italic

April 2007					September 2008		
Station	Total N <sub>2</sub> fixation (nmol N L <sup>-1</sup> h <sup>-1</sup> )	% of total N <sub>2</sub> fixation (<10 μm) (>10 μm)			Station	Total N <sub>2</sub> fixation (nmol N L <sup>-1</sup> h <sup>-1</sup> )	
<i>1</i>	<i>night</i>	<i>0.11</i>	<i>68.96</i>	<i>31.04</i>	<u>1</u>	<u>day</u>	<u>0.69</u>
<u>2</u>	<u>day</u>	<u>1.01</u>	78.36	21.64	4	day	0.06
<b>3</b>	<b>day</b>	<b>1.07</b>	<b>70.55</b>	<b>29.45</b>	<b>6</b>	<b>day</b>	<b>3.06</b>
8	day and night	6.13	67.26	32.74	8	day	4.22
<i>10</i>	<i>night</i>	<i>3.95</i>	<i>74.83</i>	<i>25.17</i>	<i>11</i>	<i>night</i>	<i>0.12</i>
<u>11</u>	<u>day</u>	<u>11.36</u>	95.15	4.85	<u>13</u>	<u>day</u>	<u>0.13</u>
<b>15</b>	<b>day</b>	<b>16.36</b>	<b>6.56</b>	<b>93.44</b>	15	day	3.51
20SP1	day and night	0.60	75.51	24.49	17	day	0.90
<u>20SP2</u>	<u>day</u>	<u>2.86</u>	55.01	44.99	20	day	5.05
<u>19SP1</u>	<u>day</u>	<u>15.54</u>	46.77	53.23	<i>20</i>	<i>night</i>	<i>2.34</i>
19SP2	day	12.90	73.78	26.22	<u>24</u>	<u>day</u>	<u>0.18</u>
<b>19SP3</b>	<b>day</b>	<b>22.77</b>	<b>63.06</b>	<b>36.94</b>	<u>29</u>	<u>day</u>	<u>1.66</u>
19SP4	day	12.52	21.02	78.98	<b>36</b>	<b>day</b>	<b>0.74</b>
<i>19SP5</i>	<i>night</i>	<i>14.62</i>	<i>26.83</i>	<i>73.17</i>	<b>28SP1</b>	<b>day</b>	<b>0.70</b>
<i>19SP6</i>	<i>night</i>	<i>18.99</i>	<i>23.80</i>	<i>76.20</i>	<i>28SP2</i>	<i>night</i>	<i>0.10</i>
<u>19SP7</u>	<u>day</u>	<u>15.70</u>	35.59	64.41	<u>28SP3</u>	<u>day</u>	<u>1.02</u>
					<i>28SP4</i>	<i>day and night</i>	<i>0.64</i>

### 3.4 Results

#### 3.4.1 Hydrographic conditions and nutrient distributions

The coastal waters of the SCS are characterized by strong tides of up to 4.5 m (Hoa et al. 2007), which cause a deep intrusion of ocean waters upstream into the Mekong River during the intermonsoon, the low discharge season. In April 2007, waters with a salinity of 0 were therefore found approximately 30 km upstream (H. Hein unpubl. data). A sample of Mekong River freshwater was taken at the station My Tho, which lies app. 50 km upstream. The lowest salinity at sampling stations in the River mouth was 14.3 (Sta. 3), and from there, salinities gradually increased to maximal values of around 34 at stations farthest offshore (Fig. 3.2A).

During SW monsoon in September 2008, the outflow was much higher so that freshwater was found in the river arms at Sta. 1 and 24 (Fig. 3.2B). The plume extended much farther offshore during that cruise; however, due to considerable swell it was impossible for our small vessel to reach sampling stations as far offshore as in April 2007. Salinities above 30 were measured at outer Sta. 8 and 20, and the maximal salinities were found at Sta. 28, ranging between 31.9 and 32.0.

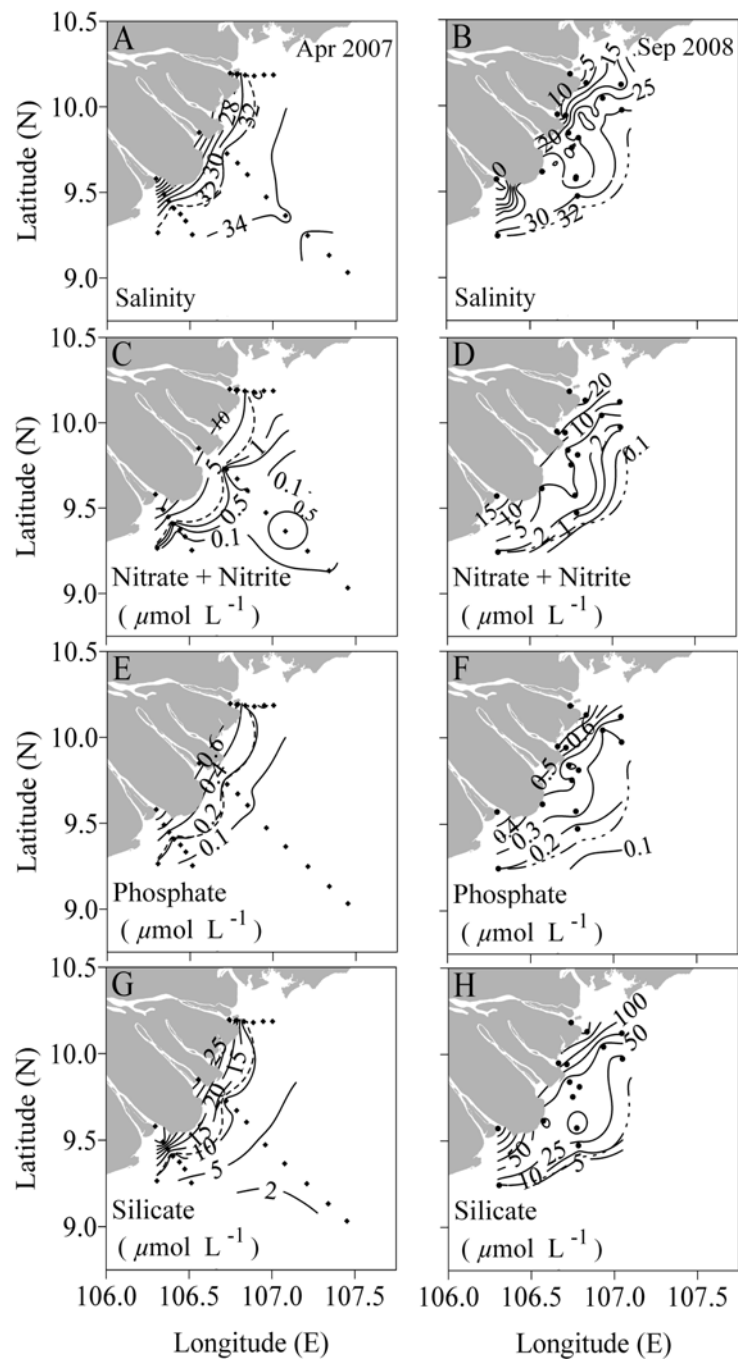


**Figure 3.2:** Salinity and nutrient distribution in the investigation area. Plots showing horizontal distributions of salinity (A, B), NO<sub>3</sub><sup>-</sup>+ NO<sub>2</sub><sup>-</sup> concentrations (C, D), PO<sub>4</sub> concentrations (E, F) and Si(OH)<sub>4</sub> concentrations correspond to April 2007 (left column) and September 2008 (right column). 2.0 µmol L<sup>-1</sup> Si(OH)<sub>4</sub> marks the limit for diatom growth. 0.1 µmol L<sup>-1</sup> denotes the detection limit for all nutrients. The dashed lines denote the salinity boundary of 32.

Based on surface salinity and nutrient distributions, we distinguish three station categories which will be referred to throughout this paper: 1) mesohaline (14.3 to 32.0), which was sampled during both cruises, 2) transitional (>32.0 to 33.5), and 3) oceanic (>33.5), whereby the latter salinities are typical for open sea water as defined by Dippner et al. (2007) for the SCS off Vietnam. Transitional- and oceanic salinities were sampled only in April 2007, and as mentioned, salinities <14.0 (0.1 – 8.9) were found only in September 2008. In order to clearly show the differences between the observed salinity gradients during lowest and highest river discharge, the salinity isoline of 32 is highlighted in all figures showing surface distributions. The salinity of 32 was also chosen because it was previously defined as a lower boundary for the occurrence of *Trichodesmium* (Jones et al. 1982; Revelante and Gilmartin 1982).

**Table 3.2:** Pearson correlation matrix comparing changes in salinity, turbidity, and nutrient concentrations. *p*-values  $\leq 0.01$  are considered significant.

	April 2007		September 2008	
	salinity	<i>p</i> -value	salinity	<i>p</i> -value
Salinity	1.000		1.000	
Turbidity	-0.723	$\leq 0.001$	-0.720	0.0125
Nitrate + nitrite	-0.944	$\leq 0.001$	-0.978	$\leq 0.001$
Phosphate	-0.916	$\leq 0.001$	-0.783	$\leq 0.001$
Silicate	-0.933	$\leq 0.001$	-0.989	$\leq 0.001$

Overall, concentrations of all nutrients showed a strong offshore gradient and were negatively correlated with salinity in April 2007; in September 2008, only NO<sub>3</sub>+NO<sub>2</sub> and Si(OH)<sub>4</sub> showed significantly negative correlations with salinity (Fig. 3.2C-H, Table 3.2). The highest concentrations of NO<sub>3</sub>+NO<sub>2</sub>, PO<sub>4</sub>, and Si(OH)<sub>4</sub> were encountered within the river arms, at Sta. 2 and 3 in April 2007, and at Sta. 1 in September 2008 (Fig. 3.2C-H). Interestingly, concentrations of 4.2 - 19.6  $\mu\text{mol L}^{-1}$  NO<sub>3</sub>+NO<sub>2</sub> and 0.4 - 1.0  $\mu\text{mol L}^{-1}$  PO<sub>4</sub> in mesohaline waters in April 2007 did not differ much from concentrations in waters with much lower salinity ( $\leq 8.9$ ) in September 2008 (17.3 - 22.3  $\mu\text{mol L}^{-1}$  NO<sub>3</sub>+NO<sub>2</sub> and 0.6 - 0.9  $\mu\text{mol L}^{-1}$  PO<sub>4</sub>); however, for concentrations of Si(OH)<sub>4</sub>, there was indeed a clear difference (18.8 – 42.6  $\mu\text{mol L}^{-1}$  in mesohaline waters in April 2007 vs. 115-176  $\mu\text{mol L}^{-1}$  at salinities  $\leq 8.9$  in September 2008) (Table 3.3). Mesohaline waters had overall similar nutrient concentrations during both investigations (Table 3.3). Transitional waters, which were only sampled in April 2007, had NO<sub>3</sub>+NO<sub>2</sub> concentrations of  $\leq 0.9$   $\mu\text{mol L}^{-1}$ , PO<sub>4</sub> of  $\leq 0.3$   $\mu\text{mol L}^{-1}$ , and Si(OH)<sub>4</sub> concentrations of  $\leq 10.1$   $\mu\text{mol L}^{-1}$ . At oceanic stations, concentrations of PO<sub>4</sub> were below detection, concentrations of NO<sub>3</sub>+NO<sub>2</sub> were mostly  $\leq 0.3$   $\mu\text{mol L}^{-1}$  besides one higher value at Sta. 14 (1.0  $\mu\text{mol L}^{-1}$ ), and concentrations of Si(OH)<sub>4</sub> were  $\leq 3.6$   $\mu\text{mol L}^{-1}$ .

**Table 3.3:** Ranges, means and standard deviations (SD) of variables for both investigations in April 2007 and September 2008, within different salinity ranges.

	April 2007				September 2008					
	Mesohaline (salinity 14.0-32.0) Range (mean ±SD)	<i>n</i>	Transitional (salinity 32.0–33.5) + Range (mean ± SD)	<i>n</i>	Oceanic (salinity >33.5) Range (mean ± SD)	<i>n</i>	salinity <14.0 Range (mean ± SD)	<i>n</i>	Mesohaline (salinity 14.0 – 32.0) × Range (mean ± SD)	<i>n</i>
Salinity	14.3 – 31.4 (24.4 ± 5.6)	10	32.6 – 33.5 (33.0 ± 0.3)	16	33.5 – 34.0 (33.8 ± 0.2)	6	0.1 – 8.9 (4.2 ± 3.9)	11	15.8 – 32.0 (25.7 ± 5.0)	49
Turbidity (NTU)	11.2 – 250.0 (68.8 ± 68.4)	10	0.4 – 20.9 (6.2 ± 5.5)	16	0.0 – 1.8 (0.5 ± 0.6)	6	37.2 – 296.0 (194 ± 107.7)	6	2.0 – 185.9 (26.3 ± 35.0)	42
Temperature (°C)	29.0 – 31.5 (30.1 ± 0.7)	10	29.4 – 30.6 (29.9 ± 0.4)	16	28.5 – 30.5 (29.4 ± 0.7)	6	27.9 – 29.2 (28.4 ± 0.3)	11	28.5 – 30.2 (28.9 ± 0.4)	49
Nitrate + Nitrite (µmol L <sup>-1</sup> ) *	4.2 – 19.6 (12.4 ± 4.4)	8	0.0 – 1.0 (0.3 ± 0.3)	13	0.0 – 1.0 (0.3 ± 0.4)	6	17.3 – 22.3 (20.4 ± 2.3)	4	1.1 – 13.0 (5.1 ± 4.3)	17
Phosphate (µmol L <sup>-1</sup> ) *	0.4 – 1.0 (0.7 ± 0.2)	8	0.1 – 0.2 (0.15 ± 0.03)	13	not detectable	6	0.6 – 0.9 (0.8 ± 0.1)	4	0.1 – 0.7 (0.4 ± 0.2)	17
Silicate (µmol L <sup>-1</sup> ) *	18.8 – 42.6 (32.0 ± 9.2)	8	4.8 – 10.1 (7.7 ± 1.7)	13	2.3 – 7.5 (3.5 ± 1.9)	6	115.5 – 176.5 (151.9 ± 259.0)	4	8.6 – 92.0 (39.4 ± 27.1)	17
N:P *	11.5 – 22.1 (17.7 ± 3.2)	8	0.8 – 5.2 (2.3 ± 1.6)	12			24.3 – 32.4 (26.9 ± 3.8)	4	3.0 – 26.2 (12.3 ± 6.4)	17
Si:N *	2.1 – 4.5 (2.8 ± 0.8)	8	4.0 – 49.3 (32.2 ± 15.0)	13	2.8 – 49.3 (18.5 ± 18.6)	4	6.7 – 8.9 (7.4 ± 1.0)	4	4.6 – 17.2 (9.1 ± 3.4)	17
Chlorophyll <i>a</i> (µg L <sup>-1</sup> )	2.2 – 3.9 (3.2 ± 0.7)	5	1.4 – 3.0 (2.1 ± 0.6)	9	0.2 – 0.4 (0.3 ± 0.1)	4	0.3 – 1.0 (0.6 ± 0.3)	4	0.2 – 1.3 (0.5 ± 0.4)	15
N <sub>2</sub> Fixation (nmol N L <sup>-1</sup> h <sup>-1</sup> )										
<10 µm	0.08 – 1.57 (0.73 ± 0.44)	5	2.63 – 14.36 (6.28 ± 3.95)	8	1.07 – 10.80 (4.95 ± 5.16)	3				
>10 µm	0.03 – 1.29 (0.40 ± 0.51)	5	1.89 – 14.47 <sup>+</sup> (8.06 ± 4.00)	8	0.55 – 15.28 (5.61 ± 8.38)	3				
Total	0.11 – 2.86 (1.13 ± 1.04)	5	5.76 – 22.77 <sup>+</sup> (14.33 ± 5.08)	8	4.00 – 16.40 (10.55 ± 6.24)	3	0.06 – 0.69 (0.26 ± 0.29)	4	0.10 – 5.05 (1.81 ± 1.70)	12
Primary Production (µmol C L <sup>-1</sup> h <sup>-1</sup> )										
<10 µm	0.01 – 0.07 (0.04 ± 0.03)	4	0.01 – 0.25 (0.11 ± 0.09)	6	0.01 – 0.04	2				
>10 µm	0.01 – 0.11 (0.06 ± 0.04)	4	0.04 – 0.45 (0.24 ± 0.19)	6	0.005 – 0.01	2				
Total	0.02 – 0.14 (0.11 ± 0.06)	4	0.05 – 0.64 (0.34 ± 0.28)	6	0.01 – 0.05	2	0.03 – 0.15 (0.07 ± 0.06)	4	0.06 – 0.68 (0.23 ± 0.17)	10

\* Sta. 23, 24, and 25 are not included due to a complete change in weather conditions;

+ includes individual measurements at time-series Sta. 19

× includes individual measurements at time-series Sta. 28

Ratios of NO<sub>3</sub>+NO<sub>2</sub> to PO<sub>4</sub> (N:P) generally decreased with increasing salinity during both investigations (Fig. 3.3, Table 3.3). N:P ratios lower than the Redfield ratio of 16:1 were largely confined to transitional waters during April 2007 (only mesohaline Sta. 6 had an N:P ratio of 11). In September 2008, N:P ratios in mesohaline waters were more variable, but below 16 at 13 out of 17 stations. In waters with salinities below 14, N:P ratios were always above 20 (Fig. 3.3, Table 3.3). Ratios of Si(OH)<sub>4</sub> to NO<sub>3</sub>+NO<sub>2</sub> (Si:N) tended to increase with increasing salinity, although this increase was not as obvious in September 2008 as in April 2007 (Table 3.3).

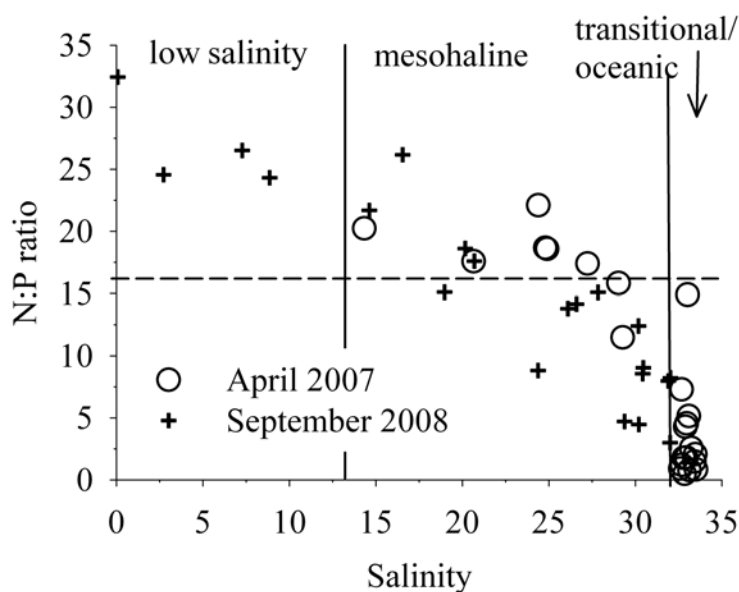


**Figure 3.3:** N:P ratios in the different salinity ranges for both cruises. The dashed line marks the Redfield ratio of 16:1

### 3.4.2 N<sub>2</sub> fixation and primary production

During both investigations, N<sub>2</sub> fixation was detectable at all stations (Fig. 3.4). In April 2007, total N<sub>2</sub> fixation rates in mesohaline surface waters ranged between 0.11 and 2.86 nmol N L<sup>-1</sup> h<sup>-1</sup> (mean 1.13 ± 1.04 nmol N L<sup>-1</sup> h<sup>-1</sup>) and increased to very high values in transitional waters (5.76- 22.77 nmol N L<sup>-1</sup> h<sup>-1</sup>, mean: 14.33 ± 5.08 nmol N L<sup>-1</sup> h<sup>-1</sup>) and oceanic waters (4.00 - 16.40 nmol N L<sup>-1</sup> h<sup>-1</sup>, mean: 10.55 ± 6.24 nmol N L<sup>-1</sup> h<sup>-1</sup>). In September 2008, N<sub>2</sub> fixation rates ranged from 0.10 to 5.05 nmol N L<sup>-1</sup> h<sup>-1</sup> in mesohaline waters (mean: 1.81 ± 1.7 nmol N L<sup>-1</sup> h<sup>-1</sup>), and from 0.06 – 0.69 nmol N L<sup>-1</sup> h<sup>-1</sup> in waters having salinities below 14 (mean: 0.26 ± 0.29 nmol N L<sup>-1</sup> h<sup>-1</sup>). Thus, the rates found in mesohaline waters were clearly higher in September 2008, and are comparable to the lower range of values from transitional waters in April 2007 (Fig. 3.4, Table 3.3).

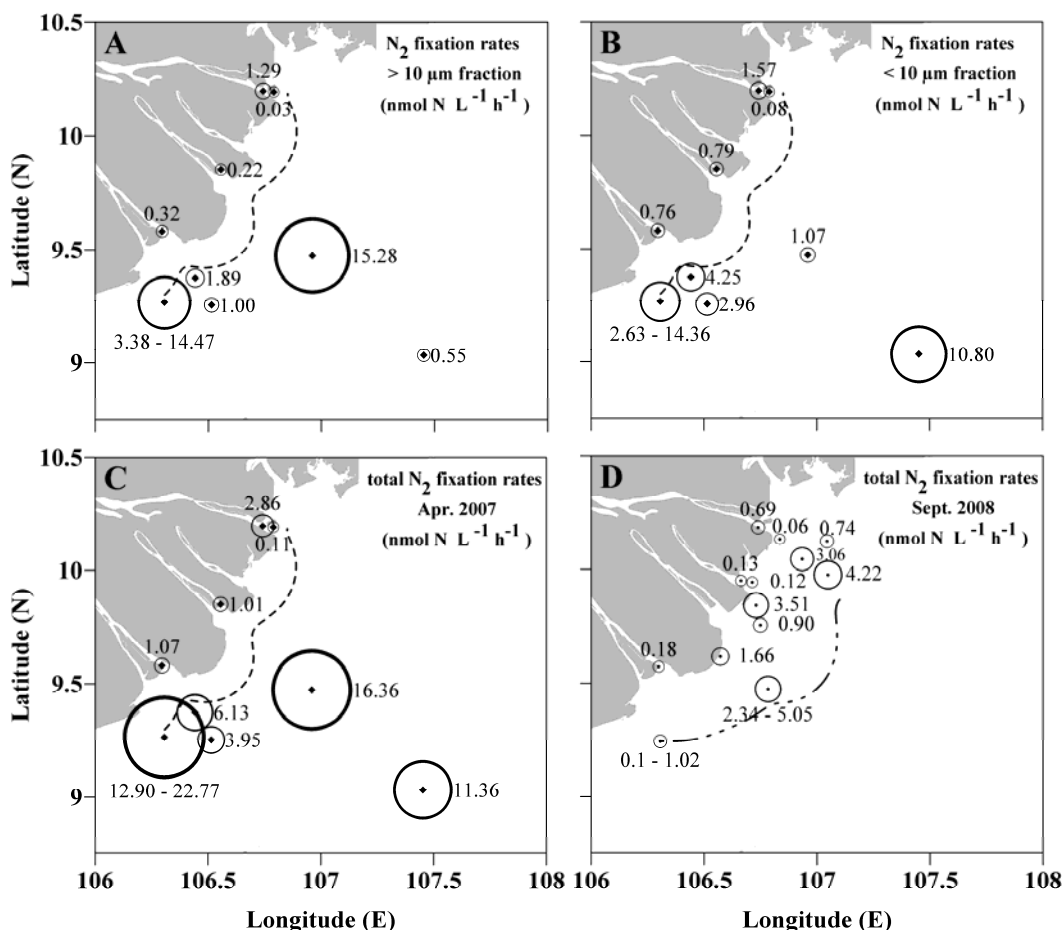


**Figure 3.4:** N<sub>2</sub> fixation rates for April 2007: (A) >10 μm size fraction (B) <10 μm size fraction, and (C) total rates. (D) Total N<sub>2</sub> fixation rates for September 2008. Symbols are scaled linearly proportional to the measured values. Rates at Sta. 19 (April 2007), 20 and 28 (September 2008) show the measured range, circle size corresponds to the mean rate. The dashed lines show the salinity boundary of 32.

During each investigation, we included three stations at which incubation periods covered the entire dark period (sunset – sunrise). In April 2007, these N<sub>2</sub> fixation rates were 0.11 nmol N L<sup>-1</sup> h<sup>-1</sup> (mesohaline waters) and 3.95 and 14.62 nmol N L<sup>-1</sup> h<sup>-1</sup> (transitional waters). In September 2008, N<sub>2</sub> fixation rates were comparable to the lower range of the April 2007 rates with 0.10, 0.12 and 2.34 nmol N L<sup>-1</sup> h<sup>-1</sup>. Furthermore, the N<sub>2</sub> fixation rates measured at night were of the same magnitude as the N<sub>2</sub> fixation rates from day-time incubations at nearby stations. In April 2007, the highest N<sub>2</sub> fixation rates of up to 22.77 nmol N L<sup>-1</sup> h<sup>-1</sup> were measured at the time-series Sta. 19 (transitional waters) and were similarly high during day and night. In September 2008, the highest N<sub>2</sub> fixation rates for day and night measurements were 5.05 and 2.34 nmol N L<sup>-1</sup> h<sup>-1</sup>, respectively (both Sta. 20, mesohaline waters).

In April 2007 we conducted size fractionation to distinguish between unicellular diazotrophs and larger diazotrophs. Both size fractions contributed different fractions to the total N<sub>2</sub> fixation, but averaged over the entire investigation area, the contributions were about equal (Table 3.3). For example, at Sta. 19, N<sub>2</sub> fixation rates in the <10 μm size fraction ranged

between 2.63 and 14.36 nmol N L<sup>-1</sup> h<sup>-1</sup>, and between 3.38 and 14.47 nmol N L<sup>-1</sup> h<sup>-1</sup> in the >10 μm size fraction (Fig. 3.5).

We evaluated the effect of light or nutrient ratios on N<sub>2</sub> fixation rates by plotting N<sub>2</sub> fixation rates against turbidity and the ratio of NO<sub>3</sub>+NO<sub>2</sub> and PO<sub>4</sub> (N:P) (Fig. 3.6). In April 2007, the two water bodies with salinity either above (transitional and oceanic waters) or below 32 (mesohaline waters) formed two distinctive clusters in terms of N<sub>2</sub> fixation rates and abiotic variables. Low N<sub>2</sub> fixation rates (<3 nmol N L<sup>-1</sup> h<sup>-1</sup>) co-occurred with salinities below 32, a turbidity above 10 NTU and N:P ratios above 10. Higher N<sub>2</sub> fixation (higher 3 nmol N L<sup>-1</sup> h<sup>-1</sup>) rates were observed at salinities above 32, turbidities below 10 NTU and N:P ratios below 10. In September 2008 N<sub>2</sub> fixation rates corresponded similar to turbidity and N:P ratios but fell in between the two clusters from April 2007 (Fig. 3.6).

Primary production rates in April 2007 were lower in waters with salinity below 32 whereas primary production in waters with a salinity above 32 was higher and more variable (Table 3.3). Similar to the N<sub>2</sub> fixation rates, the time-series station exhibited the highest rates in primary production. In September 2008, primary production rates covered the entire range measured in April 2007.

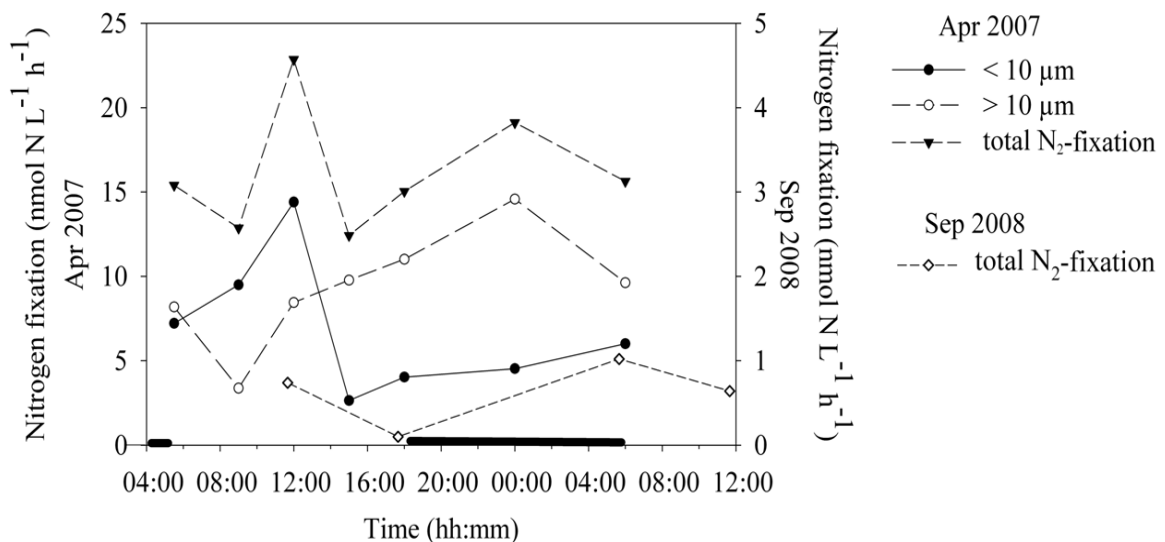


**Figure 3.5:** Course of N<sub>2</sub> fixation (total and within the different size fractions) at time-series Sta. 19 (April 2007) and Sta. 28 (September 2008). Black bars indicate night hours.

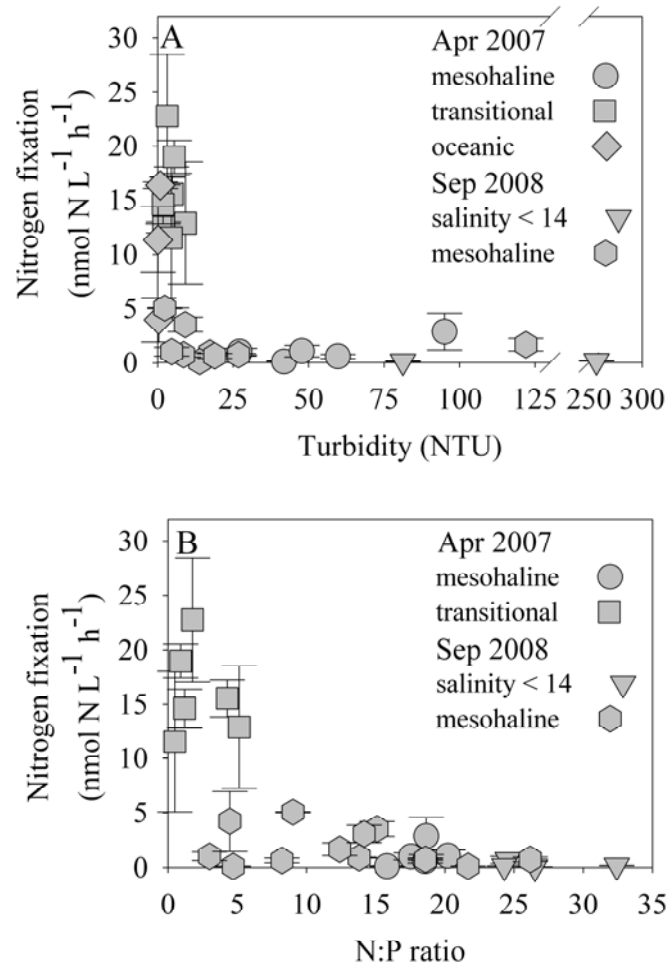


**Figure 3.6:** (A) Relationship between turbidity and total N<sub>2</sub> fixation rates. (B) Relationship between N:P ratio and total N<sub>2</sub> fixation rates. In B), no data are shown for oceanic waters since PO<sub>4</sub> was undetectable at oceanic stations in April 2007. Error bars indicate standard deviation of N<sub>2</sub> fixation rates among triplicates.

### 3.4.3 Phytoplankton species distribution

For clarity, we classified the detected phytoplankton species into three different groups, i.e., potentially symbiotic diatoms, asymbiotic diatoms, and filamentous cyanobacteria. Potentially symbiotic diatoms summarize the most common diatoms capable of hosting *Richelia intracellularis* and *Calothrix rhizosoleniae* (Carpenter 2002) and comprise *Rhizosolenia* spp., *Chaetoceros* spp., *Guinardia* spp., *Hemiaulius* spp., and *Bacteriastrum* spp. We did not microscopically investigate the presence of *Richelia intracellularis* or *Calothrix rhizosoleniae*, but nitrogenase (*nifH*) gene analysis confirmed the presence of certain heterocystous symbiotic cyanobacteria in the area (D. Bombar unpubl.), and here we rather show the distribution and abundance of diatoms that potentially hosted N<sub>2</sub> fixing symbionts. All other detected diatom species were grouped as asymbiotic diatoms. Filamentous cyanobacteria included the diazotrophs *Trichodesmium eurythraeum* and *T. thiebautii*.

Diatoms (Bacillariophyceae) were the most abundant group at all stations during both investigations, but the dominating genera differed. In April 2007, *Skeletonema* spp., *Thalassionema* spp., and *Asterionella* spp. were the dominant asymbiotic diatoms. Highest abundances (reaching 30,000 - 55,000 cells L<sup>-1</sup>) were observed in mesohaline- and transitional waters (at coastal Sta. 8, 18, 19, and 21) and decreased towards the open sea to below 1000 cells L<sup>-1</sup> (Sta. 11 - 15, Fig. 3.7A). In September 2008 the most abundant asymbiotic diatoms were the genera *Coscinodiscus*, *Thalassiosira* and *Skeletonema*. The overall abundances of asymbiotic diatoms were lower and stayed below 10,000 cells L<sup>-1</sup> (except for Sta. 27 -29, 35, and 37 where numbers ranged between 11,000 and 30,000 cells L<sup>-1</sup>). There was no offshore gradient visible as in April 2007 but numbers increased towards the southernmost Sta. 27 and 28. Overall, abundances of asymbiotic diatoms were higher in mesohaline waters (Fig. 3.7B).

Within the group of potentially symbiotic diatoms (Fig. 3.7C, D), the genus *Chaetoceros* dominated during both investigations, with highest cell densities in transitional waters in April 2007 (up to 80,700 cells L<sup>-1</sup> at Sta. 19SP6), and in mesohaline waters in September 2008 (up to 58,000 cells L<sup>-1</sup> at Sta. 32). An exception was Sta. 23 (April 2007, transitional), where *Rhizosolenia* spp. dominated, and the mesohaline Sta. 10, 11, 13, and Sta. 24 (salinity below 14) in September 2008, where *Guinardia* or *Hemiaulus* dominated. The second and third most abundant genera during both investigations were *Rhizosolenia* and *Bacteriastrum*. *Rhizosolenia* reached abundances of 6300 cells L<sup>-1</sup> (Sta. 10, oceanic) and 2850 cells L<sup>-1</sup> (Sta. 32, mesohaline) in April 2007 and September 2008, respectively. Cell densities of *Bacteriastrum* reached 5400 cells L<sup>-1</sup> (Sta. 19SP5, transitional) in April 2007 and 1800 cells L<sup>-1</sup> (Sta. 20, mesohaline) in September 2008. Overall, the abundances of potentially symbiotic diatoms seemed to increase along the flow path of the river plume (from the north towards the south) in April 2007 (Fig. 3.7C). In September 2008 only two stations showed high densities of potentially symbiotic diatoms, Sta. 32 with 63,000 cells L<sup>-1</sup> and Sta. 34 with 44,000 cells L<sup>-1</sup>, both mesohaline waters north of the middle river arm.

Filamentous cyanobacteria were most abundant in transitional- and oceanic waters in April 2007. We found highest trichome densities at transitional Sta. 9 and 16 (3300 and 5800 trichomes L<sup>-1</sup>, respectively, Fig. 3.7E). In September 2008 filamentous cyanobacteria of the genera *Anabaena* and *Spirulina* were encountered occasionally at low salinity and mesohaline stations. *Trichodesmium* was present at three mesohaline stations. For all three genera abundances were too low for a reliable count of cells or trichomes.

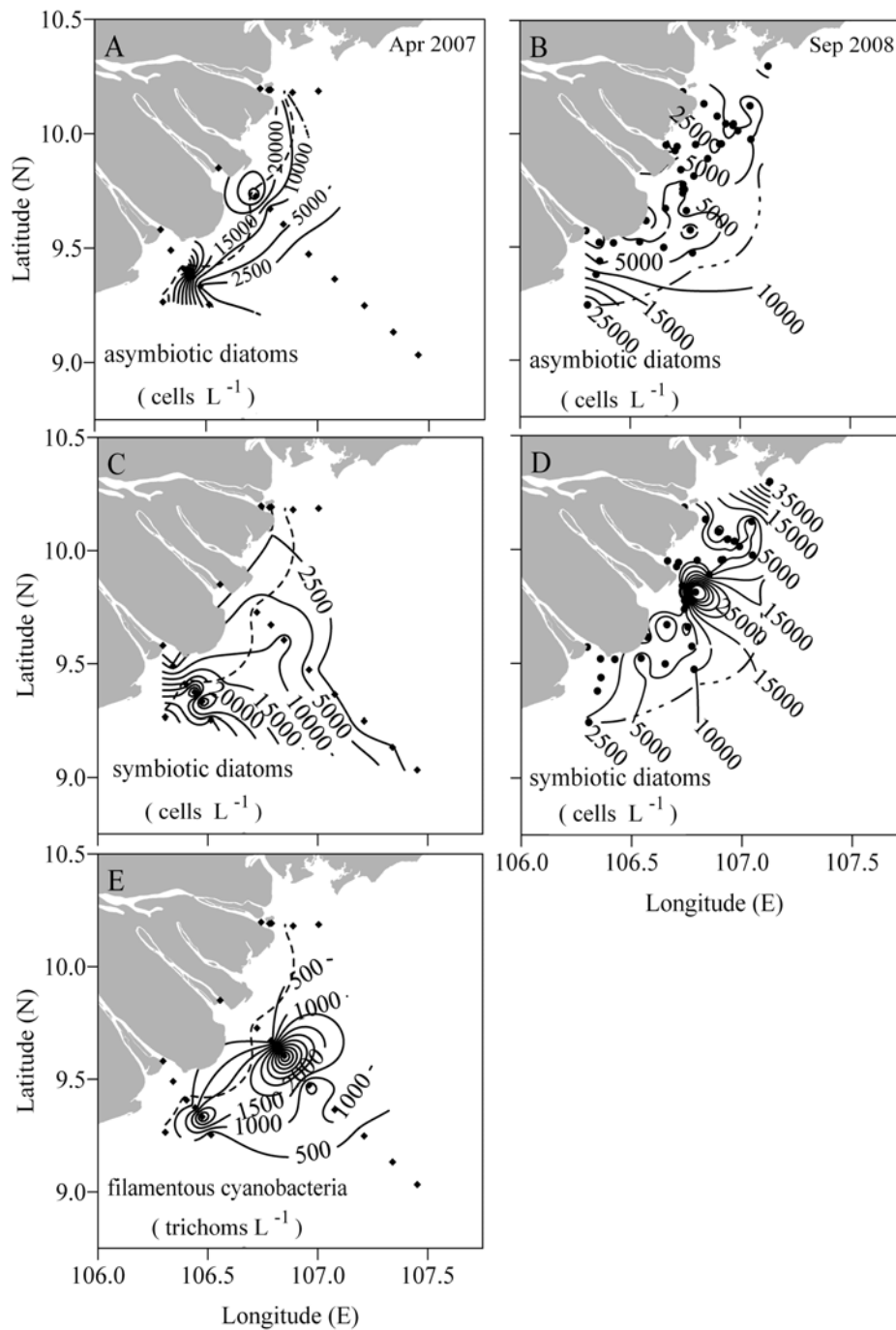


**Figure 3.7:** Phytoplankton distribution in April 2007 (left column) and September 2008 (right column): Asymbiotic diatoms (A, B), and potentially symbiotic diatoms (C, D). For April 2007, filamentous cyanobacteria are also shown (E). Possible host-species for *Richelia* and *Calothrix* include *Chaetoceros* spp., *Rhizosolenia* spp., *Bacteriastrum* spp., *Hemiaulius* spp., and *Guinardia* spp. The dashed lines show the salinity boundary of 32.

### 3.5 Discussion

#### 3.5.1 Comparison of abiotic conditions during low and high discharge

Differences in the fresh water supply of the Mekong River in the intermonsoon season in April and the SW monsoon season in September lead to a variable extension of the river plume. In April the plume flows southward along the coast and in September it reaches the oligotrophic

waters in northeast direction (Voss et al. 2006). The region covered by our station grid extended into open sea waters in April 2007, but not in September 2008. We assume that the plume reached much farther offshore in September, although we only collected waters in the mesohaline parts of the plume. Thus, only mesohaline samples can directly be compared between the two cruises regarding all parameters. Mesohaline waters covered a larger area in September 2008 but the increase in salinity and the decrease in nutrient concentrations suggest that growth conditions were similar to April 2007. Concentrations of  $\text{NO}_3 + \text{NO}_2 \leq 1.0 \mu\text{mol L}^{-1}$  can be considered to represent N-limitation for phytoplankton (Goldman and Glibert 1983), but should not affect N<sub>2</sub> fixation (Mulholland et al. 2001). N-limiting conditions were not found in the eutrophic mesohaline waters, but in transitional waters, which had detectable concentrations of  $\text{PO}_4$  and  $\text{Si(OH)}_4$ , and in oceanic waters, which were mostly depleted in both  $\text{NO}_3 + \text{NO}_2$  and  $\text{PO}_4$  (Table 3.3).

The nutrient ratios can be used to further describe the differences in growth conditions for diazotrophs. The Mekong River water from the monitoring station My Tho (50 km up-river from sta. 1) had a high N:P ratio of 42.8 and a low Si:N ratio of 4.2. These ratios clearly exceed those found at the river mouth stations in April 2007 (Sta. 1-3), where the N:P ratio was  $20.7 \pm 11.5$  (mean  $\pm$  SD;  $n=3$ ) and the Si:N ratio was  $2.6 \pm 1.1$  ( $n=3$ ). Similar N:P ratios of 30:1 were calculated from modeled TN and TP loads (Yoshimura and Takeuchi 2007). Data and model results suggest that the Mekong River water was actually P-limited. The mechanisms by which the N:P ratios decreased towards higher salinities must remain speculative here, but likely include denitrification in estuarine sediments as well as desorption of P from suspended particles or sediments as the river water mixed with ocean water (Seitzinger 1988; Jordan et al. 2008). The distribution patterns of N:P ratios show that during both low and high discharge, the mixing of Mekong- and SCS ocean waters resulted in a mixed water body in which N:P ratios were lower than the Redfield ratio, indicating favorable conditions for diazotrophs (Table 3.3). As mentioned, nutrient concentrations alone would denote mesohaline waters as largely eutrophic and therefore as an unfavorable niche for diazotrophs. However, in September 2008, N:P ratios were below 16:1 at many mesohaline stations. This is interesting, since in April 2007, N:P lower 16:1 were almost exclusively found within the comparatively narrow salinity range of transitional stations (except for mesohaline Sta. 6, N:P = 11), while  $\text{PO}_4$  was undetectable at oceanic stations. Although we did not sample transitional and oceanic waters in September 2008, our findings imply that the part of the river plume in which conditions were favorable for N<sub>2</sub> fixers covered a larger area in September 2008 than in April 2007. The  $\text{Si(OH)}_4$  concentrations in the freshwater from My Tho were about 4 fold higher than at coastal Sta. 1-3 (April 2007), but comparable to the  $\text{Si(OH)}_4$

concentrations in zero-salinity water in September 2008. High Si:N ratios should favor the growth of diatoms, as shown for a comparable environment with high fresh water inputs in the Gulf of Mexico (Turner et al. 2007). Si:N ratios tended to increase towards higher salinities in our investigation area, indicating Si(OH)<sub>4</sub> - replete conditions coincident with N-limitation. We assume that this selectively favored the growth of DDAs.

Another nutrient thought to be limiting for the growth of diazotrophs is iron (Mills et al. 2004); however, river plumes are generally not expected to be low in trace metals and preliminary results from the Mekong plume in April 2006 showed total iron concentrations of 4-6 nmol L<sup>-1</sup> in surface waters (P. Croot unpubl.). Therefore it seems unlikely that iron was limiting diazotroph growth during our investigation.

### **3.5.2 Influence of the Mekong River plume on N<sub>2</sub> fixation, primary production, and phytoplankton community composition**

As described above, N:P ratios suggest that growth conditions were most favorable for diazotrophs in mesohaline waters in September 2008, and in transitional and oceanic waters in April 2007. And indeed, the highest rates of N<sub>2</sub> fixation were found in these waters (Table 3.3, Fig. 3.4). While the exceptionally high N<sub>2</sub> fixation rates coincided with oligotrophic conditions in transitional waters in April 2007, the highest rates found in September 2008 (between 1.66 and 5.05 nmol N L<sup>-1</sup> h<sup>-1</sup>) coincided with NO<sub>3</sub>+NO<sub>2</sub> concentrations between 1.3 and 4.3 μmol L<sup>-1</sup>, which can actually not be considered oligotrophic. However, the N:P ratios were always below 16:1 in these samples, suggesting that diazotrophs indeed benefited from a PO<sub>4</sub> surplus relative to phytoplankton nutrient requirements. The magnitude of the rates found in these coastal waters is remarkable, considering that N<sub>2</sub> fixation is generally believed to be most important in areas having lowest concentrations of combined nitrogen (Capone and Carpenter 1982).

Asymbiotic diatoms were highly abundant in mesohaline waters, where the high concentrations of NO<sub>3</sub>+NO<sub>2</sub>, PO<sub>4</sub>, and Si(OH)<sub>4</sub> presumably supported their growth. Abundances of over 20,000 cells L<sup>-1</sup> were encountered close the coast in April 2007, and at southernmost stations in September 2008. At these stations, where no potential diazotrophs were found, we measured the lowest rates of N<sub>2</sub> fixation (1.13 ± 1.04 nmol N L<sup>-1</sup> h<sup>-1</sup> in April 2007). However, these rates are still similar to the highest N<sub>2</sub> fixation rates of 1.2 nmol N L<sup>-1</sup> h<sup>-1</sup> found by Voss et al. (2006) farther north in the SCS. Coinciding with highest rates of N<sub>2</sub> fixation, abundances of potentially symbiotic diatoms were highest farther away from the coast in transitional (April 2007) and mesohaline waters (September 2008). These phytoplankton distributions and the high Si:N ratios in these waters further suggest that DDAs had a growth

advantage. In contrast to the asymbiotic diatoms, abundances of DDAs seemed to increase along the flow path of the river plume (towards the south in April 2007 and towards the north in September 2008) possibly reflecting a phytoplankton community that underwent successive transformations as a response to changing nutrient conditions including incipient N-limitation and increasing Si:N ratios. Similar changes in the phytoplankton community were also seen along the Amazon River plume (Subramaniam et al. 2008), but on a much larger scale compared to the Mekong River outflow.

Unfortunately, we only speculate that the symbiotic diatoms indeed carried diazotrophic symbionts, but the picture is plausible for several reasons: 1) as mentioned, D. Bombar (unpubl.) showed that DDAs were present and actively fixed dinitrogen. 2) Other studies in comparable environments found actively fixing DDAs (Foster et al. 2008). 3) Our high rates are in line with published ones from the Amazon plume. The highest N<sub>2</sub> fixation rates encountered in the Mekong River plume were 14.47 nmol N L<sup>-1</sup> h<sup>-1</sup> within the >10 μm size fraction, and highest total rates were 22.77 nmol N L<sup>-1</sup> h<sup>-1</sup> (April 2007). These values are very similar to rates found in a DDA bloom in the Amazon River plume (~ 14 nmol N L<sup>-1</sup> h<sup>-1</sup>; Carpenter et al. 1999), but are much higher than the mean values reported by Subramaniam et al. (2008) for the same area during different seasons (around 1 nmol N L<sup>-1</sup> h<sup>-1</sup>). The high rates reported here seem rather unusual for unicellular species (Voss et al. 2004), although rates of the same magnitude were found e.g. in the pigment maximum of the Arafura Sea (Montoya et al. 2004). Blooms of *Trichodesmium* were not present in the mesohaline waters of the SCS in September 2008, further suggesting that DDAs were responsible for the high N<sub>2</sub> fixation rates encountered. According to the *nifH* data by D. Bombar (unpubl.), *Calothrix* associated with *Chaetoceros* spp. was not abundant in the area, which is puzzling, since *Chaetoceros* spp. was the most abundant diatom. It remains speculative if there were diazotroph symbionts associated with *Chaetoceros* and other diatoms in the SCS, which were not detectable with the applied QPCR oligonucleotides. This has to be resolved in future studies.

High densities of *Trichodesmium* spp. tufts were exclusively observed in waters with salinities above 32 in April 2007. Thus, *Trichodesmium* seemed to be present mainly in full marine waters and occurred only sporadically in waters which were influenced by the plume. This is in accordance with investigations in other river plumes (Carpenter et al. 1999; Foster et al. 2007, 2008). The absence of this typical marine diazotroph in mesohaline waters in September 2008 possibly shows that its growth was suppressed by the lower salinities and comparatively high concentrations of NO<sub>3</sub>+NO<sub>2</sub>.

Overall it seems that a number of changes along the aging plume determined the species composition of the phytoplankton community in a similar way to the Amazon River

plume (Subramaniam et al. 2008). Interestingly, the gradients in salinity and biogeochemical components seemed to be the same during both seasons, although the discharge volume was different. We had roughly 20 times higher discharge in September 2008, the plume was larger and therefore the mesohaline, transitional and open ocean water zones must have been larger as well. We suggest that the species composition found in April 2007 was also present in September 2008, however on larger spatial scales. This would include that DDAs became more abundant farther offshore from our easternmost station.

### 3.5.3 Ecological importance of N<sub>2</sub> fixation in the Mekong River plume

In the northern parts of the SCS N<sub>2</sub> fixation played a relatively minor role in satisfying the N demand of primary production (using a Redfield ratio of 6.6). Voss et al. (2006) reported values below 3% in the area between 11-13°N when the Mekong River plume was not present, and Chen et al. (2004) published similar values for stations around 20°N. Even during the SW monsoon season, when the Mekong River plume was stimulating N<sub>2</sub> fixation 200 km north of the river mouth, N<sub>2</sub> fixation satisfied at most 8.2% of the N demand (Voss et al. 2006). The N<sub>2</sub> fixation rates reported in this study supplied between 4.9% and 34.8% and between 1.0% and 21.7% of the total N demand of primary production in April 2007 and September 2008, respectively. These numbers are comparable to values calculated by Carpenter and others (1999) for the Amazon River plume, and exceed values found in other parts of the Atlantic (~12% with N<sub>2</sub> fixation rates of up to 2 nmol L<sup>-1</sup> h<sup>-1</sup>, Voss et al. 2004) or in the Arabian Sea (13.5% with N<sub>2</sub> fixation rates >10 nmol L<sup>-1</sup> h<sup>-1</sup>, Capone et al. 1998).

As expected, the importance of N<sub>2</sub> fixation as a nitrogen source for primary production was maximal in waters having N-limiting conditions, as shown by supplies of 13.3 – 34.8% of the N demand of primary producers in transitional waters (April 2007). It is noteworthy that this supply was still between 4.9% and 21.1% at mesohaline stations, where nutrient concentrations were high. In September 2008, N supplies by diazotrophs were in the lower range of those from April 2007 but increased with distance to the coast. We assume that in September 2008 the importance of N<sub>2</sub> fixation in fueling primary production further increased in transitional waters which we could not sample. All the aforementioned estimates of N supply are based on N<sub>2</sub> fixation measured during the time of primary production, but we also report high N<sub>2</sub> fixation rates from the night incubations. These rates were of the same magnitude as the rates measured during the day in the same area. DDAs are known to express *nifH* genes during the night (Church et al. 2005b), and we therefore propose that the rates measured during the night have to be considered in the N supply estimates as well. This suggests that even 40 - 47% of the N demand of primary production may have been satisfied

through this extra source of nitrogen. Our findings show that overall, N<sub>2</sub> fixation is important in controlling the primary production in the Mekong River plume.

This study has presented a detailed analysis of the dynamics of N<sub>2</sub> fixation in the Vietnamese coastal waters affected by the Mekong River plume. A general picture seems to emerge for the Mekong River as well as other tropical rivers: They provide ‘new’ nutrients, which are taken up quickly in the river mouth proximity and fuel phytoplankton growth, especially of diatoms. Additionally, farther offshore the excess in PO<sub>4</sub> and Si(OH)<sub>4</sub> seem to support N<sub>2</sub> fixation by a variety of diazotrophs. This may be a general phenomenon in tropical river plumes, which affect large areas of the ocean basins into which they discharge. The Amazon River plume covers thousands of km<sup>2</sup> in the tropical North Atlantic, but also in the SCS, effects of the Mekong River discharge can be seen far offshore (Voss et al. 2006). In the SCS, there are pronounced differences in discharge of water and nutrients between different monsoon seasons, and therefore the importance of the Mekong River in influencing the oceanic N- and C cycles will also differ between the seasons. We are only beginning to assess and understand these processes, but doing so seems critical for understanding the biogeochemistry of the SCS as well as for inferring hypotheses on how changes in land and water use will alter these complex dynamics.

## 4. Distribution of diazotrophic microorganisms, *nifH* gene expression and N<sub>2</sub> fixation in the Mekong River Plume during intermonsoon

### 4.1 Abstract

We have recently shown that in accordance with other tropical river plumes, high nitrogen fixation occurs in the Mekong River plume in the South China Sea, presumably due to riverine inputs of “excess” phosphorus. In April 2007, nitrogen fixation covered up to 47% of the N-demand of primary productivity; however, by light microscopy it was impossible to clearly identify the responsible diazotroph microorganisms. Here, surface samples taken in April 2007 served to investigate the horizontal distribution and activity of 9 diazotroph phylotypes, using *nifH* gene quantitative polymerase chain reaction (QPCR) and reverse transcription (RT) QPCR. Further, the *nifH* gene diversity was assessed by cloning and sequencing. Modeling of the surface water advection shows that we sampled a fixed set of water masses (salinities of 14.3-34) which had a residence time within the area that was long enough for the diazotroph community to respond to river inflow. According to QPCR, the high nitrogen fixation in the Mekong Plume was primarily carried out by *Trichodesmium* spp. and the symbiotic diatom-diazotroph associations (DDAs) *Rhizosolenia-Richelina* and *Hemiaulus-Richelina*. Unicellular cyanobacterial groups B and C and a  $\gamma$ -proteobacterial phylotype were exclusively detected and expressed *nifH* at oceanic stations, confirming that nutrient gradients in tropical river plumes induce unequal distribution patterns of diazotrophs. *NifH* clone libraries were dominated by *Trichodesmium* spp., but proteobacterial- and cluster III-like *nifH* sequences were also found, including new lineages. Such uncharacterized and potentially anaerobic prokaryotes could have resided in anoxic microzones of suspended particles, and were possibly responsible for the unexpectedly high N<sub>2</sub> fixation rates of  $1.13 \pm 1.04 \text{ nmol N L}^{-1} \text{ h}^{-1}$  at salinities of  $\leq 29$  and nitrate concentrations  $\geq 9.9 \text{ }\mu\text{mol L}^{-1}$ . This study extends the known distribution of quantitatively important oceanic diazotrophs, and shows that the Mekong River plume hosts a diverse diazotroph community, of which particularly *Trichodesmium* spp. and DDAs seem to fix nitrogen at high rates.

## 4.2 Introduction

On a global scale, biological dinitrogen ( $N_2$ ) fixation by marine pelagic prokaryotes is the most important source of biologically available nitrogen to the ocean (Karl et al. 2002; Gruber and Galloway 2008).  $N_2$  fixing microorganisms (diazotrophs) use the enzyme nitrogenase for the reduction of atmospheric  $N_2$  to ammonium. The *nifH* gene encodes for the iron-containing subunit of nitrogenase, and studies that analyzed the diversity and distribution of the *nifH* gene in marine environments have identified several new and quantitatively important diazotroph phylotypes (Zehr and McReynolds 1989; Zehr et al. 2001).

The majority of marine diazotrophs seem to be constrained to tropical and subtropical ocean regions. *Trichodesmium* spp. are non-heterocystous, filamentous cyanobacteria that can form vast blooms in warm surface waters with low concentrations of combined nitrogen (Capone et al. 1997; LaRoche and Breitbarth 2005). Other groups of diazotrophs include unicellular cyanobacteria, members of proteobacterial lineages, and relatives of anaerobic sulfate reducers (Zehr et al. 1998; 2001; Church et al. 2005a). Unicellular diazotrophic cyanobacteria are more evenly distributed in the water column than *Trichodesmium* spp. (Langlois et al. 2005; Church et al. 2005a), and likely make a substantial contribution to  $N_2$  fixation globally (Montoya et al. 2004). Another important group of diazotrophs are the symbiotic diatom-diazotroph associations (DDAs) between the heterocystous cyanobacterium *Richelia intracellularis* and *Rhizosolenia* spp. or *Hemiaulus* spp., and between *Calothrix rhizosoleniae* and *Chaetoceros* spp. (Villareal 1992; Janson et al. 1999; Foster and Zehr 2006). Although  $N_2$  fixation is recognized a key component of the marine nitrogen cycle, we are just beginning to understand the different broad-scale distributions of the various diazotrophs, and to assess their relative contributions to oceanic  $N_2$  fixation.

In the western tropical north Atlantic (WTNA), high densities of *Hemiaulus-Richelia* symbioses were found in the Amazon River plume, and rates of  $N_2$  fixation exceeded vertical nitrate fluxes (Carpenter et al. 1999). A QPCR-study, targeting *nifH*, later confirmed that these DDAs dominate in plume waters, where they presumably benefit from riverine phosphorus, silicate, and iron, while outside of the plume, *Trichodesmium* and unicellular cyanobacteria were the most abundant diazotrophs (Foster et al., 2007). Unlike *Trichodesmium* spp. and other diazotrophs, the fast-sinking DDAs efficiently contribute to the sequestration of atmospheric carbon in the deep sea (Scharek et al. 1999a,b; Mulholland 2007; Subramaniam et al. 2008). High  $N_2$  fixation in tropical river plumes, in particular carried out by DDAs, may be a general phenomenon, but few other studies in river plume systems have been conducted. The goal of

this study was to investigate diazotroph distributions and activities in the Mekong River plume, another large tropical river.

Phytoplankton growth in offshore waters of the South China Sea (SCS) is limited by nitrogen (Chen et al. 2004), and thus the environment is considered favorable for N<sub>2</sub> fixation. Moisander et al. (2008) analyzed the *nifH* diversity and abundances in the southwestern SCS and detected all groups of marine diazotrophs described above. During previous studies, we measured elevated rates of N<sub>2</sub> fixation in surface waters influenced by the Mekong River plume, but diazotrophs were not identified (Voss et al. 2006). These prior investigations took place during southwest (SW) – monsoon, when the river plume was identifiable adjacent to an upwelling area northeastward from the river mouth (around 12°N), and consequently the influences of river water and upwelling on nutrient distributions and phytoplankton species composition were possibly superimposed. In order to clarify how the Mekong River influences N<sub>2</sub> fixation and the horizontal distribution and activities of diazotrophs in the SCS, we studied the river plume during intermonsoon in April 2007, when the river discharge reaches its annual minimum. It was therefore possible to collect surface samples from the spatially constrained river plume with a high sampling resolution and without the additional influence of upwelling. Rates of <sup>15</sup>N<sub>2</sub> fixation were measured along steep gradients of salinity and nutrients and showed much higher values (up to 22.77 nmol l<sup>-1</sup> h<sup>-1</sup>) than during all previous investigations (Voss et al. 2006; Grosse et al. in press, see chapter 3). Diatoms which were potentially associated with diazotrophic symbionts *Richelia* or *Calothrix* dominated the phytoplankton community at all stations (including *Rhizosolenia* spp., *Chaetoceros* spp., *Guinardia* spp., *Hemiaulus* spp. and *Bacteriastrum* spp.), and abundances increased with the flow direction of the Mekong Plume (Grosse et al. in press, see chapter 3). We therefore assumed that DDAs would be major components of the diazotroph community. Here we used QPCR and RT- QPCR assays to estimate the *nifH* gene abundances and *nifH* gene expression of 9 diazotroph groups. Additionally, we assessed the *nifH* gene diversity along a salinity gradient. The surface flow of the river plume along the coast was simulated using a hydrodynamic model, which helped us to understand and interpret the link between the Mekong River plume and the community of diazotrophs.

## 4.3 Materials and methods

### 4.3.1 Sampling

Samples were collected along three transects (Fig. 4.1) between 15 and 20 April 2007, aboard the Vietnamese monitoring vessel BTh-0666 KN. In April, the river outflow reaches its annual

minimum of approximately  $2,500 \text{ m}^3 \text{ s}^{-1}$  (Hordoir et al. 2006), and consequently the river plume forms a relatively narrow band propagating southward along the coast. Total distances between coastal stations and stations furthest offshore were 29 km and 41 km on transects 1 and 3, respectively, and 135 km on transect 2. To describe the hydrography of the Mekong River plume and its influence on diazotroph community composition and activity throughout a complete tidal cycle, a 25 h mooring station (station 19, Fig. 4.1) was sampled between 06:00 on 18 April 2007 and 07:00 on 19 April 2007 (all times given as local time). At all stations, we recorded profiles of conductivity and temperature using a Seabird SBE19 plus sensor (Bellevue, WA, USA) with measurement error of 0.01 for salinity. Turbidity profiles were recorded with an infrared turbidity meter recording Nephelometric Turbidity Units (NTU), with a measurement error of 0.5 NTU (Seapoint, Exeter, NH, USA). A total of 25 surface water samples were taken with a 10 L Niskin bottle. At the mooring station 19, CTD profiles were recorded hourly (27 casts in total, consecutively termed as 19\_1 for cast 1 and so on), while samples were collected for nucleic acids and other parameters at 7 time points. The vertical distribution of photosynthetically active radiation (PAR) was measured using a LICOR spherical light sensor (Lincoln, NE, USA). PAR measurements were limited to stations 1, 3, 5 and 12, because the sensor was not deployable at most stations due to strong tidal currents (up to  $1.8 \text{ m s}^{-1}$ ).

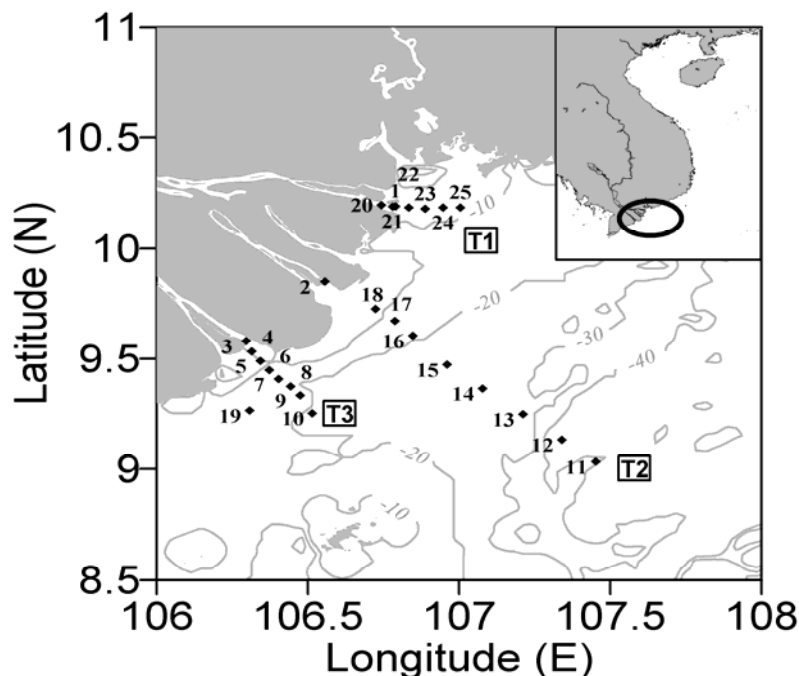


**Figure 4.1:** Map of the Mekong River Estuary showing locations of all CTD-stations on transects 1 (T1), 2 (T2) and 3 (T3).

### 4.3.2 Nutrient analyses

Surface samples for determining concentrations of nitrate ( $\text{NO}_3^-$ ), nitrite ( $\text{NO}_2^-$ ), phosphate ( $\text{PO}_4^{3-}$ ) and silicate ( $\text{Si}(\text{OH})_4$ ) were collected from 18 stations. The water samples were immediately frozen and nutrients were analyzed at the Institute of Oceanography in Nha Trang, using standard colorimetric methods (Grasshoff 1983). These methods usually reach a precision of  $0.05 \mu\text{mol L}^{-1}$  for  $\text{NO}_3^-$ ,  $0.01 \mu\text{mol L}^{-1}$  for  $\text{NO}_2^-$ ,  $0.01 \mu\text{mol L}^{-1}$  for  $\text{PO}_4^{3-}$ , and  $0.1 \mu\text{mol L}^{-1}$  for  $\text{Si}(\text{OH})_4$ . However, due to the local circumstances (nutrient traces in the only available distilled water), we could not achieve a precision better than  $0.05 \mu\text{mol L}^{-1}$  for  $\text{NO}_3^-$ ,  $\text{NO}_2^-$ , and  $\text{PO}_4^{3-}$ . Nutrient ratios (N:P, Si:N) were therefore not calculated for samples having unreliable concentrations  $\leq 0.1 \mu\text{mol L}^{-1}$ . Nutrients are hereafter termed N for  $\text{NO}_3^- + \text{NO}_2^-$ , P for  $\text{PO}_4^{3-}$ , and Si for  $\text{Si}(\text{OH})_4$ .

### 4.3.3 $\text{N}_2$ fixation

Rates of  $\text{N}_2$  fixation were measured in triplicate surface water samples at 16 stations, using the tracer assays described by Montoya et al. (1996). At each station, three 2.3-L polycarbonate bottles were filled and sealed with Teflon coated butyl-rubber septa, and 2 ml of  $^{15}\text{N}_2$  gas (Sercon, Cheshire, UK, 99 atom%) were added with a syringe. The bottles were incubated for 6 h on deck under simulated *in situ* conditions, using neutral density screening (50%) and surface sea water for cooling, and incubations were terminated by gentle filtration over precombusted Whatman GF/F filters. The remaining protocols followed Montoya et al. (1996).

### 4.3.4 Nucleic acid sampling and extraction

DNA and RNA samples were collected from the surface at 18 stations, including samples from 11 transect stations and 7 samples from the mooring station 19. Seawater from the Niskin bottle was collected into 2-L, acid washed polycarbonate bottles. Immediately after sampling, between 150 mL and 1100 mL (depending on turbidity) was filtered onto  $0.2 \mu\text{m}$  pore size Durapore (Millipore, Billerica, MA, USA) filters, held in 25 mm diameter Sartorius filter holders, using a peristaltic pump. For DNA samples, seawater was size fractionated by pre-filtering through  $10\text{-}\mu\text{m}$  pore size Isopore filters (Millipore). The filters were removed, placed into 1.5-mL cryovials and stored in liquid nitrogen until arrival in the lab, where they were stored at  $-80^\circ\text{C}$ .

A FastDNA® Pro Soil kit (MPI Biomed, Solon, OH, USA) was used for DNA extraction. We closely followed the manufacturer's extraction protocol, which includes a purification step for humic substances. RNA was extracted using a modified Qiagen (Valencia,

CA, USA) RNeasy kit protocol. Sample filters were transferred into sterile bead beater tubes containing 350  $\mu\text{L}$  of RLT buffer from the kit, 1%  $\beta$ -mercaptoethanol, and 30  $\mu\text{L}$  of 0.1-mm glass beads (Biospec Products, Bartlesville, OK, USA). The tubes were agitated in a bead beater for 2 min, filters were removed, and the tubes were centrifuged for 1 min at 8,000 g. The supernatants were transferred to Qiagen shredder columns, centrifuged for 2 min at the maximum speed, and then transferred to clean 1.5-mL microcentrifuge tubes. The RNA purification was completed by using RNeasy spin columns, following the manufacturer's protocol. An on-column DNase step was included with a 1-h incubation. The RNA was eluted in 35  $\mu\text{L}$  of RNase-free water and stored at  $-80^{\circ}\text{C}$ .

#### 4.3.5 *nifH* PCR, cloning, sequencing, and sequence analysis

The diversity of the diazotroph populations was investigated by amplifying, cloning and sequencing a 359-base-pair (bp) fragment of the *nifH* gene from surface water samples taken at eight stations (2, 3, 8, 10, 12, 15, 18, and 19\_1, 5:30). We used a nested PCR approach with degenerate primers (Zehr and Turner 2001). Amplified products were cloned into pGEM-T vectors (Promega, Madison, WI, USA), and sequenced to both directions at the University of California Berkeley sequencing facility, using SP6 or T7 primers. Sequences were trimmed and integrity-checked using phred-phrap (Ewing et al. 1998). For each sample, sequences were considered different if they differed by more than one bp. Fifty-seven representative sequences were deposited in GenBank under accession numbers GQ475428-GQ475484. For phylogenetic analyses, the edited sequences were translated and imported into an aligned ARB database (Zehr et al. 2003).

#### 4.3.6 cDNA synthesis

RNA was reverse transcribed using Super-Script III first strand cDNA synthesis kit (Invitrogen, Carlsbad, CA, USA), following the manufacturer's protocol. The 20- $\mu\text{L}$  reactions contained 5  $\mu\text{L}$  of RNA template, 0.5  $\mu\text{mol L}^{-1}$  reverse primer *nifH2* (Zehr and Turner 2001), 0.5  $\text{mmol L}^{-1}$  dNTP mixture, 2  $\mu\text{L}$  of 10 x RT-buffer, 5  $\text{mmol L}^{-1}$   $\text{MgCl}_2$ , 10  $\text{mmol L}^{-1}$  dithiothreitol, 2 U  $\mu\text{L}^{-1}$  RnaseOUT (Invitrogen), and 10 U  $\mu\text{L}^{-1}$  reverse transcriptase (RT). Negative control reactions included a reaction with no RT and sample RNA, (controls for DNA contamination) and a reaction with RT but template replaced with water. Reaction conditions were as follows:  $50^{\circ}\text{C}$  for 50 min,  $85^{\circ}\text{C}$  for 5 min, then tubes were placed on ice. Subsequently, 1  $\mu\text{L}$  of Rnase H was added to each reaction mixture, and tubes were incubated at  $37^{\circ}\text{C}$  for 20 min to eliminate residual RNA. The cDNA was stored at  $-20^{\circ}\text{C}$ .

**Table 4.1:** Primer and probe sets used in this study

Taxonomic group	Species/clone	Forward primer 5' – 3'	Probe	Reverse primer 5' – 3'	Reference
Cyanobacteria	Group A (unicellular)	AGCTATAACAACGTTTTATGCGTTGA	TCTGGTGGTCCTGAGCCTGGA	ACCACGACCAGCACATCCA	Church et al. (2005a)
Cyanobacteria	Group B (unicellular)	TGGTCCTGAGCCTGGAGTTG	TGTGCTGGTCGTGGTAT	TCTTCTAGGAAGTTGATGGA GGTGAT	Church et al. (2005a)
Cyanobacteria	Group C (unicellular)	ATACCAAGGAATCAAGTGTGTTGAGT	CGGTGGTCCCGAGCCTGGAG	ACCACGACCAG CACATCCA	Foster et al. (2007)
Cyanobacteria	<i>Trichodesmium</i>	GACGAAGTATTGAAGCCAGGTTTC	CATTAAGTGTGTTGAATCTGGTG GTCCTGAGC	CGGCCAGCGCAACCTA	Church et al. (2005a)
Cyanobacteria	Het-1	CGGTTTCCGTGGTGTACGTT	TCCGGTGGTCCTGA GCCTGGTGT	AATACCACGACC CGCACAAC	Church et al. (2005b)
Cyanobacteria	Het-2	TGGTTACCGTGATGTACGTT	TCTGGTGGTCCTGA GCCTGGTGT	AATGCCGCGACCA GCACAAC	Foster et al. (2007)
Cyanobacteria	Het-3	CGGTTTCCGTGGCGTACGTT	TCTGGTGGTCCAGAACCTGGTGT	AATACCACGACCA GCACAAC	Foster et al. (2007)
$\gamma$ - Proteobacterium	24809A11	CGGTAGAGGATCTTGAGCTTGAA	AAGTGCTTAAGGTTGGCTTT GGCGACA	CAAGTGCGTGGAGT CAGGTG	Moisander et al. (2008)
$\alpha$ - Proteobacterium	24809A06	TCTGATCCTGAACTCCAAAAGCA	ACCGTGCTGCACCTGGCCG	GAAATGGGTTCCGG TTGAGGA	Moisander et al. (2008)

### 4.3.7 Quantitative PCR and RT-QPCR

Nine Taq-Man® primer-probe sets that were previously designed for oceanic diazotroph microbes were used (Table 4.1). In the following, we refer to the quantified *nifH* genes and transcripts of cyanobionts with the abbreviations R-R for *Rhizosolenia-Richelia*, H-R for *Hemiaulus-Richelia*, and C-C for *Chaetoceros-Calothrix*, assuming that the cyanobionts were not free living, but associated with their respective diatom hosts.

QPCR reactions were conducted in a 7500 Real-Time PCR system (Applied Biosystems, Foster City, CA, USA). QPCR reactions for samples were run in triplicate. Standard curves and PCR efficiency tests were carried out as described previously (Short et al. 2004; Short and Zehr, 2005). Primer and probe sets specific for DDA species and *Trichodesmium* spp. were used to detect targets in DNA extracts from both the 10 µm and 0.2 µm pore size filters, and gene copy abundances in the two size fractions were pooled. Standard curve linear regression  $r^2$  values were  $>0.98$  for all reactions. Amplification efficiencies were  $\geq 98.1\%$  in all samples, except for one lower value in the sample from station 12 (95.7% in a reaction targeting *Trichodesmium* spp. DNA). Thus, all QPCR reactions were considered uninhibited. If only two of the three replicates produced an amplification signal, the target was noted as detected, but not quantifiable.

### 4.3.8 Transformation onto Lagrangian coordinates and a Lagrangian tracer experiment

We used a circulation model to characterize spatial and temporal patterns of the river plume propagation along the coast during intermonsoon flow conditions. Karfeld et al. (unpublished data) have simulated the circulation in the Mekong estuary, using an updated version of the numerical HAMburg Shelf Ocean Model (HAMSOM) (Backhaus 1985, Pohlmann 2006). HAMSOM is a three-dimensional, baroclinic, primitive equation model with a free surface (Backhaus 1985). We used a temporal resolution of 2.5 minutes, and a horizontal grid resolution of  $1/60^\circ$ . To validate the model results, the hydrographic measurements from our study were used (Hein et al. 2007).

We carried out two Lagrangian tracer experiments in surface currents calculated by HAMSOM. In the first experiment, we transformed our sampling stations onto Lagrangian coordinates (fixed in time). This technique eliminates the bias due to “tidal aliasing”, i.e. the wrong picture of the distribution of hydrographic parameters on fixed oceanographic stations which can result from the intermittent sampling of station transects across tide-advected water masses over time periods of several days (Brockmann and Dippner 1987). By the assumption

of no vertical mixing, this technique allows the reconstruction of quasi-synoptic observations of the hydrography. Station coordinates were transformed using the reference time of station 25, the last station sampled (4 April 2007, 8:30). In the second experiment, one tracer was released every h for a model run of 335 h from stations 1, 2 and 3, (9 April 2007, 00:00 until 22 April 2007, 00:00). This experiment aimed at resolving the temporal scales at which the river plume flows along the coast, and at visualizing the frontal dynamics in this tidally driven estuary. In both experiments, surface advection incorporated the effects of tides, river runoff, wind stress and remote forcing due to boundary currents.

### **4.3.9 Statistical analyses**

Statistical tests for normality (Shapiro-Wilk), correlations, linear regressions, curve fittings and one-way analysis of variance on ranks (Kruskal-Wallis) were performed in SPSS 15.0 for Windows and Grapher 6.0 (Golden Software Inc.).

## **4.4 Results**

### **4.4.1 Lagrangian tracer experiments**

Figure 4.2 shows the positions of the sampling stations and isolines of salinity and turbidity in the geographically fixed- and synchronized Lagrangian station grids. After transformation, the spatial distributions of both salinity and turbidity reveal stronger gradients on all three transects. This becomes especially clear at stations 14-18 on transect 2, and stations 5-10 on transect 3. The results of the tracer release experiment show the extension of the river plume front and the alongshore propagation of the plume in a south-westerly direction (Fig. 4.3). The “oldest” tracers are found furthest offshore, and especially tracers originating from station 3 spread in a southwesterly direction along a straight line. Within 335 h, the tracers covered a net distance of approximately 46 km across the shelf and a maximum alongshore distance of 63 km.

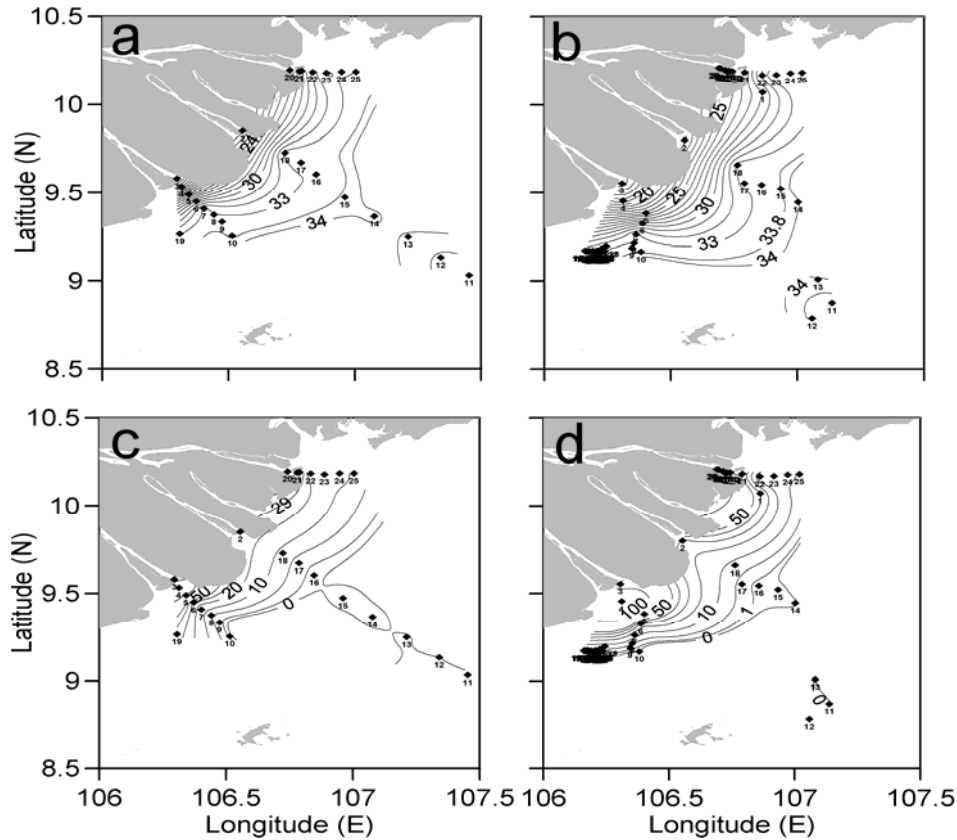


**Figure 4.2:** a) Horizontal distribution of surface salinity for Eulerian station coordinates; b) same as a), but for stations transformed onto Lagrangian coordinates. Contour intervals of salinity are 1, except for the 33.8 isoline; c) and d), horizontal distribution of surface turbidity (selected isolines of Nephelometric turbidity units, NTU) in the Eulerian and the Lagrangian coordinate system, respectively.

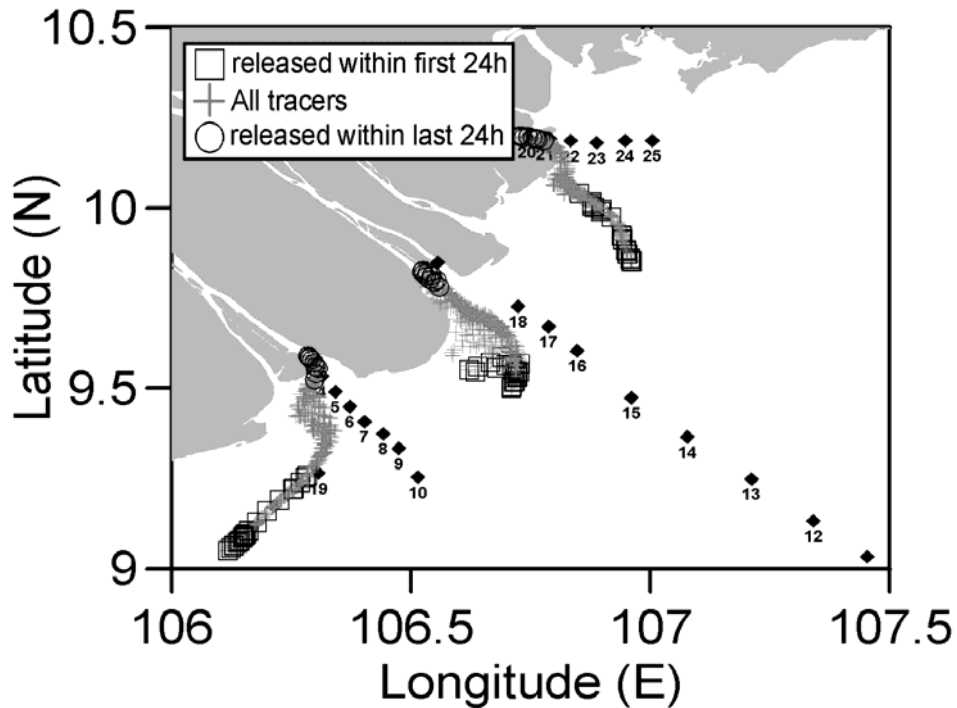


**Figure 4.3:** The propagation of the Mekong River plume between 9 April 2007, 00:00 and 22 April 2007, 00:00, as shown by results of a Lagrangian tracer experiment using the HAMSOM model. From coordinates of stations 1, 2 and 3, one tracer was released every hour for a model run of 335 h. The Eulerian sampling stations are included in this figure to show their position relative to the modeled plume propagation.

#### 4.4.2 Environmental conditions

Sea surface salinity ranged from 14.3 (station 3) to 34.0 (station 13) (Fig. 4.2b). Surface salinities at offshore stations 11 and 12 (33.6-33.8) were slightly lower compared to the further inshore stations 13 (34.0), 14 (34.0) and 15 (33.9). At the mooring station 19, surface salinities measured hourly by CTD ranged from 29.1 to 33.2, while the samples for nucleic acids taken at 7 time points had salinities between 32.6 and 33.1. Sea surface temperatures varied from 28.5°C to 31.5°C in the entire area, with the lowest temperatures at the oceanic stations 11 and 12, and the highest temperature at the riverine station 3.

**Table 4.2:** Pearson correlation matrix comparing changes in salinity, turbidity, and nutrient concentrations in surface waters. p-values  $\leq 0.01$  are considered significant.

	Salinity	p-value
Salinity	1.000	
Turbidity	-0.778	$\leq 0.001$
Nitrate	-0.822	$\leq 0.001$
Nitrite	-0.603	$\leq 0.001$
Phosphate	-0.919	$\leq 0.001$
Silicate	-0.931	$\leq 0.001$

Nutrient concentrations and sea surface turbidity showed strong offshore gradients and were negatively correlated with salinity (Table 4.2). The horizontal distributions of nutrients can be viewed in chapter 3, Fig. 3.2 C, E and G. Maximum nutrient concentrations were detected at coastal stations on transects 3 (19.6  $\mu\text{mol L}^{-1}$  of N and 0.97  $\mu\text{mol L}^{-1}$  P at station 3, and 42.6  $\mu\text{mol L}^{-1}$  of Si at station 5). Stations 10-12 were depleted in both N and P while the lowest Si concentration measured in the area was 2.3  $\mu\text{mol L}^{-1}$  (stations 11, 12). Concentrations of N had a positive relationship with P ( $p < 0.01$ , Spearman rank correlation,  $r_s = 0.88$ ) and Si ( $p < 0.01$ , Spearman rank correlation,  $r_s = 0.90$ ) (Fig. 4.4a, b). The regression lines have positive x-axis intercepts, suggesting that on average significant amounts of P and Si remained in N-depleted waters. At stations 19\_15, 19\_21 and at station 23, N concentrations were at the detection limit while P concentrations between 0.1 and 0.2  $\mu\text{mol L}^{-1}$  and Si concentrations between 2.3 and 6.1  $\mu\text{mol L}^{-1}$  were measured. There was a significant ( $p < 0.001$ ) negative relationship between surface salinity and the ratios of N to P (Fig. 4.4c). Ratios of Si to N were not significantly correlated with salinity or turbidity. Si:N ratios remained below 5 at surface salinities between 14.3 and 29.3, and at salinities greater 32.6, they varied between 2.8 and 49.3 (Fig. 4.4d).

Highly turbid surface waters were largely confined to the area where depths were shallower than 20 m (Fig. 4.1, Fig. 4.2d). At stations 1, 3, and 5, where turbidity was between

42 and 79 NTU, PAR decreased to less than 50% of the surface value within the first meter of the water column, and to less than 1% at 2-m depth (data not shown). In contrast, at station 12, surface turbidity was below detection (<0.5 NTU), and PAR was still 40% of the surface value at 5 m depth.

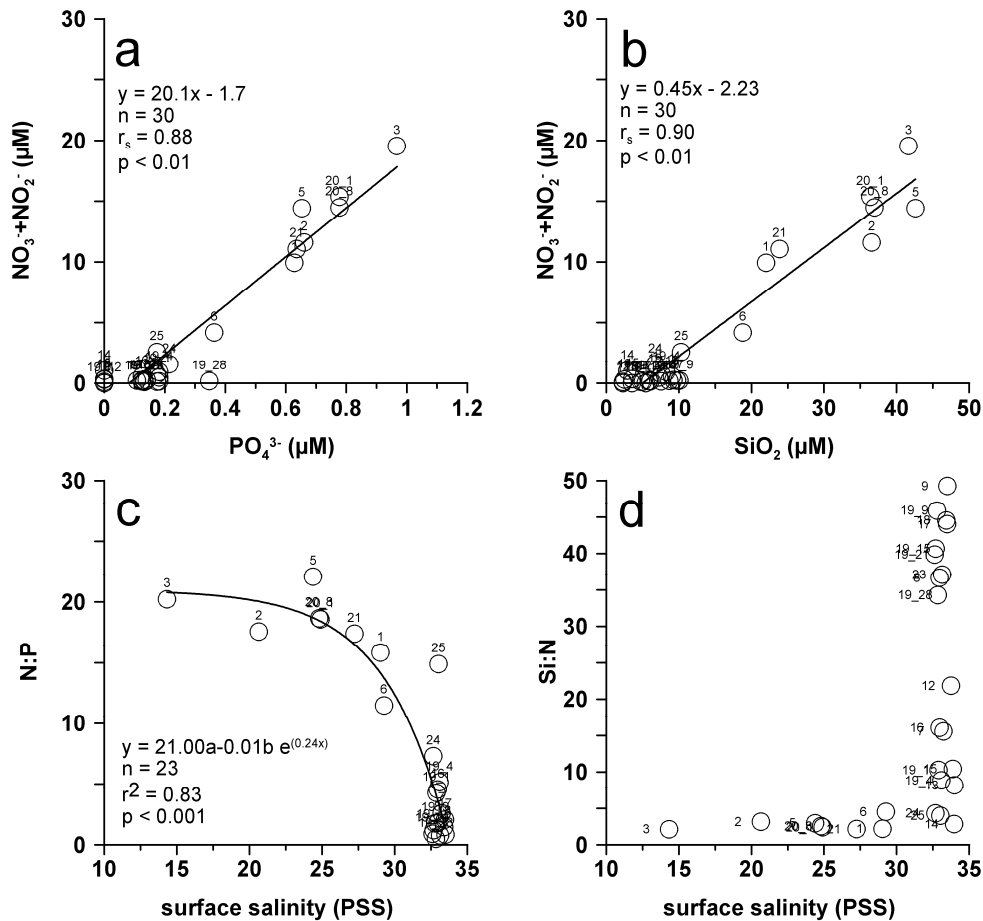


**Figure 4.4:** Relationship between a)  $\text{PO}_4^{3-}$  and  $\text{NO}_3 + \text{NO}_2^-$  concentrations, b)  $\text{SiO}_2$  and  $\text{NO}_3 + \text{NO}_2^-$  concentrations, c) salinity and N:P ratios, and d) salinity and Si:N ratios. Numbers above data points indicate sampling stations.

Based on the environmental parameters, the stations that were sampled for  $\text{N}_2$  fixation assays and/or nucleic acids were grouped as plume-, transitional- and oceanic stations (Table 4.3). Plume stations had surface salinities ranging from 14.3 to 29.0, and were characterized by highest nutrient concentrations ( $\text{N} \geq 9.9 \mu\text{M}$ ,  $\text{P} \geq 0.6 \mu\text{M}$ ,  $\text{Si} \geq 22.0 \mu\text{M}$ ) and highest turbidities ( $\text{NTU} \geq 27$ ). At oceanic stations (surface salinities 33.6-33.9), nutrient concentrations were low or undetectable ( $\text{N} \leq 0.3 \mu\text{M}$ ,  $\text{P}$  below detection,  $\text{Si} \leq 3.6 \mu\text{M}$ ) and turbidity was  $\leq 1$  NTU. Transitional stations (salinities 32 to 33.5) had intermediate nutrient concentrations ( $\text{N} \leq 0.9 \mu\text{M}$ ,  $\text{P} \leq 0.3 \mu\text{M}$ ,  $\text{Si} \leq 10.1 \mu\text{M}$ ), and turbidity was clearly higher than at oceanic stations (2-9 NTU).

**Table 4.3:** Mean *nifH* gene copy- and transcript abundances (in parentheses) in surface waters off the Mekong River mouth in April 2007. Only phylotypes for which *nifH* genecopies and/or transcripts were quantifiable are shown. Stations are classified from lowest to highest surface salinity, and capital letters P, T and O in the first column denote river Plume-, Transitional-, and Oceanic stations, respectively. N concentrations ( $\text{NO}_3^- + \text{NO}_2^-$ ), N:P ratios and total rates of  $\text{N}_2$  fixation (mean  $\pm$  s.d.,  $n=3$ ) are also shown. Time refers to sampling time for  $\text{N}_2$  fixation assays and nucleic acids from the same Niskin bottle. nd: not detected.

Surface salinity	Station	Sampling date & time	$\mu\text{mol N L}^{-1}$ ; N:P ratio	$\text{N}_2$ fixation (nmol N $\text{L}^{-1} \text{h}^{-1}$ )	<i>Rhizosolenia</i> - <i>Richelia</i> (het-1)	<i>Hemiaulus</i> - <i>Richelia</i> (het-2)	<i>Trichodesmium</i> spp.	Group B	Group C	$\gamma$ -proteo bacteria
14.3	3	16. Apr. 07, 11:30	19.6; 20.2	$1.07 \pm 0.52$	nd (nd)	nd (nd)	$3.0 \times 10^4$ (nd)	nd (nd)	nd (nd)	nd (nd)
20.7	2	16. Apr. 07, 06:00	11.6; 17.6	$1.01 \pm 0.31$	nd (nd)	$4.5 \times 10^3$ (nd)	$5.7 \times 10^3$ (nd)	nd (nd)	nd (nd)	nd (nd)
P 24.4	5	16. Apr. 07, 14:30	14.4; 22.1	-	nd (nd).	nd (nd)	nd (nd)	nd (nd)	nd (nd)	nd (nd)
24.9	20_1	19. Apr. 07, 15:00	14.0; 18.6	$0.59 \pm 0.19$	nd (nd)	nd (nd)	$2.1 \times 10^3$ (nd)	nd (nd)	nd (nd)	nd (nd)
29.0	1	15. Apr. 07, 17:00	9.9; 15.8	$0.11 \pm 0.06$	nd (nd)	nd (nd)	nd (nd)	nd (nd)	nd (nd)	nd (nd)
32.6	19_21	19. Apr. 07, 00:00	0.1; 0.9	$18.99 \pm 1.53$	nd (nd)	$2.5 \times 10^3$ (d)	$5.3 \times 10^3$ (nd)	nd (nd)	nd (nd)	nd (nd)
32.7	19_15	18. Apr. 07, 18:00	0.1; 1.2	$14.62 \pm 1.77$	$1.6 \times 10^3$ ( $9.8 \times 10^3$ )	$8.6 \times 10^2$ ( $1.1 \times 10^4$ )	$1.2 \times 10^5$ ( $1.1 \times 10^4$ )	nd (nd)	nd (nd)	nd (nd)
32.8	19_9	18. Apr. 07, 12:00	0.2; 1.8	$22.77 \pm 5.69$	nd (nd)	nd (nd)	$3.6 \times 10^4$ (d)	nd (nd)	nd (nd)	nd (nd)
32.8	19_27	19. Apr. 07, 06:00	0.2; 0.5	$11.56 \pm 6.50$	$1.0 \times 10^3$ ( $1.6 \times 10^3$ )	$4.0 \times 10^2$ (nd)	$2.4 \times 10^4$ ( $6.9 \times 10^3$ )	nd (nd).	nd (nd)	nd (nd)
32.9	19_1	18. Apr. 07, 05:30	0.7; 4.3	$15.54 \pm 1.71$	d (nd)	nd (nd)	$2.0 \times 10^5$ (nd)	nd (nd)	nd (nd)	nd (nd)
33.0	8	16. Apr. 07, 17:00	0.3; 1.8	$5.76 \pm 0.70$	$5.7 \times 10^3$ ( $2.3 \times 10^4$ )	$5.1 \times 10^2$ ( $1.2 \times 10^4$ )	$9.3 \times 10^4$ ( $2.5 \times 10^4$ )	nd (nd)	nd (nd)	nd (d)

**Table 4.3** (continued)

	Surface salinity	Station	Sampling date & time	$\mu\text{mol N L}^{-1}$ ; N:P ratio	$\text{N}_2$ fixation ( $\text{nmol N L}^{-1} \text{h}^{-1}$ )	<i>Rhizosolenia</i> - <i>Richelia</i> (het-1)	<i>Hemiaulus</i> - <i>Richelia</i> (het-2)	<i>Trichodesmium</i> spp.	Group B	Group C	$\gamma$ -proteo bacteria
	33.0	19_12	18. Apr. 07, 15:00	0.0; -	$12.52 \pm 0.5$	nd ( $5.6 \times 10^2$ )	nd ( $4.7 \times 10^2$ )	$5.7 \times 10^3$ ( $1.3 \times 10^4$ )	nd (nd)	nd (nd)	nd (nd)
T	33.1	19_4	18. Apr. 07, 09:00	0.9; 5.1	$12.90 \pm 5.64$	$1.0 \times 10^3$ ( $4.4 \times 10^3$ )	$3.3 \times 10^2$ ( $1.2 \times 10^3$ )	$5.4 \times 10^4$ ( $3.8 \times 10^5$ )	nd (nd)	nd (nd)	nd (nd)
	33.4	18	17. Apr. 07, 16:00	0.2; 1.5	-	$2.4 \times 10^3$ (nd)	nd (nd)	$2.3 \times 10^4$ (nd)	nd (nd)	nd (nd)	nd (nd)
	33.6	11	17. Apr. 07, 06:00	0.0; -	$11.36 \pm 3.04$	$6.7 \times 10^4$ ( $2.0 \times 10^6$ )	$1.0 \times 10^3$ ( $1.3 \times 10^4$ )	$2.3 \times 10^3$ (nd).	nd ( $3.3 \times 10^2$ )	$1.3 \times 10^3$ ( $4.7 \times 10^4$ )	$7.5 \times 10^2$ ( $8.8 \times 10^4$ )
O	33.7	10	16. Apr. 07, 18:20	0.0; -	$3.95 \pm 2.06$	$4.6 \times 10^4$ ( $1.4 \times 10^6$ )	$1.5 \times 10^3$ ( $1.4 \times 10^4$ )	$2.4 \times 10^5$ ( $3.0 \times 10^4$ )	$5.4 \times 10^3$ ( $3.7 \times 10^5$ )	nd ( $1.1 \times 10^4$ )	$3.3 \times 10^3$ ( $2.8 \times 10^4$ )
	33.8	12	17. Apr. 07, 07:00	0.1; -	-	$3.4 \times 10^3$ ( $5.2 \times 10^4$ )	nd ( $5.8 \times 10^3$ )	nd (nd)	nd (nd)	nd ( $2.0 \times 10^4$ )	$1.0 \times 10^3$ ( $3.1 \times 10^4$ )
	33.9	15	17. Apr. 07, 13:30	0.3; -	$16.36 \pm 0.30$	$9.0 \times 10^3$ (d)	nd (nd)	$1.0 \times 10^4$ ( $7.7 \times 10^3$ )	$5.2 \times 10^2$ (nd)	$4.0 \times 10^2$ ( $7.9 \times 10^2$ )	$5.6 \times 10^2$ ( $5.4 \times 10^3$ )

### 4.4.3 N<sub>2</sub> fixation

Rates of N<sub>2</sub> fixation were measured at several stations within the plume (stations 1-3, & 20\_1), transitional waters (8, 18 & 19) and within oceanic waters (10, 11, & 15) (Table 4.3). N<sub>2</sub> fixation was detectable at all of these stations. Daytime N<sub>2</sub> fixation overall ranged from 0.59 nmol N L<sup>-1</sup> h<sup>-1</sup> (station 20\_1) to 22.77 nmol N L<sup>-1</sup> h<sup>-1</sup> (station 19\_9). The highest rates of N<sub>2</sub> fixation were detected at transitional and oceanic stations having surface salinities  $\geq 32.6$  and relatively low nutrient concentrations ( $\leq 0.9, 0.4, 10.1 \mu\text{mol L}^{-1}$  of N, P and Si, respectively, Table 4.3). The rates of N<sub>2</sub> fixation are discussed in more detail in Grosse et al. (in press., see chapter 3).

### 4.4.4 Abundances of diazotrophs and *nifH* gene expression

Spatial distribution and gene expression of diazotrophic populations was determined at all stations where N<sub>2</sub> fixation was measured, and additionally at stations 5, 12, and 18 (Table 4.3). The *C-C* symbiosis,  $\alpha$ -proteobacteria, and group A unicellular cyanobacteria were not detectable or quantifiable in any of the samples.

The greatest *nifH* abundances and gene expression of the large diazotrophs (*Trichodesmium* spp., R-R and H-R), were found at the oceanic and transitional stations (Fig. 4.5, Table 4.3). These stations had overall low N:P ratios ( $\leq 5.1$ ), low N concentrations ( $\leq 0.9 \mu\text{mol N}$ ), and had highest N<sub>2</sub> fixation rates. Unicellular diazotrophs (group B, C, and  $\gamma$ -proteobacteria) were exclusively quantifiable and expressing *nifH* in samples from oceanic stations, which had N concentrations of  $\leq 0.3 \mu\text{mol L}^{-1}$  and P concentrations below detection (Table 4.3, Fig. 4.5).

The H-R ( $4.5 \times 10^3$  *nifH* gene copies L<sup>-1</sup>) and *Trichodesmium* spp. ( $5.7 \times 10^3$  *nifH* gene copies L<sup>-1</sup>) phylotypes were also found at the plume station 2, where N concentrations and the N:P ratio were high ( $11.6 \mu\text{mol L}^{-1}$ ; 17.6). However, *nifH* expression was not detected and N<sub>2</sub> fixation rates was comparatively reduced ( $1.01 \pm 0.31$  nmol N L<sup>-1</sup> h<sup>-1</sup>). Similarly, *Trichodesmium* spp. was present with no detectable *nifH* gene expression at the plume station 20\_1 ( $2.1 \times 10^3$  *nifH* gene copies L<sup>-1</sup>) and station 3 ( $3.0 \times 10^4$  *nifH* gene copies L<sup>-1</sup>), which also had high N concentrations, high N:P, and low N<sub>2</sub> fixation (Table 4.3).

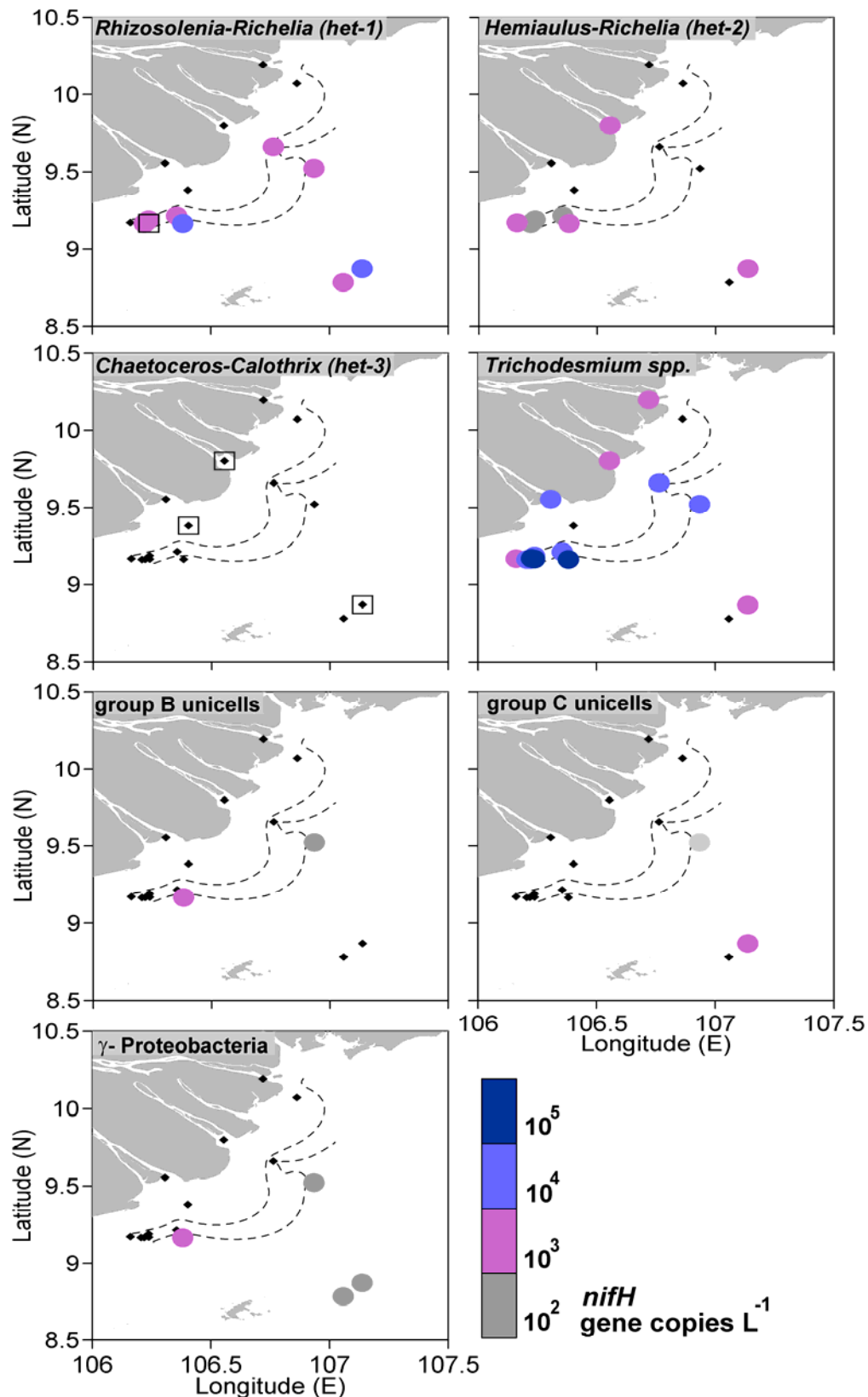


**Figure 4.5:** Horizontal distribution of *nifH* gene copies  $L^{-1}$  of the three different DDA, *Trichodesmium* spp., unicellular group B and C cyanobacteria, and  $\gamma$ -Proteobacteria. Black squares indicate samples in which *nifH* gene copies were detected but not quantifiable. Diamonds indicate sampled stations where *nifH* gene copies of the different phylotypes were not detected. The dashed lines define the salinity range between 32 and 33.5, i.e. the transitional zone.

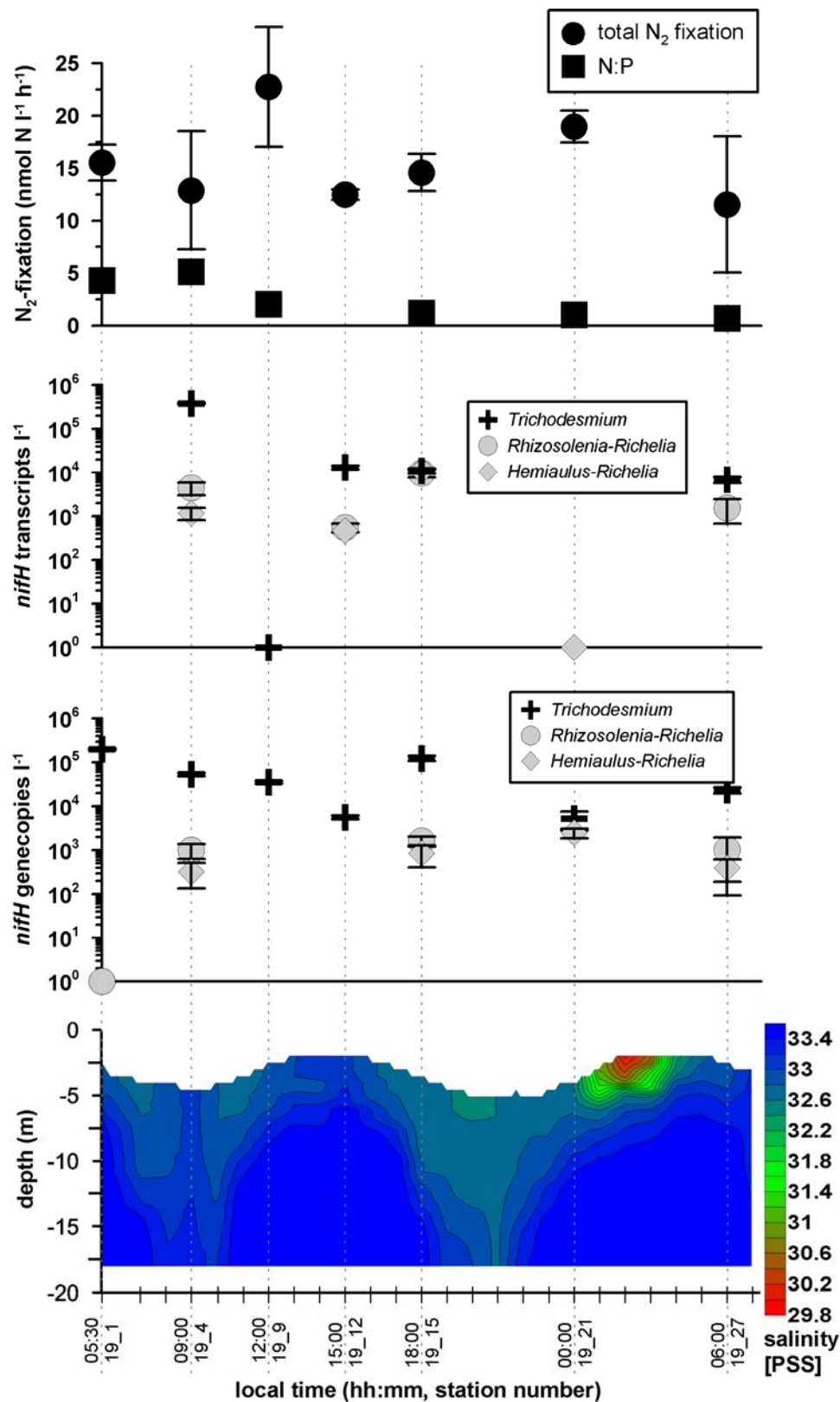


**Figure 4.6:** *NifH* gene copies / transcripts of phylotypes detected at mooring station 19, which was occupied between 5:30 on April 18<sup>th</sup> 2007 and 7:00 on April 19<sup>th</sup>. Also shown are rates of  $N_2$  fixation and N:P ratios. Tick marks indicate hourly CTD measurements, and dotted lines mark time points of sampling for nucleic acid, nutrients, and  $N_2$  fixation incubations. The contour plot of salinity was tide corrected, so that the declining/elevating surface values indicate low and high tide, respectively. Data points of *nifH* gene copies or transcripts on the x-axis indicate samples that where *nifH* was detected but not quantifiable.

Gene expression for the larger diazotrophs (*Trichodesmium* spp., H-R, R-R) was unexpectedly high in some samples taken later in the photoperiod (station 8, 17:00 and station 10, 18:00). Group C and the  $\gamma$ -proteobacterial phylotype had relatively stable *nifH* transcript abundance regardless of the time of sampling (stations 10-12, & 15).

DNA and RNA were sampled at station 19 every 3-6 h to assess the variability in both *nifH* copies and transcript abundance in transitional waters (Fig. 4.6). There was no clear correspondence between low tides and low salinities at station 19. However, isolines of salinity showed a mixed water column during low tide and a more stratified water column during high tide (Fig. 4.6). With a few exceptions, *nifH* gene copies and transcripts of R-R, H-R, and *Trichodesmium* spp. were detected in most of the samples (Fig. 4.6; Table 4.3). Unicellular diazotrophs were never detected at station 19. *NifH* gene abundance of *Trichodesmium* spp. fluctuated little with changing water masses, and the highest abundances were recorded at sampling points 19\_1 (05:30, salinity of 32.9) and 19\_15 (18:00, salinity of 32.7). DDAs were not as consistently detected and reached highest abundances at sampling points 19\_15 (18:00, salinity of 32.7) and 19\_21 (00:00, salinity of 32.6). *NifH* expression for all 3 of these larger diazotrophs remained high (around  $10^4$  *nifH* transcripts L<sup>-1</sup>) late into the photoperiod (19\_15, 18:00), which was also observed at station 10. In the 12:00 sample (19\_9), *Trichodesmium* spp. was present ( $3.6 \times 10^4$  *nifH* gene copies L<sup>-1</sup>), but *nifH* transcription remained undetectable for all 3 of the larger diazotrophs, although N<sub>2</sub> fixation was high ( $22.77 \pm 5.69$  nmol N L<sup>-1</sup> h<sup>-1</sup>).

#### 4.4.5 *nifH* diversity and phylotype distributions

A total of 82 *nifH* sequences were recovered from the 8 clone libraries amplified from surface samples, of which 52 sequences were considered unique. These sequences fell into clusters I and III according to the lineages defined by Zehr et al. (2003). Twenty-four of the 82 total sequences (29%) were within the cyanobacterial lineage and had >95% amino acid sequence identity to *Trichodesmium erythraeum*. These sequences were recovered from oceanic and transitional stations 10, 15, 18 and 19\_1 (05:30), where high abundances of *nifH* gene copies of *Trichodesmium* spp. were also detected by QPCR. Sequences belonging to unicellular cyanobacterial groups B and C as well as heterocystous *Richelia* symbionts did not appear in the clone libraries.

The 45 remaining cluster I sequences, which stem from all stations except station 15, had a high identity with a diverse group of proteobacterial sequences. Twelve sequences from stations 2-3, 10, 18, and 19\_1 had high sequence identity (96-100% protein identity) with proteobacterial sequences recovered in April 2006 in the SCS (EU052326, EU052438), and one sequence from station 12 had 99% amino acid sequence identity with the  $\gamma$ -proteobacterial

sequence that was used to design the QPCR primer probe set used in this study (EU052413) (Moisander et al. 2008). This sequence had 98% identity at the protein level with a  $\gamma$ -proteobacterial *nifH* sequence from the subtropical North Pacific (DQ269145) (Church et al. 2005b). Thirteen sequences from stations 2, 3, 10, 12, had between 90% and 98% protein identity with sequences retrieved from the rhizosphere of the salt marsh cordgrass *Spartina alterniflora* (Lovell et al. 2000), or with a sequence amplified from endophytes of rice roots (AF331989). Another 18 sequences from stations 2, 3, 18 and 19\_1 were most similar to sequences isolated from soil (EU913012, 91-94% protein identity), or estuarine sediments (EU381318, 87-90% protein identity).

Thirteen sequences recovered from stations 2, 8, and 18 were more similar to cluster III- like sequences. Nine sequences from station 8 were most similar (91-97% amino acid sequence identity) to sequences recovered from surface waters of the Gulf of Aqaba (Red Sea, EU151779) (Foster et al. 2009) and from the Chesapeake Bay water column (AY224021). Also in this cluster III group there were 3 sequences from stations 2 and 18 that were similar (99% protein identity) to sequences retrieved from the rhizosphere of the salt marsh cordgrass (Lovell et al. 2000). One sequence (station 18) had 98% identity at the protein level to a sequence recovered from sediments in Jiaozhou Bay, China (FJ686527). The closest cultivated relatives with sequences in cluster III were anaerobic sulfate reducers (genus *Desulfovibrio*, 86-90% protein identity).

## 4.5 Discussion

### 4.5.1 Hydrography of the Mekong River plume during intermonsoon and classification of stations

The spatial and temporal scales at which the river plume propagated based on the model output are consistent with typical patterns observed during intermonsoon in April (Fig. 4.3) (Hordoir et al. 2006). Due to the low discharge of approximately  $2,500 \text{ m}^3 \text{ s}^{-1}$ , a relatively small river plume is formed, and in the absence of monsoonal wind forcing, it gets deflected in a southwesterly direction by the Coriolis force (Hordoir et al. 2006). The tracers originating from station 3 stretched out as a line, displaying the position of a frontal jet formed by a strong horizontal density gradient (Fig. 4.3). The tracers were transported with maximum speed at the offshore boundary of the plume. However, the alongshore transport by surface advection over a time period of 14 days was only 63 km. Consequently, there was only limited spatial displacement of the sampling stations by the transformation onto Lagrangian coordinates (Fig. 4.2). Thus, we assume that during our 5-day study, we did not sample different water masses

which successively flowed through the study area, but that we rather sampled a fixed set of water masses in which the marine phytoplankton community responded to riverine influence.

The classification of stations 10 and 15 as oceanic stations was slightly ambiguous, given that they lay close to the plume (Fig. 4.3) and had Si concentrations of  $3.5 \mu\text{mol L}^{-1}$ , which are higher than typical offshore Si concentrations in the SCS. In contrast, stations 11 and 12 were clearly too far offshore to be influenced by the river plume, and had surface salinities and nutrient concentrations that are indistinguishable from values measured in surface waters much further offshore (east of  $108.8^\circ\text{E}$ ) during intermonsoon in April 2006 (salinity of  $33.7 \pm 0.1$ , Si concentrations of  $2.3 \pm 0.1$ , while N and P concentrations were at the detection limit;  $n = 10$ ). The higher Si concentrations at stations 10 and 15 could either be due to earlier entrainment of plume water, or vertical mixing with bottom waters richer in nutrients. However, given that these stations had “offshore” surface salinities, we classified them as oceanic stations (Table 4.3). The relatively low maximum surface salinities in the SCS, compared to other open ocean sites, are explained by the large importance of river runoff for the SCS as a whole, especially in the southern part of the basin (Shaw and Chao 1994).

#### 4.5.2 Influence of the river plume on the distribution and activity of different diazotrophs

Tropical rivers were initially thought to support new production solely by introducing dissolved nitrogen ( $\text{NO}_3^-$ ,  $\text{NO}_2^-$ ,  $\text{NH}_4$ ) to the coastal zone; therefore, the observation that they can fuel marine  $\text{N}_2$  fixation further offshore was new and unexpected (Carpenter et al. 1999). Observations in the WTNA and the eastern equatorial Atlantic have shown that riverine inputs can favor the growth of diazotrophs, and in particular DDAs (Foster et al. 2007, 2008). The recognized importance of these symbiotic associations in the N and C cycling of the tropical North Atlantic prompted interest in whether similar scenarios could be found in other tropical river plumes around the world (Subramaniam et al. 2008). Here, we investigated a coastal area in the SCS that was partly influenced by the Mekong River plume. To our knowledge, this is the first study describing *nifH* gene expression and  $\text{N}_2$  fixation in the Mekong river plume, and we found several diazotrophs to be abundant and highly active throughout transitional and oceanic stations.

At plume stations, which were most directly affected by the river inflow, the high N concentrations of  $\geq 9.9 \mu\text{mol L}^{-1}$  likely suppressed  $\text{N}_2$  fixation of marine diazotrophs (Mulholland et al. 2001). Consequently, although *H-R* and *Trichodesmium* spp. were sometimes present at these stations, *nifH* expression was undetectable, and rates of  $\text{N}_2$  fixation were comparably low (Table 4.3).

At all transitional stations, concentrations of N were  $\leq 0.9 \mu\text{mol L}^{-1}$ , which represent N-limitation for phytoplankton growth (Goldman and Glibert 1983), but may not affect  $\text{N}_2$  fixation activity by diazotrophs (Mulholland et al. 2001). Concentrations of P were detectable, and N:P ratios were clearly lower than the Redfield ratio of 16:1, indicating a N deficiency relative to phytoplankton nutrient requirements (Fig. 4.4c, Table 4.3). Such conditions favor diazotrophs in general, and indeed, we found high *nifH* gene abundances of DDAs and *Trichodesmium* spp. at these stations (Table 4.3). At the mooring station 19, the QPCR data do not resolve whether one of the detected phylotypes dominated in a particular water mass (Fig. 4.6). However, the highest abundances of *Trichodesmium* spp. were not found during the most stratified conditions and highest salinities (e.g. 19\_12 at 15:00), but during time points when the river plume was clearly present (19\_1 at 5:30, 19\_15 at 18:00, Fig. 4.6). Overall, abundances of *Trichodesmium* spp. were not different between transitional and oceanic stations (Kruskal Wallis,  $p = 0.644$ ), but abundances of DDAs were greater at the oceanic stations in comparison to the transitional stations (Kruskal Wallis,  $p = 0.027$  for pooled abundances of R-R and H-R).

When interpreting rates of  $\text{N}_2$  fixation and *nifH* gene expression, it has to be considered that stations were sampled during various times of the day (Table 4.3). There is strong evidence for temporal segregation of *nifH* gene expression in unicellular cyanobacteria, *Trichodesmium* spp., and DDAs (Church et al. 2005b). Thus, transcripts detection is dependent on time of sampling. Due to the inherent diurnal periodicity of  $\text{N}_2$  fixation activity in the different species, it is important to compare rates of  $\text{N}_2$  fixation only between stations at which experimental incubations were initiated at similar times of day. A comparison of morning stations 11, 19\_1, 19\_4, 19\_27 or mid-day stations 15 and 19\_9 shows that rates of  $\text{N}_2$  fixation were equal or higher at transitional stations compared to oceanic stations (Table 4.3). The rates of  $\text{N}_2$  fixation at all but one of the transitional stations were an order of magnitude higher than the maximal surface rates that we measured previously in the SCS ( $1.1 \text{ nmol N L}^{-1} \text{ h}^{-1}$ ) (Voss et al. 2006). These results are overall not compatible with the conception that nutrient-rich riverine inputs suppress  $\text{N}_2$  fixation, and rather suggest that there was a positive influence of river water constituents on marine diazotrophs. At the transitional stations, N:P ratios were all clearly lower than the Redfield ratio of 16:1, suggesting an important role of “excess” P in enhancing  $\text{N}_2$  fixation.

The discrepancy between *nifH* expression and rates of  $\text{N}_2$  fixation at many stations (10, 15, 19\_1, 19\_9, 19\_21) make it difficult to infer from *nifH* transcript abundances whether conditions at some stations were more favorable for  $\text{N}_2$  fixation than at other stations. The snapshots of transcriptional activity at the time points of sampling (when  $\text{N}_2$  fixation

incubations were initiated), did obviously not represent the mean response of the diazotroph community, and the overall potential for N<sub>2</sub> fixation was only revealed by the rate measurements which integrate the N<sub>2</sub> fixation activity of the whole diazotroph community over several hours. However, the *nifH* expression data can be viewed as qualitative information about the phylotypes which were present and actively participating in N<sub>2</sub> fixation, and these seemed to be exclusively DDAs and *Trichodesmium* spp. at transitional stations. This implies that primarily these large diazotrophs were able to grow under riverine influence.

The high *nifH* transcript abundances of *Trichodesmium* spp. and DDAs which were sometimes detected later in the photoperiod (stations 8, 10, 19\_15) indicate that these diazotrophs continued fixing N<sub>2</sub> after sunset, possibly by using energy reserves from photosynthesis. In the subtropical North Pacific, Church et al. (2005b) found *nifH* transcript abundances of *Trichodesmium* spp. and R-R in the order of 10<sup>4</sup> *nifH* transcripts L<sup>-1</sup> in samples taken at midnight. Thus, possibly *Trichodesmium* spp. and DDAs were responsible for the high rates of N<sub>2</sub> fixation at stations 8 and 19\_15, given that group B unicellular diazotrophs, which are known to fix N<sub>2</sub> exclusively during nighttime, were undetectable. It is also possible that there were diazotrophs fixing N<sub>2</sub> at night which were not detected by any QPCR oligonucleotides used in this study.

Based on microscopy, diatoms of the genera *Rhizosolenia* and *Hemiaulus*, which potentially associate with *Richelia intracellularis*, were present at all stations and reached highest abundances at transitional- and oceanic stations (station 19, 7, 8, 10, see chapter 3.4.3). We therefore assumed that DDAs would be dominant diazotrophs in waters influenced by the Mekong River plume. Diatoms require silica for growth, so bloom formation was presumably initiated close to the shore, where Si concentrations of 32.0 ± 9.2 μmol L<sup>-1</sup> (mean of all plume stations) were measured. These diatoms must have been mainly asymbiotic at plume stations, given that *Richelia* was only present at station 2 (associated with *Hemiaulus*). DDA *nifH* gene copies and transcripts were found much more frequently and in high abundances at transitional stations (Table 4.3). This indicates that the proportion of diatoms associated with N<sub>2</sub> fixing *Richelia* increased in these waters, as a result of incipient N-limitation (≤ 0.9 μmol N L<sup>-1</sup>) after the plume waters mixed with nutrient-depleted oceanic water. Si and P were still available at transitional stations (Fig. 4.4a-d), suggesting that conditions were favorable for DDA growth. Batch culture experiment with *Rhizosolenia* showed that the percentage of *Rhizosolenia* cells associated with *Richelia* increased from 5% to 65% within 12 days under N-deplete conditions (Villareal 1990). Since these progressions were observed during a culture study, it cannot be assumed that they equally occur in the field within a diatom bloom under N-limiting conditions. However, according to our modeling approach, the river plume flow

would cover the distances between plume stations and transitional stations on timescales of <14 days (Fig. 4.3). We therefore speculate that the greater abundances of DDA *nifH* genes at transitional stations represent a diatom population in which the proportion of cyanobionts increased as the river plume mixed with nutrient-poor ocean water and the resultant N-limitation selected for diazotrophy.

*Trichodesmium* spp. was frequently detected and actively expressing *nifH* at transitional stations, yet in April 2006, *nifH* gene abundances of *Trichodesmium* spp. increased with distance from the Mekong River plume (Moisander et al. 2008). Greatest abundances of *Trichodesmium* spp. are generally found offshore in areas characterized by lowest concentrations of combined N (Capone et al. 1997, LaRoche and Breitbarth 2005). In the WTNA, *Trichodesmium* spp. was also most abundant in oligotrophic regions that were less influenced by the Amazon River plume, while DDAs and particularly *H-R* clearly dominated over all other phylotypes in mesohaline waters (salinities between 31.0 and 34.9) (Foster et al. 2007). In our investigation area, *Trichodesmium* spp. as well as DDAs seemed to be important members of the diazotroph community in waters influenced by the Mekong plume. Interestingly, we only detected unicellular cyanobacterial diazotrophs (groups B and C) at oceanic stations, which is in line with distribution patterns in the WTNA and in other areas where greatest abundances of these phylotypes were found in high salinity waters having lowest N concentrations (Church et al. 2005a, 2008; Foster et al. 2007).

Langlois et al. (2005) proposed that temperature additionally constrains the distribution of unicellular cyanobacterial diazotrophs, since in the tropical and subtropical Atlantic these *nifH* sequence types were primarily found in waters of <26°C. The relatively high surface water temperatures in the SCS and especially in the Mekong River plume may represent an upper tolerance extent for these unicellular cyanobacterial diazotrophs, which would partly explain why they were only sporadically detected or absent during our study. Overall, our data confirm that tropical rivers are responsible for unequal distribution patterns of the different marine diazotroph phylotypes. In September 2008 during SW monsoon, we again found large diatom blooms and high rates of N<sub>2</sub> fixation within the plume (see chapter 3). This suggests that DDAs can also be quantitatively important diazotrophs when discharge from the Mekong is at its maximum and the plume affects an area extending at least up to 12.5°N and 110.5°E (Voss et al. 2006).

By using cloning and sequencing techniques, proteobacterial *nifH* sequences were found in samples from almost all stations, and cluster III like *nifH* sequences were recovered from samples representing plume- and transitional stations. Some samples likely contained cells that were flushed into the estuary attached to suspended particles, since we recovered

proteobacterial and cluster III - like *nifH* sequences that were similar to sequences from the rhizosphere of cord grass or from endophytes of rice plants. However, there were also many sequences presumably of marine origin, which were similar to sequences obtained from offshore waters of the SCS, the North Pacific, and the Red Sea. Whether all of these sequences represent active marine diazotrophs remains unclear. Strict anaerobe diazotrophs such as *Desulfovibrio* spp. and other representatives of cluster III could reside in O<sub>2</sub>-reduced microenvironments within large suspended particles. Possibly, such prokaryotes were partly responsible for the detectable rates of N<sub>2</sub> fixation within highly turbid, nutrient rich waters at station 2 and 3.

Interestingly, the sequence which was most similar to the oceanic  $\gamma$ -proteobacterial sequence (EU052413, Moisander et al. 2008) was only found at an oceanic station (station 12), in accordance with the results from QPCR. In April 2006,  $\gamma$ -proteobacterial *nifH* genes were found exclusively within the upper 50 m of the water column, suggesting that these diazotrophs might have a light-dependent metabolism (Moisander et al. 2008). It is also noteworthy that the abundances of  $\gamma$ -proteobacterial *nifH* transcripts were relatively high in this study, compared to transcript abundances reported from the oligotrophic North Pacific (Church et al. 2005b).

The abundances of *nifH* genes reported in this study are subject to the known caveats of *nifH* gene quantifications by QPCR described earlier (e.g. Foster et al. 2009). The interpretation of *nifH* gene copy abundances as cell abundances is assumptive, given that multiple *nifH* gene copies per genome (so far only precluded for *Trichodesmium* spp. and group B cyanobacteria), or multiple genomes per cell could exist. A particular caveat of this study is that we did not normalize *nifH* gene abundances of *Richelia* to the number of heterocyst and non-heterocystous cells within a trichome, since epifluorescence microscopy to analyze the cyanobionts was not available. Nevertheless, the data are useful to identify the presence of the different diazotrophs, and *nifH* gene abundances can be compared between different stations sampled during our study.

This study has presented data on the distribution and activity of diazotroph microorganisms in the Mekong River plume. Within a relatively narrow salinity range spanning transitional and oceanic stations (32.6 - 33.9), we found high abundances of *nifH* genes and transcripts of *Trichodesmium* spp. and *Richelia intracellularis* associated with *Rhizosolenia* and *Hemiaulus*. Active unicellular cyanobacterial and proteobacterial phylotypes were only detected in oceanic waters. Possibly, temperature- or nutrient requirements exclude certain unicellular diazotrophs from river plumes, but it remains to be shown whether other proteobacteria or anaerobe diazotrophs are active in the eutroph parts of the plume. The highest rates of N<sub>2</sub>

fixation were found in transitional waters between the region directly influenced by the plume and the open ocean. These data overall confirm that the Mekong River sets favorable conditions for large diazotrophs like *Trichodemsium* and DDAs. The low N:P- and high Si:N ratios in waters having salinities  $\geq 32.6$  suggest an important role of “excess” P in enhancing  $N_2$  fixation, and that an ecological advantage for DDA species existed. Whether DDAs become dominant diazotrophs within a plume possibly depends on the discharge volume, since higher discharge leads to the formation of a larger mesohaline/transitional zone, and thereby provides the setting for selective processes to occur on longer timescales.

The decreased N:P ratios are likely due to desorption of P from suspended riverine particles, as has been shown for the Amazon River plume and other river systems (Chase and Sayles 1980; Jordan et al. 2008). N-losses via denitrification or anammox might also play a role in changing nutrient ratios. It is unlikely that iron was limiting  $N_2$  fixation in our investigation area, since measurements from April 2006 in waters with a salinity of 32.7 had concentrations of total iron of 4-6 nmol L<sup>-1</sup> (P. Croot, unpublished data). Given that nitrogenase activity of photoautotrophic diazotrophs is directly linked to photosynthesis (Gallon 2001), it is conceivable that  $N_2$  fixation was light-limited at some transitional- and plume stations. Turbidity-values characteristic for oligotrophic ocean regions (<1 NTU) were only found at salinities  $\geq 33.0$ . To test our assumptions, future studies should include measurements of trace metals and other N-species (NH<sub>4</sub>, dissolved organic N), since these are likely important factors influencing diazotrophy in the Mekong River plume and other tropical river plumes. There is now more proof that the enhancement of marine  $N_2$  fixation by tropical rivers could substantially influences global oceanic  $N_2$  fixation, and an important next step will be to understand how these interactions will be altered by changes in land and water use.

## 5. Conclusions and Perspectives

Upwelling systems and river plumes strongly influence the biogeochemistry of tropical oceans, but their importance relative to permanent diffusive processes in supplying nutrients and in shaping phytoplankton community structures remains poorly known. The SCS provides the opportunity to study nutrient inputs from upwelling and Mekong River discharge, which both mainly occur during the SW monsoon when the open SCS is stratified and N-limitation prevails. In the framework of this thesis, upwelling, diffusive inputs and river discharge were for the first time investigated in detail, and the results indicate that these nutrient sources have distinguishable influences on carbon and nitrogen cycling as well as on phytoplankton species composition in the SCS.

In the upwelling area, pronounced differences were found between the upwelling zone and the adjacent offshore zone regarding the magnitude of primary productivity and vertical  $\text{NO}_3^-$  supply. Upwelling-induced  $\text{NO}_3^-$  fluxes were almost an order of magnitude higher than diffusive  $\text{NO}_3^-$  supply, and this was mirrored in the observed zonal differences in rate measurements. These findings highlight the importance of the Vietnamese upwelling for the biogeochemistry of the SCS. It seems that upwelled nutrients were rapidly taken up by phytoplankton within the euphotic zone, with little residual  $\text{NO}_3^-$  left to be advected further offshore by Ekman transport. From these patterns, it can be concluded that the maximal upwelling-induced productivity of the Vietnamese upwelling was described, which is comparable to other important upwelling areas of the world. In order to quantify the upwelling-induced primary productivity in the SCS on a larger scale, future studies should include to investigate the processes that occur within the offshore jet that protrudes from the Vietnamese coast between approx.  $12^\circ\text{N}$  and  $13^\circ\text{N}$  during SW monsoon. This jet advects upwelled water and phytoplankton into the central, oligotrophic SCS, but it remains unclear to which extent it triggers new production (Tan and Shi 2009).

The study of the upwelling area encompassed two years which had different upwelling intensities due to differences in climate forcing. The rate measurements presented here are the first *in situ* data describing the biological response to El Niño modulated upwelling intensity off Vietnam, and this aspect deserves further investigations in the future for several reasons. In upwelling areas where  $\text{NO}_3^-$  availability is high, blooms of diatoms tend to develop, which play an important role in sustaining relatively short food chains and in export production (Bode et al. 1997; Wilkerson et al. 2000; Ryther 1969). In contrast, under conditions of weaker upwelling and/or in aged upwelling waters, picoplankton rather dominates, relative more regenerated production takes place, and potential for sedimentation is reduced (Joint et al. 2001; Joint and

Wassmann 2001). Both in July 2003 and 2004, diatoms were indeed the most abundant phytoplankton species in the upwelling zone off Vietnam (Loick et al. 2007). However, the observed El Niño modulation of the upwelling intensity and related biological responses suggests that there can be pronounced variability in phytoplankton community composition, standing stocks, and inherently export production between different years.

For some eastern boundary upwelling systems, e.g. off Oregon, California, and off Peru, El Niño related decreases in new productivity and chlorophyll standing stocks have been well described (Wilkerson et al. 1987; Corwith and Wheeler 2002), but for the SCS, we are just beginning to assess these phenomena. An analysis of the Comprehensive Ocean Atmosphere Data Set (COADS) for the period 1950-1990 showed that compared to the climatological mean, warmer SST and lower wind speeds can be found in the SCS in post El Niño years, while in post La Niña years, SST are colder and wind speeds are higher (Dippner et al. unpubl.). Preliminary model estimates suggest that the primary productivity of the Vietnamese upwelling may be up to 118% higher in post La Niña years compared to post El Niño years (Dippner et al., unpubl.). The Institute of Oceanography, Nha Trang, has monitored phytoplankton- and zooplankton species occurring in Vietnamese coastal waters for more than 30 years (L. Nguyen, pers. com.), and it would be interesting to analyze whether there are variations in these data that correspond to the climate anomalies documented in the COADS data set. Such analyses might help in investigating the proposed variability of ecosystem functioning.

Variations in upwelling intensity off Vietnam will also be mirrored in the standing stocks of higher trophic levels and ultimately fishery yields in Vietnamese coastal waters. According to the Vietnamese Ministry of Fisheries, marine fishing represents a key source for domestic consumption and export, with nearly 1.3 million tons of wild catches in 2001, which account for roughly 64% of total fish catches in Vietnam (Tri 2002). A large share of these catches occurs in the shelf waters off southeastern Vietnam, i.e. within the upwelling area (<http://www.fao.org/fi/oldsite/FCP/en/VNM/profile.htm>). Therefore, future studies should also investigate how the varying upwelling intensity and primary productivity affects the local marine fisheries. These studies are all the more important since also global warming will affect the Vietnamese upwelling in the long term. Goes et al. (2005) have revealed that the western Arabian Sea is becoming more productive due to a steepened land-ocean thermal gradient which causes a stronger SW monsoon and inherently intensified upwelling and phytoplankton blooming. This is most likely an exemplary scenario of what can be expected to occur in the monsoon-induced upwelling system of the SCS.

There is growing evidence that a serious underestimation of global oceanic  $N_2$  fixation seems to be the principal reason for the “missing” N in the oceanic nitrogen budget. The results of this thesis add to this evidence by showing that tropical river plumes are sites where  $N_2$  fixation can occur at very high and ecologically significant rates, in contradiction to the hypothesis that the river constituents would suppress  $N_2$  fixation in the open ocean (Fig. 5.1). While similar observations have been made in the Amazon River plume, it is important to document that this phenomenon occurs in other tropical river plumes. The results presented here go beyond the studies from the Amazon plume and show significant  $N_2$  fixation occurring at night in the plume. The most important diazotroph species were *Trichodesmium* and DDAs (Fig. 5.1). High silicate availability is likely to induce a shift towards the dominance of DDAs in river plumes. In the Mekong Plume, we found considerable  $N_2$  fixation even on stations near the river mouth, i.e. under N-replete conditions. Some marine cyanobacteria and proteobacteria were shown to lack genes for both  $NO_3^-$  and  $NO_2^-$  transporters (Moore et al. 2002; Moran et al. 2007). Possibly, the proteobacterial- and cluster III like *nifH* sequences recovered from stations which had N replete conditions could represent such ecotypes that cannot use any other N source besides  $NH_4^+$  and atmospheric  $N_2$ , but this has to be investigated in future studies.

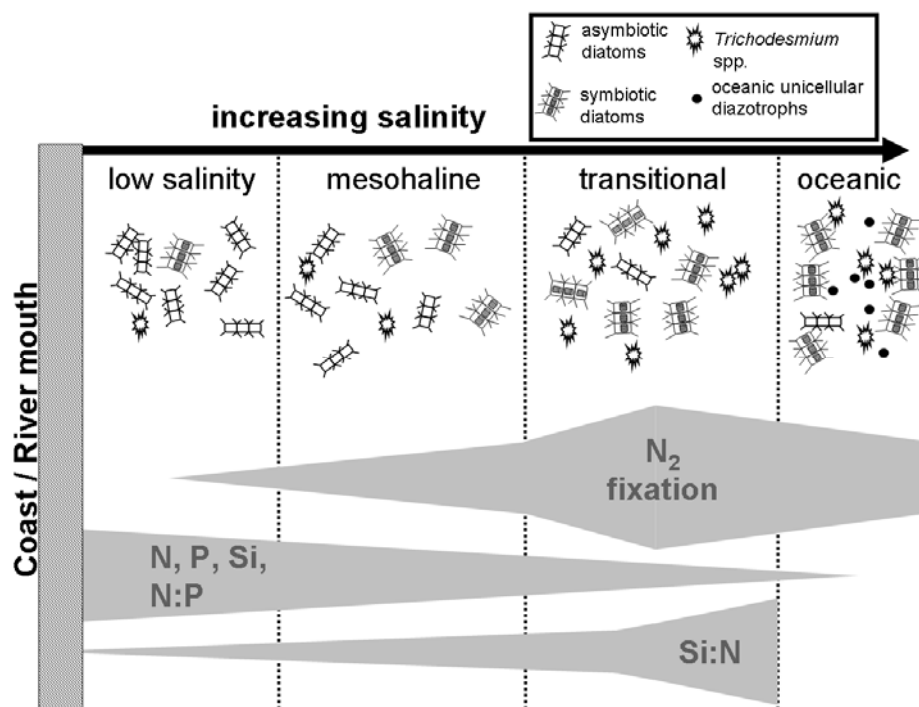


**Figure 5.1:** Sketch summarizing the patterns of  $N_2$  fixation, diazotroph distributions, and nutrient dynamics found in the Mekong River plume. Discharge of nutrients triggers growth of phytoplankton, primarily consisting of diatoms which are mainly asymbiotic in low salinity and mesohaline waters. As the mixing with nutrient-poor ocean water progresses, nutrients are drawn down until nitrogen becomes limiting. Concurrently, P and Si remain available, or P is even added from particles and sediment (see Text, Jordan et al. 2008), and this selects for diazotrophs including *Trichodesmium* and DDAs. According to QPCR, oceanic unicellular diazotrophs including cyanobacteria and  $\gamma$ -proteobacteria, seem constrained to oceanic waters. However, *nifH* diversity suggests that other proteobacteria and prokaryotes belonging to cluster III are possibly active  $N_2$  fixers in low salinity waters.

In the oligotrophic surface ocean, detectable  $N_2$  fixation appears as a relatively common feature. In contrast, biogeochemical conditions in estuaries and river plumes can vary on short time scales and are spatially very heterogeneous, and it therefore appears likely that  $N_2$  fixation occurs as stochastic “events”, wherever conditions become favorable for diazotrophs. Such inputs are difficult to measure by field sampling efforts. The Mekong Plume is an example which highlights that once  $N_2$  fixation is “switched on” in estuaries and river plumes farther offshore, it can occur at substantial rates, presumably due to the high availability of limiting nutrients ( $PO_4^{3-}$ , iron). It remains a challenge of future research to reliably integrate these inputs over larger spatial scales. This can only be achieved by a complete assessment of the diversity of marine diazotrophs, and by a good understanding of when and due to which environmental settings diazotroph microbes realize their genetic potential. As the variety of physiological and ecological factors that control oceanic  $N_2$  fixation gets better known, regional and global ecosystem models can be improved in order to allow for a more realistic quantification of diazotroph inputs, and for predictions of how environmental change will affect them.

In the Mekong Plume,  $PO_4^{3-}$  appeared to be an important regulation factor in promoting  $N_2$  fixation. Some further thoughts on nutrient dynamics which were not included in detail in manuscripts 3 or 4 shall be discussed here, since they are interesting regarding future research questions. As mentioned,  $N_2$  fixation at river-influenced sites has been controversial, and especially estuaries have traditionally been viewed as unfavorable sites for  $N_2$  fixation because of the availability of fixed nitrogen species, including  $NH_4^+$  which is a known suppressor of nitrogenase activity (Mulholland et al. 2001). Further, it was suggested that the elevated turbulence of estuarine waters as well as grazing controls could prevent the formation of diazotroph cyanobacterial blooms (Moisander et al. 2002, Chan et al. 2006). However, an important aspect is that rivers can deliver large amounts of inorganic particles, including particulate inorganic phosphorus. For the Amazon River plume, it was calculated that the phosphorus load discharged in particulate form can be 15 times greater than the soluble reactive  $PO_4^{3-}$  load (Chase and Sayles 1980). The release of  $PO_4^{3-}$  from inorganic particles is not accompanied by a release of N, and this should favor oceanic diazotrophs, for which  $PO_4^{3-}$  is the most important limiting factor besides iron (Mills et al. 2004). Once particulate phosphorus is deposited in an estuary, it can be converted to biologically available  $PO_4^{3-}$  in anoxic layers of sediments, through processes that are enhanced by increasing salinity, and the  $PO_4^{3-}$  diffuses into the overlying waters (see Jordan et al. 2008 for details). This could explain the gradual decrease of N:P ratios with increasing salinity that we found in waters influenced by the Mekong plume. An indication for this comes from a comparison of the concentration

changes of  $\text{PO}_4^{3-}$  and  $\text{Si}(\text{OH})_4$  within the salinity gradient (Fig. 5.2). In Figure 5.2, the black solid line connects the oceanic- and freshwater concentrations of  $\text{Si}(\text{OH})_4$ , and thus represents the line of ideal mixing between the end members riverine- and open sea water. Clearly, the concentration changes of  $\text{Si}(\text{OH})_4$  seem to be largely due to conservative mixing. In contrast, concentrations of  $\text{PO}_4^{3-}$  largely fall above a mixing line, possibly indicating release from sediments to occur. Concentrations of  $\text{NO}_3^- + \text{NO}_2^-$  (not shown) fall closer to a mixing line than  $\text{PO}_4^{3-}$ . It maybe appears simplistic to assume that only two types of water were mixed (riverine and open sea water), but according to the water mass analysis by Dippner et al. (2007), besides the Mekong outflow there are only open sea water and Gulf of Thailand water (during SW monsoon) to be considered in the area, and those water masses are depleted in nutrients. Thus, although sedimentary denitrification might also explain low N:P ratios, we assume that the release of dissolved  $\text{PO}_4^{3-}$  from sedimentary particles could play an important role in the Mekong estuary.

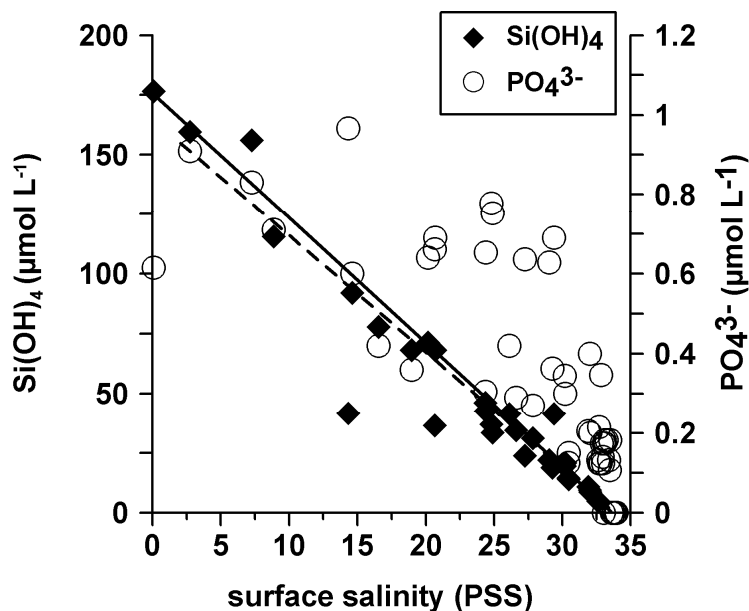


**Figure 5.2:** Concentrations of dissolved  $\text{Si}(\text{OH})_4$  and  $\text{PO}_4^{3-}$  vs. salinity for surface waters collected in April 2007 and September 2008 in the Mekong plume. The solid black line and the dashed line are the lines of ideal mixing for  $\text{Si}(\text{OH})_4$  and  $\text{PO}_4^{3-}$ , respectively.

Future studies could include molecular methods to test the hypothesis that oceanic diazotrophs respond to transient supplies of  $\text{PO}_4^{3-}$ , e.g. by rivers. For example, the *pboA* gene (involved in alkaline phosphatase synthesis) is expressed under P-stress in *Trichodesmium* (Dyhrman et al. 2002), and its analysis is useful to test for phosphate limitation of diazotrophs in the SCS or elsewhere. Alternatively, a promising approach is to target expression levels of genes involved in membrane phosphate transport (*pstS*), since these genes are typically highly regulated in picocyanobacteria and would thus give immediate information about the response of microorganisms to concentration changes of this specific nutrient (Scanlan et al. 2009).

Overall, the results from the Vietnamese German research cooperation provide a valuable basis for future research, which should include investigations on how the SCS pelagic ecosystem will respond to climate change and increasing direct anthropogenic pressures. According to Halpern et al. (2008), the SCS is among oceanic sites that are most strongly affected by human activities. Regarding the riverine influence on ocean biogeochemistry, the construction of dams, increased fertilizer use, increased sewage loading and mangrove destruction in the Mekong basin are of particular interest. These perturbations will affect sediment loads, freshwater discharge, nutrient fluxes and nutrient ratios, and will therefore alter the structure and functioning of the pelagic ecosystem in the SCS which we are just beginning to understand.

## Bibliography

- Allen, A. E., M. G. Booth, M. E. Frischer, P. G. Verity, J. P. Zehr, and S. Zani. 2001. Diversity and detection of nitrate assimilation genes in marine bacteria. *Appl. Environ. Microbiol.* **67**: 5343–5348.
- Altabet, M. A., R. Francois, D. W. Murray, and W. L. Prell. 1995. Climate-related variations in denitrification in the Arabian Sea from sediment  $^{15}\text{N}/^{14}\text{N}$  ratios. *Nature* **373**: 506-509
- Backhaus, J. O. 1985. A Three-Dimensional Model for the Simulation of Shelf Sea Dynamics. *Di. hydrogr. Z.* **38**: 165-187
- Barber, R. T., M. P. Sanderson, S. T. Lindley, F. Chai, J. Newton, C. C. Trees, D. G. Foley and F. P. Chavez. 1996. Primary productivity and its regulation in the equatorial Pacific during and following the 1991-1992 El Niño. *Deep-Sea Res. II* **43**(4-6): 933-969.
- Barber, R. T., J. Marra, R. C. Bidigare, L. A. Codispoti, D. Halpern, Z. Johnson, M. Latasa, R. Goericke and S. L. Smith. 2001. Primary productivity and its regulation in the Arabian Sea during 1995. *Deep-Sea Res. II* **48**: 1127-1172.
- Behrenfeld, M., and P. Falkowski. 1997. Photosynthetic rates derived from satellite-based chlorophyll concentration. *Limnol. Oceanogr.* **42**(1): 1–20.
- Beman, J. M., K. R. Arrigo, and P. A. Matson. 2005. Agricultural runoff fuels large phytoplankton blooms in vulnerable areas of the ocean. *Nature* **434**: 211-214
- Bergquist, B. A., and E. A. Boyle. 2006. Iron isotopes in the Amazon River system: Weathering and transport signatures. *Earth and Planetary Science Letters* **248**: 54-68.
- Berman-Frank, I., J. T. Cullen, Y. Shaked, R. M. Sherrell, and P. G. Falkowski. 2001. Iron availability, cellular iron quotas, and nitrogen fixation in *Trichodesmium*. *Limnol. Oceanogr.* **46**: 1249–1277
- Bode, A., J. A. Botas, and E. Fernandez. 1997. Nitrate storage by phytoplankton in a coastal upwelling environment. *Mar. Biol.* **129**: 399–406
- Bonnet, S., I. C. Biegala, P. Dutrieux, L. O. Slemons, and D. Capone. 2009. Nitrogen fixation in the western equatorial Pacific: Rates, diazotrophic cyanobacterial size class distribution, and biogeochemical significance. *Global Biogeochem. Cycles*, **23**: GB3012, doi:10.1029/2008GB003439, 2009.
- Brink, K. H., B. H. Jones, J. C. van Leer, C. N. K. Mooers, D. W. Stuart, M. R. Stevenson, R. C. Dugdale and G. W. Heburn. 1981. Physical and biological structure and variability in an upwelling centre off Peru near 15°S during March, 1977, pp. 473-495. *In*: F. A. Richards [ed.], Coastal Upwelling, Washington, American Geophysical Union.

- Brockmann, C. W., and J. W. Dippner. 1987. Tidal correction of hydrographic measurements. *Dt. hydrogr. Z.* **40**: 241-260.
- Bronk, D. A., P. M. Glibert, and B. B. Ward. 1994. Nitrogen uptake, dissolved organic nitrogen release, and new production. *Science* **265**: 1843- 1846
- Capone, D. G., and E. J. Carpenter. 1982. Nitrogen fixation in the Marine Environment. *Science* **217**: 1140-1142.
- Capone, D. G., J. P. Zehr, H. W. Paerl, B. Bergman, and E. J. Carpenter. 1997. *Trichodesmium*, a globally significant marine cyanobacterium. *Science* **276**: 1221-1229.
- Capone, D. G., A. Subramaniam, J. P. Montoya, M. Voss, C. J. A. M. Humborg, R. L. Siefert, and E. J. Carpenter. 1998. An extensive bloom of the N<sub>2</sub>-fixing cyanobacteria *Trichodesmium erythraeum* in the central Arabian Sea. *Mar. Ecol. Prog. Ser.* **172**: 281-292.
- Capone, D. G., J. A. Burns, J. P. Montoya, A. Subramaniam, C. Mahaffey, T. Gunderson, A. F. Michaels and E. J. Carpenter. 2005. Nitrogen fixation by *Trichodesmium* spp.: An important source of new nitrogen to the tropical and subtropical North Atlantic Ocean. *Global Biogeochem. Cycles*, **19**: 1-17.
- Caron, D. A., E. L. Lim, G. Miceli, J. B. Waterbury, and F. W. Valois. 1991. Grazing and utilization of chroococcoid cyanobacteria and heterotrophic bacteria by protozoa in laboratory cultures and a coastal plankton community. *Mar. Ecol. Prog. Ser.* **76**(3): 205–217.
- Carpenter, E. J., J. P. Montoya, J. Burns, M. R. Mulholland, A. Subramaniam, and D. G. Capone. 1999. Extensive bloom of a N<sub>2</sub>-fixing diatom/cyanobacterial association in the tropical Atlantic Ocean. *Mar. Ecol. Prog. Ser.* **185**: 273-283
- Carpenter, E. J. 2002. Marine cyanobacterial symbioses. *Biology and Environment: Proceedings of the Royal Irish Academy* **102**: 15-18
- Carpenter, E. J., and D. G. Capone. 2008. Nitrogen fixation in the marine environment pp. 141-184. In Capone, D. G., D. Bronk, M. Mulholland, and E. J. Carpenter [eds.]. Nitrogen in the marine environment, 2nd edition. Elsevier Science
- Carr, M. E., M. A. M. Friedrichs, M. Schmeltz, M. N. Aita, D. Antoine, K. R. Arrigo, et al. 2006. A comparison of global estimates of marine primary production from ocean color. *Deep-Sea Res. II* **53**: 741–770
- Chan, F., R. L. Marino, R. W. Howarth, and M. L. Pace. 2006. Ecological constraints on planktonic nitrogen fixation in saline estuaries. II. Grazing controls on cyanobacterial population dynamics. *Mar. Ecol. Prog. Ser.* **309**: 41-53
- Chao, S. Y., P. T. Shaw and S. Y. Wu. 1996. El Niño modulation of the South China Sea circulation. *Progr. Oceanogr.* **38**: 51-93.

- Chase, E. M. and F. L. Sayles. 1980. Phosphorus in suspended sediments of the Amazon River. *Estuarine and Coastal Marine Sciences* **11**: 383-391.
- Chavez, F. P., and J. R. Toggweiler. 1995. Physical estimates of global new production: The upwelling contribution. In Summerhayes, C. P., K. C. Emeis, M. V. Angel, R. L. Smith, and B. Zeitschel [eds.], *Upwelling in the Oceans; Modern Processes and Ancient Records*. Wiley, New York. pp. 313–321
- Chen, Y., B. Dominic, M. T. Mellon, and J. P. Zehr. 1998. Circadian rhythm of nitrogenase gene expression in the diazotrophic filamentous nonheterocystous cyanobacterium *Trichodesmium* sp. Strain IMS 101. *J. Bacteriol.* **180**(14): 3598-3605
- Chen, Y. L., H. Y. Chen, and Y. H. Lin. 2003. Distribution and downward flux of *Trichodesmium* in the South China Sea as influenced by the transport from the Kuroshio Current. *Mar. Ecol. Prog. Ser.* **259**: 47-57.
- Chen, Y. L., H. Y. Chen, D. M. Karl and M. Takahashi. 2004. Nitrogen modulates phytoplankton growth in spring in the South China Sea. *Cont. Shelf Res.* **24**: 527-541.
- Chen, Y. L. 2005. Spatial and seasonal variations of nitrate-based new production and primary production in the South China Sea. *Deep-Sea Res. I.* **52**: 319-340.
- Chou W-C, Y-L. Chen, D. D. Sheu, Y-Y. Shih, C-A. Han, C. L. Cho, C-M. Tseng, and Y-J. Yang 2006. Estimated net community production during the summertime at the SEATS time-series study site, northern South China Sea: Implications for nitrogen fixation. *Geophys. Res. Lett.* **33**: L22610, doi:22610.21029/22005GL025365
- Church, M. J., B. D. Jenkins, D. M. Karl, and J. P. Zehr. 2005a. Vertical distributions of nitrogen-fixing phylotypes at Stn ALOHA in the oligotrophic North Pacific Ocean. *Aquat. Microb. Ecol.* **38**: 3-14.
- Church, M. J., C. M. Short, B. D. Jenkins, D. M. Karl, and J. P. Zehr. 2005b. Temporal patterns of nitrogenase gene (*nifH*) expression in the oligotrophic North Pacific Ocean. *Appl. Environ. Microbiol.* **71**: 5362-5370.
- Church, M. J., K. M. Björkman, and D. M. Karl. 2008. Regional distribution of nitrogen-fixing bacteria in the Pacific Ocean. *Limnol. Oceanogr.*, **53**(1): 63-77.
- Claustre, H., and J.-C. Marty. 1995. Specific phytoplankton biomasses and their relation to primary production in the tropical North Atlantic. *Deep-Sea Res. I.* **42**(8): 1475-1493.
- Clean Water Team (CWT). 2004. Turbidity fact sheet, FS-3.1.5.0 (Turb). In: *The clean water team guidance compendium for watershed monitoring and assessment, version 2.0*. Division of Water Quality, California State Water Resource Control Board (SWRCB), Sacramento, CA:  
[www.swrcb.ca.gov/water\\_issues/programs/swamp/docs/cwt/guidance/3150fs.pdf](http://www.swrcb.ca.gov/water_issues/programs/swamp/docs/cwt/guidance/3150fs.pdf)

- Cochlan, W. P., P. J. Harrison, and K. L. Denman. 1991. Diel periodicity of nitrogen uptake by marine phytoplankton in nitrate-rich environments. *Limnol. Oceanogr.* **36**(8): 1689-1700.
- Codispoti, L. A. 2007. An oceanic fixed nitrogen sink exceeding 400 TgNa<sup>-1</sup> vs the concept of homeostasis in the fixed-nitrogen inventory. *Biogeosciences* **4**: 233–253
- Collos, Y. and G. Slawyk. 1976. Significance of cellular nitrate content in natural populations of marine phytoplankton growing in shipboard cultures. *Mar. Biol.* **34**: 27-32.
- Conley, D. J. 1997. Riverine contribution of biogenic silica to the oceanic silica budget. *Limnol. Oceanogr.* **42**(4): 774-777
- Corwith, H. L., and P. A. Wheeler. 2002. El Niño related variations in nutrient and chlorophyll distributions off Oregon. *Prog. Oceanogr.* **54**: 361–380.
- Davey, M., G. A. Tarran, M. M. Mills, C. Ridame, R. J. Geider, and J. LaRoche. 2008. Nutrient limitation of picophytoplankton photosynthesis and growth in the tropical North Atlantic. *Limnol. Oceanogr.* **53**:1722-1733
- Dekas, A. E., R. S. Poretsky, and V. J. Orphan. 2009. Deep-Sea archaea fix and share nitrogen in methane-consuming microbial consortia. *Science* **326**: doi: 10.1126/science.1178223
- Deutsch, C., J. L. Sarmiento, D. M. Sigman, N. Gruber, and J. P. Dunne. 2007. Spatial coupling of nitrogen inputs and losses in the ocean. *Nature* **445**: 163-167.
- Dippner, J., K. V. Nguyen, H. Hein, T. Ohde, and N. Loick. 2007. Monsoon induced Upwelling off the Vietnamese Coast. *Ocean Dynamics* **57**: 46-62.
- Dore, J. E., and D. M. Karl. 1996. Nitrification in the euphotic zone as a source for nitrite, nitrate, and nitrous oxide at Station ALOHA. *Limnol. Oceanogr.* **41**: 1619-1628
- Ducklow, H. W., D. K. Steinberg, and K. O. Buesseler. 2001. Upper ocean carbon export and the biological pump. *Oceanography* **14**(4): 50-58
- Dugdale, R. C. and J. J. Goering. 1967. Uptake of new and regenerated forms of nitrogen in primary productivity. *Limnol. Oceanogr.* **12**: 196-206.
- Dugdale, R. C., F. P. Wilkerson, and A. Morel. 1990. Realization of new production in coastal upwelling areas: A means to compare relative performance. *Limnol. Oceanogr.* **35**(4): 822-829.
- Dyhrman S. T., E. A. Webb, D. M. Anderson, J. W. Moffett, and J. B. Waterbury. 2002. Cell-specific detection of phosphorus stress in *Trichodesmium* from the western north Atlantic. *Limnol. Oceanogr.* **47**:1832-1836
- Egge, J. K., and D. L. Asknes, 1992. Silicate as regulating nutrient in phytoplankton competition. *Mar. Ecol. Prog. Ser.* **83**: 281-289.
- Eppley, R. W., T. T. Packard and J. J. MacIsaac 1970. Nitrate reductase in Peru current phytoplankton. *Mar. Biol.* **6**: 195-199.

- Eppley, R. W., and B. J. Peterson. 1979. Particulate organic matter flux and planktonic new production in the deep ocean. *Nature* **282**: 677–680
- Ewing, B., L. Hillier, M.C. Wendl, and P. Green. 1998. Base-calling of automated sequencer traces using phred. I. Accuracy assessment. *Genome Res.* **8**: 175-185.
- Falkowski, P. G. 1997. Evolution of the nitrogen cycle and its influence on the biological sequestration of CO<sub>2</sub> in the ocean. *Nature* **387**: 272-275
- Falkowski, P. G., E. A. Laws, R. T. Barber, and J. W. Murray. 2003. Phytoplankton and their role in primary, new, and export production. pp. 99-121. *In* M. J. R. Fasham [ed.]: *Ocean Biogeochemistry*. Springer Verlag Berlin Heidelberg.
- Fang, W., G. Fang, P. Shi, Q. Huang, and Q. Xie. 2002. Seasonal structure of upper layer circulation in the southern South China Sea from in-situ observations. *J. Geophys. Res.* **107**: 3202, doi:10.1029/2002JC001343
- Farnelid, H., and L. Riemann. 2008. Heterotrophic N<sub>2</sub>-fixing bacteria: Overlooked in the marine nitrogen cycle? pp. 409-423. *In* G. N. Couto [ed.], *Nitrogen Fixation Research Progress*. Nova Science Publishers, Inc.
- Fay, P. 1992. Oxygen relations of nitrogen fixation in cyanobacteria. *Microbiol. Rev.* **56**(2): 340-373
- Field, C. B., M. J. Behrenfeld, J. T. Randerson, and P. Falkowski. 1998. Primary production of the biosphere: Integrating terrestrial and oceanic components. *Science* **281**: 237–240
- Foster, R. A., and J. P. Zehr. 2006. Characterization of diatom-cyanobacteria symbioses on the basis of *nifH*, *hetR* and 16S rRNA sequences. *Environ. Microbiol.* **8**: 1913-1925.
- Foster, R. A., A. Subramaniam, C. Mahaffey, E. J. Carpenter, D. G. Capone, and J. P. Zehr. 2007. Influence of the Amazon River plume on distribution of free-living and symbiotic cyanobacteria in the western tropical North Atlantic Ocean. *Limnol. Oceanogr.* **52**: 517-532.
- Foster, R. A., A. Subramaniam, and J. P. Zehr. 2008. Distribution and activity of diazotrophs in the Eastern Equatorial Atlantic. *Environ. Microbiol.* **11**: 741-750, doi: 10.1111/j.1462-2920.2008.01796.x
- Foster, R. A., and G. D. O'Mullan. 2008. Nitrogen-fixing and nitrifying symbioses in the marine environment. pp. 1197-1218. *In* Capone, D. G., D. Bronk, M. Mulholland, and E. J. Carpenter [eds.]. *Nitrogen in the marine environment*, 2nd edition. Elsevier Science.
- Foster, R. A., A. Paytan, and J. P. Zehr. 2009. Seasonality of N<sub>2</sub> fixation and *nifH* gene diversity in the Gulf of Aqaba (Red Sea). *Limnol. Oceanogr.* **54**(1): 219-233.
- Gallon, J. R. 2001. N<sub>2</sub> fixation in phototrophs: adaptation to a specialized way of life. *Plant Soil* **230**. 39–48.

- Gaye, B., M. G. Wiesner, and N. Lahajnar. 2009. Nitrogen sources in the South China Sea, as discerned from stable nitrogen isotopic ratios in rivers, sinking particles, and sediments. *Mar. Chem.* doi:0.1016/j.marchem.2009.04.003.
- Gill, A. E., and W. L. Donn. 1982. Atmosphere-Ocean Dynamics. International Geophysics Series. Academic Press, London
- Goes, J. I., P. G. Thoppil, H. R. Gomes, and J. T. Fasullo. 2005. Warming of the Eurasian landmass is making the Arabian Sea more productive. *Science* **308**: 545-547. doi: 10.1126/science.1106610
- Goldman, J. C., and P. M. Glibert. 1983. Kinetics of inorganic nitrogen uptake by phytoplankton. pp. 233-274. In E. J. Carpenter, and D. G. Capone [eds.], Nitrogen in the marine environment. Academic Press.
- Gómez, F., K. Furuya, and S. Takeda. 2005. Distribution of the cyanobacterium *Richelia intracellularis* as an epiphyte of the diatom *Chaetoceros compressus* in the western Pacific Ocean. *J. Plankton Res.* **27**: 323–330 doi:10.1093/plankt/fbi007
- Grasshoff, K. 1983. Determination of nutrients. pp. 125-188. In K. Grasshoff, M. Ehrhardt, and K. Kremling [eds.], Methods of Seawater Analysis, 2nd edition. Verlag Chemie.
- Graziano L. M., R. J. Geider, W. K. W. Li, M. Olaizola. 1996. Nitrogen limitation of North Atlantic phytoplankton: Analysis of physiological condition in nutrient enrichment experiments. *Aquat. Microb. Ecol.* **11**:53-64
- Gruber, N., and J. L. Sarmiento. 1997: Global patterns of marine nitrogen fixation and denitrification. *Global Biogeochem. Cycles* **11**(2): 235-266.
- Gruber, N., and J. L. Sarmiento. 2002. Large-scale biogeochemical/physical interactions in elemental cycles. pp. 337–399. In A. R. Robinson, J. J. McCarthy, and B. J. Rothschild [eds.] "The Sea: Biological–Physical Interactions in the Oceans. Vol. 12, Wiley, New York..
- Gruber, N. and J. N. Galloway. 2008. An Earth-system perspective of the global nitrogen cycle. *Nature* **451**: 293-296. doi:10.1038/nature06592
- Gruber, N. 2008. The marine nitrogen cycle: Overview and Challenges. pp. 1-43. In Capone, D. G., D. Bronk, M. Mulholland, and E. J. Carpenter [eds.]. Nitrogen in the marine environment, 2nd edition. Elsevier Science.
- Halpern, B. S., S. Walbridge, K. A. Selkoe, C. V. Kappel, F. Micheli, C. D'Agrosa, J. F. Bruno, K. S. Casey, C. Ebert, H. E. Fox, R. Fujita, D. Heinemann, H. S. Lenihan, E. M. P. Madin, M. T. Perry, E. R. Selig, M. Spalding, R. Steneck, and R. Watson. 2008. A global map of human impact on marine ecosystems. *Science* **319**: 948-952 [DOI: 10.1126/science.1149345]
- Hansell, D. A., N. R. Bates, and D. B. Olson. 2004. Excess nitrate and nitrogen fixation in the North Atlantic Ocean. *Mar. Chem.* **84**: 243-265

- Hallegraeff, G. M. 1995. Harmful algal blooms: A global overview. pp. 1-22. *In* Hallegraeff, G. M., D. M. Anderson, and A. D. Cembella. [eds.], *Manual on harmful marine microalgae*. IOC Manual and Guides, No. 33, UNESCO.
- Hein, H., B. Karfeld, T. Pohlmann. 2007. Mekong water dispersion: measurements and consequences for the hydrodynamical modeling. *Journal of Water Resources and Environmental Engineering, Special Issue, August 2007*: 21-28
- Hellerman, S., and M. Rosenstein. 1983. Normal monthly wind stress over the world ocean with error estimation. *J. Phys. Oceanogr.* **13**: 1093-1104.
- Hewson, I., S. R. Govil, D. G. Capone, E. J. Carpenter, and J. A. Fuhrman. 2004. Evidence of *Trichodesmium* viral lysis and potential significance for biogeochemical cycling in the oligotrophic ocean. *Aquat. Microb. Ecol.* **36**: 1–8.
- Ho, L. T. V., N. H. Nhan, E. Wolanski, T. T. Cong, and H. Shigekoa. 2007. The combined impact on the flooding in Vietnam's Mekong River delta of local man-made structures, sea level rise, and dams upstream in the river catchment. *Estuar. Coast. Shelf Sci.* **71**: 110-116.
- Holl, C. M. and J. P. Montoya. 2005. Interactions between nitrate uptake and N<sub>2</sub>-fixation in *Trichodesmium*. *J. Phycol.* **41**: 1178-1183
- Hordoir, R., K. D. Nguyen, and J. Polcher. 2006. Simulating tropical river plumes, a set of parameterizations based on macroscale data: A test case in the Mekong Delta region. *J. Geophys. Res. - oceans* **111**: C09036, doi:10.1029/2005JC003392.
- Hu, J., H. Kawamura, H. Hong and Y. Qi. 2000. A review on the currents in the South China Sea: Seasonal circulation, South China Sea warm current and Kuroshio intrusion. *Journal of Oceanography* **56**: 607-624.
- Hu, J., H. Kawamura, H. Hong, F. Kobayashi, and D. Wang. 2001. 3-6 months variation of sea surface height in the South China Sea and its adjacent ocean. *Journal of Oceanography* **57**(1): 69-78.
- Huntsman, S. A., and R. T. Barber. 1977. Primary production off northwest Africa: the relationship to wind and nutrient conditions. *Deep-Sea Res.* **24**: 25-33.
- Isobe, A., and T. Namba. 2001. The circulation in the upper and intermediate layers of the South China Sea. *Journal of Oceanography* **57**: 93-104.
- Janson, S., J. Wouters, B. Bergman, and J. C. Carpenter. 1999. Host specificity in the *Richelia*-diatom symbiosis revealed by hetR gene sequence analysis. *Envir. Microbiol.* **1**: 431–438
- Jenkins, W. J. 1988. Nitrate flux into the euphotic zone near Bermuda: *Nature* **331**: 521–523.
- Jenkins, W. J., and S. C. Doney. 2003. The subtropical nutrient spiral. *Global Biogeochem. Cycles*, **17**(4): doi:10.1029/2003GB002085.

- Johnson, K. S., V. A. Elrod, S. E. Fitzwater, J. N. Plant, F. P. Chavez, S. J. Tanner, R. M. Gordon, D. L. Westphal, K. D. Perry, J. Wu, and D. M. Karl. 2003. Surface ocean - lower atmosphere interactions in the Northeast Pacific Ocean gyre: Aerosols, iron and the ecosystem response: *Global Biogeochem. Cycles* **17**: doi:10.1029/2002GB002004.
- Joint, I., and P. Wassmann. 2001. Lagrangian studies of the Iberian upwelling system- An introduction. A study of the temporal evolution of surface production and fate of organic matter during upwelling on and off the NW Spanish continental margin. *Prog. Oceanogr.* **51**: 217–220.
- Joint, I., A. P. Rees, and E. M. S. Woodward. 2001a. Primary production and nutrient assimilation in the Iberian upwelling in August 1998. *Prog. Oceanogr.* **51**, 303–320.
- Jones G. B., C. Burdon-Jones, and F. G. Thomas. 1982. Influence of *Trichodesmium* red tides on trace metal cycling at a coastal station in the Great Barrier Reef Lagoon. *Oceanol. Acta* **4**: 319-326.
- Jordan, T. E., J. C. Cornwell, W. R. Boynton, and J. T. Anderson. 2008. Changes in phosphorus biogeochemistry along an estuarine salinity gradient: The iron conveyer belt. *Limnol. Oceanogr.* **53**: 172-184.
- Karl, D. M., R. Letelier, D. Hebel, L. Tupas, J. Dore, J. Christian and C. D. Winn. 1995. Ecosystem changes in the North Pacific subtropical gyre attributed to the 1991-92 El Niño. *Nature* **373**: 230-234
- Karl, D. M., J. R. Christian, J. E. Dore, D. V. Hebel, R. M. Letelier, L. M. Tupas, and C. D. Winn. 1996. Seasonal and interannual variability in primary production and particle flux at station ALOHA. *Deep Sea Res. Pt. II* **43**, 539-568
- Karl, D. M., J. E. Dore, R. Lukas, A. F. Michaels, N. R. Bates, and A. Knap. 2001. Building the Long-term Picture: The U.S. JGOFS Time-series Programs. *Oceanography* **14** (4), 6-17
- Karl, D. M., B. Michaels, B. Bergman, D. G. Capone, E. J. Carpenter, R. Letelier, F. Lipschultz, H. W. Paerl, D. M. Sigman and L. Stal. 2002. Dinitrogen fixation in the world's oceans. *Biogeochemistry*, **57**, 47-98.
- Karl, D. M., N. R. Bates, S. Emerson, P. J. Harrison, C. Jeandel, O. Llinás, K.-K. Liu, J.-C. Marty, A. F. Michaels, J. C. Miquel, S. Neuer, Y. Nojiri and C. S. Wong. 2003. Temporal Studies of Biogeochemical Processes Determined from Ocean Time-Series Observations During the JGOFS Era. pp. 239-267. *In* M. J. R. Fasham [ed.], *Ocean Biogeochemistry: The Role of the Ocean Carbon Cycle in Global Change*, IGBP Series. Springer, New York.
- Kirchman, D. L., P. A. Wheeler. 1998. Uptake of ammonium and nitrate by heterotrophic bacteria and phytoplankton in the sub-Arctic Pacific. *Deep-Sea Res. Pt. I* **45**. 347-365.

- Kirshtein, J. D., H. W. Paerl, and J. P. Zehr. 1991. Amplification, cloning, and sequencing of a *nifH* segment from aquatic microorganisms and natural communities. *Appl. Environ. Microbiol.* **57**(9): 2645-2650
- Kondo, J. 1975. Air-Sea bulk transfer coefficients in diabatic conditions. *Boundary Layer Meteorology*, **9**, 91-112.
- Korzun, V. I. 1978. World water balance and water resources of the earth, *In* V.I. Korzun [ed.] UNESCO series studies and reports in hydrology No.25. Paris
- Kudela, R. M. 2008. Silicon:Nitrogen Interactions in the Marine Environment. p. 1589-1626. *In* Capone, D. G., D. Bronk, M. Mulholland, and E. J. Carpenter [eds.]. Nitrogen in the marine environment, 2nd edition. Elsevier Science.
- Kustka, A. B., S. A. Sanudo-Wilhelmy, E. J. Carpenter, D. G. Capone, and J. A. Raven. 2003. A revised estimate of the iron use efficiency of nitrogen fixation, with special reference to the marine cyanobacterium *Trichodesmium* spp. (cyanophyta). *J. Phycol.* **39**: 12-25.
- Langlois, R. J., J. LaRoche, and P. A. Raab. 2005. Diazotrophic Diversity and Distribution in the Tropical and Subtropical Atlantic Ocean. *Appl. Environ. Microb.* **71**(12), 7910-7919.
- LaRoche, J., and E. Breitbart. 2005. Importance of the diazotrophs as a source of new nitrogen in the ocean. *J. Sea Res.* **53**, 67-91.
- Laws, E. A., P. G. Falkowski, W. O. Smith Jr., H. Ducklow, and J. McCarthy. 2000. Temperature effects on export production in the open ocean. *Global Biogeochem. Cy.* **14** (4), 1231-1246
- Ledwell, J. R., A. J. Watson and C. S. Law. 1993. Evidence for slow mixing across the pycnocline from an open-ocean tracer-release experiment. *Nature* **364**, 701-703.
- Lee, K., D. M. Karl, R. Wannikhof, and J. Z Zhang. 2002. Global estimate of net carbon production in the nitrate-depleted tropical and sub-tropical ocean: *Geophys. Res. Lett.* **29**, p. 10.1029/2001GL014198.
- Lewis, M. R., W. G. Harrison, N. S. Oakey, D. Hebert, and T. Platt. 1986. Vertical nitrate fluxes in the oligotrophic ocean. *Science* **234**, 870-873.
- Liu, K. K., S. Y. Chao, P. T. Shaw, G. C. Gong, C. C. Chen and T. Y. Tang. 2002. Monsoon-forced chlorophyll distribution and primary production in the South China Sea: observations and a numerical study. *Deep-Sea Res.* **49**, 1387-1412.
- Loick, N., J. W. Dippner, H. Doan-Nhu, I. Liskow, and M. Voß. 2007. Pelagic nitrogen dynamics in the Vietnamese upwelling area according to stable nitrogen and carbon isotope data. *Deep-Sea Res. Pt. I*, **54**, 596-607.

- Longhurst, A., S. Sathyendranath, T. Platt and C. Caverhill. 1995. An estimate of global primary production in the ocean from satellite radiometer data. *J. Plankton Res.* **17**(6): 1245-1271
- Lovell, C. R., Y. M. Piceno, J. M. Quattro, and C. E. Bagwell. 2000. Molecular Analysis of Diazotroph Diversity in the Rhizosphere of the Smooth Cordgrass, *Spartina alterniflora*. *Appl. Environ. Microb.* **66**(9): 3814-3822.
- Lu, X. X. and R. Y. Siew. 2005. Water discharge and sediment flux changes in the lower Mekong River. *Hydrol. Earth Syst. Sc. Discussions* **2**: 2287-2325.
- MacIsaac, J. J. 1978. Diel cycles of inorganic nitrogen uptake in a natural phytoplankton population dominated by *Gonyaulax polyedra*. *Limnol. Oceanogr.*, **23**, 1-9.
- MacIsaac, J. J., R. C. Dugdale, R. T. Barber, D. Blasco, and T. T. Packard. 1985. Primary production cycle in an upwelling center. *Deep-Sea Res.* **32**(5), 503-529.
- Mague, T. H., N. M. Weare, and O. Holm-Hansen. 1974. Nitrogen fixation in the North Pacific Ocean. *Mar. Biol.* **24**: 109-119
- Mahaffey, C., R. G. Williams, G. A. Wolff, N. Mahowald, W. Anderson, and M. Woodward. 2003. Biogeochemical signatures of nitrogen fixation in the eastern North Atlantic: *Geophys. Res. Lett.* **30**. doi:10.1029/2002GL016542
- Mahaffey, C., A. F. Michaels, and D. G. Capone. 2005. The conundrum of marine N<sub>2</sub> fixation. *Am. J. Sci.* **305**: 546-595
- Marra, J. and R. T. Barber 2005. Primary productivity in the Arabian Sea. *Progr. Oceanogr.* **65**, 159-175.
- Mehta, M. P., J. A. Huber, and J. A. Baross. 2005. Incidence of novel and potentially archaeal nitrogenase genes in the deep Northeast Pacific Ocean. *Environ. Microbiol.* **7**(10): 1525-34.
- Mellor, G. L. and T. Yamada. 1974. A Hierarchy of Turbulence Closure Models for Planetary Boundary Layers. *Journal of Atmospheric Sciences*, **31**, 1791-1806.
- Michaels, A. F., N. R. Bates, K. O. Buesseler, C. A. Carlson, and A. H. Knap. 1994. Carbon-cycle imbalances in the Sargasso Sea: *Nature* **372**: 537-540
- Michaels, A. F., D. Olson, J. L. Sarmiento, J. W. Ammerman, K. Fanning, R. Jahnke, A. H. Knap, F. Lipschultz, and J. M. Prospero. 1996. Inputs, losses and transformations of nitrogen and phosphorus in the pelagic North Atlantic Ocean. *Biogeochemistry*, **35**, 181-226.
- Michaels, A. F., D. M. Karl, and D. G. Capone. 2001. Element stoichiometry, new production and nitrogen fixation. *Oceanography* **14**: 68-77
- Mills, M. M., C. Ridame, M. Davey, J. La Roche, and R. J. Geider. 2004. Iron and phosphorus co-limit nitrogen fixation in the eastern tropical North Atlantic. *Nature* **429**: 292-294.
- Moisander, P. H., J. L. Hench, K. Kononen, and H. W. Paerl. 2002. Small-scale shear effects

- on heterocystous cyanobacteria. *Limnol. Oceanogr.*, **47**(1), 2002, 108–119
- Moisander, P. H., R. A. Beinart, M. Voss, and J. P. Zehr. 2008. Diversity and abundance of diazotrophic microorganisms in the South China Sea during intermonsoon. *The ISME Journal* **2**: 954-967, doi:10.1038/ismej.2008.51
- Montoya, J. P., M. Voss, P. Kähler and D. G. Capone. 1996. A Simple, High-Precision, High-Sensitivity Tracer Assay for N<sub>2</sub> Fixation. *Appl. Environ. Microb.* **62**(3), 986-993.
- Montoya, J. P., E. J. Carpenter, and D. G. Capone. 2002. Nitrogen fixation and nitrogen isotope abundance in zooplankton of the oligotrophic North Atlantic. *Limnol. Oceanogr.* **47**: 1617–1628
- Montoya, J. P., C. M. Holl, J. P. Zehr, A. Hansen, T. A. Villareal, and D. G. Capone. 2004. High rates of N<sub>2</sub> fixation by unicellular diazotrophs in the oligotrophic Pacific Ocean. *Nature* **430**, 1027-1031.
- Montoya, J. P., M. Voss, and D. G. Capone. 2007. Spatial variation in N<sub>2</sub>-fixation rate and diazotroph activity in the Tropical Atlantic. *Biogeosciences* **4**, 369–376
- Moore, L. R., A. F. Post, G. Rocap, and S. W. Chisholm. 2002. Utilization of different nitrogen sources by the marine cyanobacteria *Prochlorococcus* and *Synechococcus*. *Limnol. Oceanogr.* **47**(4): 989-996
- Moran, M. A., R. Belas, M. A. Schell, J. M. González, F. Sun, and others. 2007. Ecological Genomics of Marine Roseobacters. *Appl. Environ. Microb.* **73**(14): 4559–4569
- Mulholland, M. R., K. Ohki and D. G. Capone. 2001. Nutrient controls on nitrogen uptake and metabolism by natural populations and cultures of *Trichodesmium* (cyanobacteria). *J. Phycol.*, **37**, 1001-1009
- Mulholland, M. R. 2007. The fate of nitrogen fixed by diazotrophs in the ocean. *Biogeosciences* **4**: 37-51.
- Needoba, J. A., R. A. Foster, C. Sakamoto, J. P. Zehr, and K. S. Johnson. 2007. Nitrogen fixation by unicellular diazotrophic cyanobacteria in the temperate oligotrophic North Pacific Ocean. *Limnol. Oceanogr.* **52**, 1317–1327
- Neuer, S., R. Davenport, T. Freudenthal, G. Wefer, O. Llinás, M.-J. Rueda, D. K. Steinberg, and D. M. Karl. 2002. Differences in the biological carbon pump at three subtropical ocean sites, *Geophys. Res. Lett.*, **29**(18), 1885, doi:10.1029/2002GL015393.
- Nittrouer, C. A., G. J. Brunskill, and A. G. Figueiredo. 1995. Importance of tropical coastal environments. *Geo-Mar. Lett.* **15**: 121-126.
- Nguyen, A. D., H. H. G. Savenije, D. N. Pham, and D. T. Tang. 2008. Using salt intrusion measurements to determine the freshwater discharge distribution over the branches of a multi-channel estuary: The Mekong Delta case. *Estuar. Coast. Shelf Sci.* **77**: 433-445.

- O'Neil, J. M. and M. R. Roman. 1992. Grazers and associated organisms of *Trichodesmium*, pp. 61–73. *In* Carpenter, E. J., Capone, D. G., and Rueter, J., [eds.], *Marine Pelagic Cyanobacteria: Trichodesmium and Other Diazotrophs*. Kluwer, Dordrecht
- Oschlies, A. 2002. Nutrient supply to the surface waters of the North Atlantic: a model study. *J. Geophys. Res.* **107**, doi:0.1029/2000JC000275. pdf
- Paerl, R. W., R. A. Foster, B. D. Jenkins, J. P. Montoya, and J. P. Zehr. 2008. Phylogenetic diversity of cyanobacterial *narB* genes from various marine habitats. *Environ Microbiol* **10**(12). 3377-3387. doi:10.1111/j.1462-2920.2008.01741.x
- Perry, G. D., P. D. Duffy, and A. N. L. Miller. 1996. An extended data set of river discharges for validation of general circulation models. *J. Geophys. Res.* **101**. 21339 - 21349.
- Plattner, G. K., N. Gruber, H. Frenzel, and J. C. McWilliams. 2005. Decoupling marine export production from new production. *Geophys. Res. Lett.* **32**, L11612, doi:10.1029/2005GL022660
- Pohlmann, T. 1987. A three-dimensional circulation model of the South China Sea, pp. 245-268. *In* J. C. J. Nihoul and B. M. Jamart [eds.]. *Three-dimensional models of marine and estuarine dynamics*. Elsevierer Oceanography Series
- Pohlmann, T. 2006. A meso-scale model of the central and southern North Sea: Consequences of an improved resolution. *Cont. Shelf Res.* **26**. 2367 – 2385.
- Redfield, A. C. 1958. The biological control of chemical factors in the environment. *Am. Sci.* **46**, 205-221.
- Revelante N., and M. Gilmartin. 1982. Dynamics of phytoplankton in the Great Barrier Reef lagoon. *J. Plankton Res.* **4**: 47–76.
- Ryther, J. H. 1969. Photosynthesis and fish production in the sea. *Science* **166**: 72
- Sambrotto, R. N., G. Savidge, C. Robinson, P. Boyd, T. Takahashi, D. M. Karl, C. Langdon, D. Chipman, J. Marra, and L. Codispoti. 1993. Elevated consumption of carbon relative to nitrogen in the surface ocean. *Nature* **363**: 248–250.
- Sanudo-Wilhelmy, S. A., A. B. Kustka, C. J. Gobler, D. A. Hutchins, M. Yang, K. Lwiza, J. Burns, D. G. Capone, J. A. Raven, and E. J. Carpenter. 2001. Phosphorus limitation of nitrogen fixation by *Trichodesmium* in the central Atlantic Ocean. *Nature* **411**: 66-69.
- Scanlan, D. J., M. Ostrowski, S. Mazard, A. Dufresne, L. Garczarek, W. R. Hess, A. F. Post, M. Hagemann, I. Paulsen, and F. Partensky. 2009. Ecological Genomics of Marine Picocyanobacteria. *Microbiol. Mol. Biol. R* **73**:249-299
- Scharek, R., M. Latasa, D. M. Karl, and R. R. Bidigare. 1999a. Temporal variations in diatom abundance and downward vertical flux in the oligotrophic North Pacific gyre. *Deep Sea Res. Pt. I* **46** (6), 1051–1075.

- Scharek, R., L. M. Tupas, and D. M. Karl. 1999b. Diatom fluxes to the deep sea in the oligotrophic North Pacific gyre at Station ALOHA. *Mar. Ecol. Progr. Ser.* **182**, 55-67.
- Seitzinger, S. P. 1988. Denitrification in freshwater and coastal marine ecosystems: Ecological and geochemical significance. *Limnol. Oceanogr.* **33**: 702-724.
- Shaw, P. T. and S. Y. Chao. 1994. Surface circulation in the South China Sea. *Deep-Sea Res. Pt. I* **41**: 1663-1683.
- Short, S. M., B. D. Jenkins, and J. P. Zehr. 2004. Spatial and Temporal Distribution of Two Diazotrophic Bacteria in the Chesapeake Bay. *Appl. Environ. Microb.* **70**(4), 2186-2192.
- Short, S. M. and J. P. Zehr. 2005. Quantitative analysis of *nifH* genes and transcripts from aquatic environments. *Methods Enzymol.* **397**: 380-394.
- Sigman, D. M., and K. L. Casciotti. 2001. Nitrogen isotopes in the ocean. pp. 1884 – 1894. In Thorpe, S., and K. Threbbion [Eds.], *Encyclopedia of Ocean Sciences*, Elsevier Verlag, New York
- Stewart, W. D. P., G. P. Fitzgerald, and R. H. Burris. 1967. *In situ* studies on N<sub>2</sub> fixation, using the acetylene reduction technique: *PNAS* **58**: 2071.
- Subramaniam, A., P. L. Yager, E. J. Carpenter, C. Mahaffey, K. Bjorkman, S. Cooley, A. B. Kustka, J. P. Montoya, S. A. Sanudo-Wilhelmy, R. Shipe, and D. G. Capone. 2008. Amazon River enhances diazotrophy and carbon sequestration in the tropical North Atlantic Ocean. *PNAS* **105**: 10460-10465.
- Tan, S. C. and G. Y. Shi. 2009. Spatiotemporal variability of satellite-derived primary production in the South China Sea, 1998-2006. *J. Geophys. Res.* **114**, G03015, doi:10.1029/2008JG000854, 2009
- Tang, D.-L., H. Kawamura, H. Doan-Nhu, and W. Takahashi. 2004a. Remote sensing oceanography of a harmful algal bloom off the coast of southeastern Vietnam. *J. Geophys. Res.* **109**, doi:10.1029/2003JC002045, 2004), 1-7.
- Tang, D.-L., H. Kawamura, T. Van Dien, and M.-A. Lee. 2004b. Offshore phytoplankton biomass increase and its oceanographic causes in the South China Sea. *Mar. Ecol. Progr. Ser.* **268**, 31-41.
- Thomas, W. H. 1966. Surface nitrogenous nutrients and phytoplankton in the northeastern tropical Pacific ocean. *Limnol. Oceanogr.* **15**, 393–400
- Thomas, H., V. Ittekkot, C. Osterroht, B. Schneider. 1999. Preferential recycling of nutrients—the ocean’s way to increase new production and to pass nutrient limitation? *Limnol. Oceanogr.* **44**(8): 1999 - 2004.
- Tri, D. L. 2002. Vietnam Report on Fisheries. 15th Standing Committee on Tuna and Billfish Honolulu, Hawaii, 22 - 27/7/2002

- Tseng, C.-M., G. T. F. Wong, I.-I. Lin, C.-R. Wu, and K. K. Liu. 2005. A unique seasonal pattern in phytoplankton biomass in low-latitude waters in the South China Sea. *Geophys. Res. Lett.* **32**, L08608, doi:10.1029/2004GL022111
- Turner, R. E., N. N. Rabalais, R. B. Alexander, G. McIsaac, and R. W. Howarth. 2007. Characterization of nutrient, organic carbon, and sediment loads and concentrations from the Mississippi River into the Northern Gulf of Mexico. *Estuaries and Coasts* **30**: 773-790.
- Utermöhl, V. H. 1958. Quantitative estimation of phytoplankton abundance and volume. *Mitt. Inter. Ver. Theor. Angew. Limnol.* **9**: 1-38. (Published in German: Zur Vervollkommnung der quantitativen Phytoplankton-Methodik).
- Veldhuis, M. J. W., G. W. Kraay, J. D. L. Van Bleijswijk, and M. A. Baars. 1997. Seasonal and spatial variability in phytoplankton biomass, productivity and growth in the northwestern Indian Ocean: the southwest and northeast monsoon, 1992-1993. *Deep-Sea Res. Pt. I*, **44**(3), 425-449.
- Venrick, E. L. 1974. The distribution and significance of *Richelia intracellularis* in the North Pacific central gyre. *Limnol. Oceanogr.* **19**, 437-445
- Villareal, T. A. 1990. Laboratory Culture and Preliminary Characterization of the Nitrogen-Fixing *Rhizosolenia*-*Richelia* Symbiosis. *Mar. Ecol.* **11**(2): 117-132.
- Villareal, T. A. 1992. Marine nitrogen-fixing diatom-cyanobacteria symbioses, p. 163-175. In E. J. Carpenter, D. G. Capone, and J. G. Rueter [eds.], *Marine pelagic cyanobacteria: Trichodesmium and other Diazotrophs*. Kluwer.
- Voss, M., P. Croot, K. Lochte, M. Mills, and I. Peeken. 2004. Patterns of nitrogen fixation along 10°N in the tropical Atlantic. *Geophys. Res. Lett.* **31**: L23S09, doi:10.1029/2004GL020127
- Voss, M., D. Bombar, N. Loick and J. W. Dippner. 2006. Riverine influence on nitrogen fixation in the upwelling region off Vietnam, South China Sea. *Geophys. Res. Lett.* **33**, L07604, doi:10.1029/2005GL025569, 2006.
- Walsh, J. J. 1991. Importance of continental margins in the marine biogeochemical cycling of carbon and nitrogen. *Nature* **350**: 53-55
- Walsh, J. J. 1996. Nitrogen fixation within a tropical upwelling ecosystem: Evidence for a Redfield budget of carbon/nitrogen cycling by the total phytoplankton community. *J. Geophys. Res.* **101** (C9). 20,607-20,616.
- Wasmund, N., I. Topp, and D. Schories. 2006. Optimising the storage and extraction of chlorophyll samples. *Oceanologia* **48**: 125-144.

- Wilkerson, F. P., R. C. Dugdale, and R. T. Barber. 1987. Effects of El Niño on new, regenerated, and total production in eastern boundary upwelling systems. *J. Geophys. Res.-Oceans* **92**, 14347–14353.
- Wilkerson, F. P., R. C. Dugdale, R. M. Kudela, and F. P. Chavez. 2000. Biomass and productivity in Monterey Bay, California: Contribution of the large phytoplankton. *Deep Sea Res. Pt. II* **47**, 1003–1022.
- Wong G. T. F., S.-W. Chung, F.-K. Shiah, C.-C. Chen, L.-S. Wen, and K.-K. Liu. 2002. Nitrate anomaly in the upper nutricline in the northern South China Sea - Evidence for nitrogen fixation. *Geophys. Res. Lett.* **29**. doi:2010.1029/2002GL015796
- Wu, J., S. W. Chung, L. S. Wen, K.-K. Liu, Y.-L. Chen, H.-Y. Chen, and D. M. Karl. 2003. Dissolved inorganic phosphorus, dissolved iron, and *Trichodesmium* in the oligotrophic South China Sea. *Global Biogeochem. Cy.* **17**(1), 8-1-8-10.
- Wyrtki, K. 1961. Physical Oceanography of the Southeast Asian waters. UC San Diego: Scripps Institution of Oceanography. Retrieved from:  
<http://www.escholarship.org/uc/item/49n9x3t4>
- Xie, S.-P., Q. Xie, D. Wang, and W. T. Liu. 2003. Summer upwelling in the South China Sea and its role in regional climate variations. *J. Geophys. Res.* **108** (C8), 17-1-17-13.
- Yool, A., A. P. Martin, C. Fernandez, and D. R. Clark. 2007. The significance of nitrification for oceanic new production. *Nature* **447**, 999-1002, doi:10.1038/nature05885
- Yoshimura C., and K. Takeuchi. 2007. Estimation of nutrient runoff processes in the Mekong River Basin using a distributed hydrological model. *Journal of Japan Society of Hydrology & Water Resources* **20**: 493-504.
- Zehr, J. P. and L.A. McReynolds. 1989. Use of Degenerate Oligonucleotides for Amplification of the *nifH* Gene from the Marine Cyanobacterium *Trichodesmium thiebautii*. *Appl. Environ. Microb.* **55**: 2522-2526
- Zehr, J. P., and D. G. Capone. 1996. Problems and promises of assaying the genetic potential for nitrogen fixation in the marine environment. *Microbial Ecol.* **32**: 263–281
- Zehr J. P., M. T. Mellon, and S. Zani. 1998. New nitrogen-fixing micro-organisms detected in oligotrophic oceans by amplification of nitrogenase (*nifH*) genes. *Appl. Environ. Microb.* **64**: 3444–3450.
- Zehr, J. P., J. B. Waterbury, P. J. Turner, J. P. Montoya, E. Omoregie, G. F. Steward, A. Hansen, and D. M. Karl. 2001. Unicellular cyanobacteria fix N<sub>2</sub> in the subtropical North Pacific ocean. *Nature* **412**, 635-638.

- Zehr J. P. and P. J. Turner. 2001. Nitrogen fixation: Nitrogenase genes and gene expression, pp 271–286. In J. H. Paul [ed.] *Methods in Microbiology: Marine Microbiology*. Academic Press: London, UK.
- Zehr, J. P. and B. B Ward. 2002. Minireview: Nitrogen Cycling in the Ocean: New Perspectives on Processes and Paradigms. *Appl. Environ. Microb.* **68**: 1015 - 1024
- Zehr, J. P., B. D. Jenkins, S. M. Short, and G. F. Steward. 2003. Nitrogenase gene diversity and microbial community structure: a cross-system comparison. *Environ. Microbiol.* **5**(7): 539-554
- Zehr, J. P., J. P. Montoya, B. D. Jenkins, I. Hewson, E. Mondragon, C. M. Short, M. J. Church, A. Hansen, and D. M. Karl. 2007. Experiments linking nitrogenase gene expression to nitrogen fixation in the North Pacific subtropical gyre. *Limnol. Oceanogr.* **52**(1): 169–183
- Zehr, J. P. and H. W. Paerl. 2008. Molecular ecological aspects of nitrogen fixation in the marine environment, pp. 481-525. In D. L. Kirchman [ed.], *Microbial Ecology of the Oceans*. 2nd edition, Wiley-Blackwell.
- Zehr, J. P., S. R. Bench, B. J. Carter, I. Hewson, F. Niazi, T. Shi, H. J. Tripp, and J. P. Affourtit. 2008. Globally Distributed Uncultivated Oceanic N<sub>2</sub>-Fixing Cyanobacteria Lack Oxygenic Photosystem II. *Science* **322**: 1110-1112. doi:10.1126/science.1165340
- Zhang, J.-Z., R. Wanninkhof, and K. Lee. 2001. Enhanced new production observed from the diurnal cycle of nitrate in an oligotrophic anticyclonic eddy. *Geophys. Res. Lett.* **28**(8): 1579-1582..

## Publications, Manuscripts, and Conferences

This PhD has been part of an interdisciplinary project in which results from different scientists intertwine. The contents of chapters 2 and 3 have already been published in peer-reviewed journals. Chapter 4 has been submitted to an international journal, and another part of my work is being prepared for submission. The author contributions to each manuscript are outlined in the following:

### Publications in peer-reviewed journals

- **Bombar, D.**, J. W. Dippner, H. N. Doan, L. N. Ngoc, I. Liskow, N. Loick-Wilde, and M. Voss (2010), Sources of new nitrogen in the Vietnamese upwelling region of the South China Sea, *J. Geophys. Res.*, doi:10.1029/2008JC005154, (in press).  
Contributions: D. B., N. L. W., M. V. (sampling, rate measurements, chlorophyll measurements), I. L., D.B. and N. L. W. (nutrient analyses, isotope measurements). J. W. D. (calculations of diffusion coefficients). Concept and first editions of manuscript: D. B., J. W. D. Revisions of manuscript: D. B., J. W. D., M. V., N. L. W., H. N. D., L. N. N.
- Grosse, J., **D. Bombar**, H. N. Doan, L. N. Nguyen, and M. Voss. The Mekong River plume fuels nitrogen fixation and determines phytoplankton species distribution in the South China Sea during the low and high discharge season. *Limnology and Oceanography* (in press, accepted March 15<sup>th</sup>, 2010).  
Contributions: D. B., J.G. (sampling, rate measurements, chlorophyll- and nutrient measurements in April 2007, with help from A. Rathmeyer), D. B. (sampling, rate measurements, chlorophyll- and nutrient measurements in September 2008, with help from F. Korth, I. Liskow and M.V.). H. N. D and L. N. N. (phytoplankton cell counts with help from members of their workgroup). CTD and other sensor measurements: B. Karfeld and H. Hein. Isotope measurements by I. Liskow. Concept and first edition of manuscript: J. G., D. B., M. V. Revisions of manuscript: D. B., J. G., M. V.
- Voss, M., **D. Bombar**, N. Loick, and J. W. Dippner (2006), Riverine influence on nitrogen fixation in the upwelling region off Vietnam, South China Sea, *Geophys. Res. Lett.*, 33, L07604, doi:10.1029/2005GL025569.  
This manuscript is part of the diploma thesis of D. B.

### Manuscripts submitted or in preparation

- **Bombar, D.**, P. H. Moisaner, J. W. Dippner, R. A. Foster, M. Voss, B. Karfeld, and J. P. Zehr. Distribution of diazotrophic microorganisms, *nifH* gene expression and N<sub>2</sub> fixation in the Mekong River Plume during intermonsoon. *Marine Ecology Progress Series* (submitted).  
Contributions: D. B. (*nifH* sampling), D. B., P. H. M., R. A. F. (*nifH* PCR, QPCR, RT-QPCR). J. W. D. and B. K. (Lagrangian tracer experiments). Concept and first edition of manuscript: D. B., P. H. M. Revisions of manuscript: D. B., P. H. M., R. A. F., B. K., M. V., J. P. Z.

- **Bombar, D.**, J. W. Dippner, F. Korth, N. Loick-Wilde, I. Liskow, L. N. Ngoc, H. N. Doan, and M. Voss. A mesocosm experiment reproduces the positive influence of the Mekong River discharge on nitrogen fixation in the South China Sea. (in preparation). Contributions: D. B., F. K., N. L. W., M. V. (sampling, rate measurements, chlorophyll- and nutrient measurements, with help from R. Peinert and M. Schmidt). H. N. D and L. N. N. (phytoplankton cell counts with help from members of their workgroup). I. L., D. B. (Isotope measurements). J. W. D. (modeling). Concept and first edition of manuscript: D. B., J. W. D., M. V.

### Talks and poster presentations at conferences and workshops

- **Bombar, D.**, J. W. Dippner, N. Loick-Wilde, J. Grosse, and M. Voss. (2009). Nitrogen cycling in the South China Sea: Upwelling, river input and nitrogen fixation. GfÖ 2009: Dimensions of ecology- from global change to molecular ecology. Conference of the Ecological Society of Germany, Austria and Switzerland, Bayreuth, Germany, 14.-18. September 2009
- **Bombar, D.**, P. H. Moisander, J. W. Dippner, R. A. Foster, M. Voss, B. Karfeld, and J. P. Zehr. (2009). A Molecular Approach to Study Diazotrophy in the Mekong River Plume. Final workshop of the project 'Land-Ocean-Atmospheric Interactions in the Coastal Zone of Southern Vietnam'. Deutsche Forschungsgemeinschaft. Nha Trang, Vietnam, 25. November 2009
- **Bombar, D.**, P. H. Moisander, M. Voss, J. Grosse, and J. P. Zehr (2009). Abundance of diazotrophic microorganisms and nitrogenase gene (*nifH*) expression in the Mekong River Plume during Intermonsoon (Poster). American Society of Limnology and Oceanography. Nice, France, 25-30 Jan. 2009
- **Bombar, D.**, J. Dippner, M. Voss, and N. Loick. (2008). An assessment of different sources of new nitrogen during monsoon-forced upwelling off the Vietnamese Coast (Poster). American Society of Limnology and Oceanography. Orlando, Florida, 2-9 Mar. 2008
- **Bombar, D.** (2006). Regulation factors of productivity in the Vietnamese upwelling area. National Ocean Science workshop of the Vietnamese Ministry of Science and Technology. Nha Trang, Vietnam, 30. Nov. - 01. Dez. 2006

## Acknowledgements

*I would like to thank my supervisor, PD Dr. Maren Voss, for giving me the chance to continue the participation in the Vietnamese-German research project after my diploma thesis. Her great supervision and continuous readiness for discussions helped me to keep the necessary focus, and to shape initial ideas into feasible plans. The collaboration with PD Dr. Joachim W. Dippner has been a pleasure, and this thesis has been greatly upvalued by his inputs and explanations about physical oceanography, so I am very grateful. Dr. J. Waniek was a member of my thesis committee and I want to thank her for encouraging discussions.*

*The workgroup “Mariner Stickstoffkreislauf” at IOW is a great team of dedicated, helpful, hard working people who always supported me. I want to especially thank Iris Liskow for introducing me to stable isotope measurements and for her participation in the planning and realization of field- and lab work in Vietnam. Likewise, Frederike Korth, Natalie Loick-Wilde and Matthias Schmidt deserve big thanks for all their help in Vietnam, and for starring in a photo-love-story that is now under consideration to be turned into a major Vietnamese TV series... I also acknowledge Natalies proofreading expertise. Dr. Hai Nhu Doan, Dr. Lam Nguyen Ngoc and their whole team at ION have been great hosts and colleagues to us and were of course instrumental in planning and conducting all of the field work. Further, Dr. Rolf Peinert has been most valuable in organizing the 2nd phase of the VG project, and without his organizational and diplomatic efforts, clearly there would have been no field sampling or mesocosm experiments. A special thanks also goes out to A. Rathmeyer (alias MacGyver), who has an astonishing creativity in technical matters and thereby enabled us to overcome many difficulties while preparing and conducting the 1<sup>st</sup> Mekong cruise and experiments. The friendly crew of the monitoring vessel BTh-0666KN is acknowledged for cruising us safely around the Mekong estuary.*

*I also feel very grateful to Prof. Dr. Jonathan P. Zehr and his workgroup for welcoming me at UC Santa Cruz. Especially, Pia Moisander, M. Ochiai, R. Beinart, Rachel Foster, M. Hogan, I. Henson, R. Paerl and E. Mondragon helped me to learn and apply the molecular methods and made my stay in Santa Cruz unforgettable. I am also very thankful to the German Academic Exchange Service (DAAD) for enabling me this experience abroad.*

*Many people at the IOW have become my friends, and made the time there most enjoyable. I want to thank the whole group of “Dipl-Docs” and postdocs for the nice times we had during institute events, conferences, every-day “Cafe Seeblick” lunch breaks, and for sharing thoughts and concerns regarding the PhD life. Special thanks go to Christian, Lars and Sabine for the fun times we shared as former office mates.*

*Last but not least, I want to deeply thank my family, friends, and Ruth for all the support and patience.*

## **Erklärung**

Ich versichere hiermit an Eides statt, dass ich die vorliegende Arbeit selbstständig angefertigt und ohne fremde Hilfe verfasst habe, keine außer den von mir angegebenen Hilfsmitteln und Quellen dazu verwendet habe und die den benutzten Werken inhaltlich und wörtlich entnommenen Stellen als solche kenntlich gemacht habe.

Rostock, den

Deniz Bombar

## Curriculum vitae

### DENIZ BOMBAR

Date and place of birth:  
15. February 1978  
Worms, Germany

---

### Education

- |                     |   |
|---------------------|---|
| 6/2006 until 8/2009 | Ph. D. Biological Oceanography at the Leibniz Institute of Baltic Sea Research<br>Thesis Advisor: Dr. habil. Maren Voss<br>Thesis Title: Regulation factors of productivity, nitrogen fixation and phytoplankton species composition in the upwelling area and the Mekong estuary off Southern Central Vietnam, South China Sea |
| 4/2002 – 1/2006     | Postgraduate studies in Biology at the University of Rostock, Germany.<br>Diploma thesis at the Leibniz Institute for Baltic Sea Research.<br>Thesis Title: Nitrogen fixation as a source of new nitrogen in the Vietnamese upwelling area  |
| 4/2000 – 3/2002     | Undergraduate studies in Biology at Johannes-Gutenberg-University, Mainz, Germany.  |

### Professional Education

- |                 |  |
|-----------------|--|
| 8/1999 – 2/2000 | Apprenticeship as emergency medical technician |
|-----------------|--|

### Schools

- |               |   |
|---------------|---|
| 8/1988–6/1998 | Rudi Stephan Gymnasium Worms, Abitur (Final grade 2,2)    |
| 8/1994-7/1995 | School year abroad: El Dorado High school, Placentia, USA |
| 1984–1988     | Ernst Ludwig elementary school in Worms                   |